2007

Sensitivity of thermal properties of pavement materials using mechanistic-empirical pavement design guide

Satish Reddy Chintakunta
Iowa State University

Sensitivity of thermal properties of pavement materials using mechanistic-empirical pavement design guide

by

Satish Reddy Chintakunta

A thesis submitted to the graduate faculty

in partial fulfillment of the requirements for the degree of

MASTER OF SCIENCE

Major: Engineering Mechanics

Program of Study Committee:
Halil Ceylan, Co-Major Professor
Thomas Rudolphi, Co-Major Professor
Vinay Dayal
Kejin Wang

Iowa State University

Ames, Iowa

2007

Table of Contents

List of Tables

List of Figures

Acknowledgements

I would like to take this opportunity to express my deep appreciation and gratitude to my major professors, Prof. Halil Ceylan and Prof. Thomas Rudolphi, for their suggestions on such an interesting problem and providing me constant guidance throughout this study. Their encouragement and motivation during my graduate studies has enabled me to earn wealth of knowledge and conduct research in a fruitful manner. Without their guidance and support this masters thesis could not have been successfully completed.

I would also like to express my deep thanks to my research group members for their valuable suggestions and ideas. Their support and encouragement during the group meetings and personal interaction motivated me to pursue my research interests successfully. I also wish to thank Federal Highway Administration and my advisors Jim Sherwood, Eric Weaver, Katherine Petros and other at Turner Fairbank Highway Research Center for constantly providing guidance and also for providing funding for this project. Finally, I wish to thank my friends especially Emin Kutay, Martin Kathleen, Jiang Ming Wei for their support and help during my thesis.

Abstract

Pavement design procedures available in the literature do not fully take advantage of mechanistic design concepts, and as a result, heavily rely on empirical approaches. However, reliance on empirical solutions can be reduced by introducing mechanistic–empirical methods, now adopted in the newly released Mechanistic-Empirical Pavement Design Guide (MEPDG). Thermal properties like, coefficient of thermal expansion (CTE), thermal conductivity, heat capacity, surface shortwave absorptivity, ultimate shrinkage strain, mix coefficient of thermal contraction, which control the flow of heat through pavements constitute the primary inputs to MEPDG.

A study was undertaken to compare the sensitivity of thermal input parameters on the performance of concrete and flexible pavements using MEPDG Version 1.0. Effect of climate on the pavement performance was also evaluated. Results from all the simulations showed that almost all of the cases produce reasonable values for transverse cracking, faulting, punchouts, rutting, alligator cracking, IRI. The transverse cracking model in jointed plain concrete pavement (JPCP) is sensitive to coefficient of thermal expansion (CTE), thermal conductivity and climate. Faulting values are sensitive to dowels, thermal conductivity, co-efficient of thermal expansion, surface shortwave absorptivity (SSA) and climate zone. Punchouts are most sensitive to CTE. In flexible pavements airvoid content, traffic volume, and thickness of the asphalt layer, SSA and climate zone are the most sensitive parameters which affect rutting and alligator cracking. However, there are cases for which model predictions disagree with prevailing knowledge in pavement engineering. This study also revealed some problems associated with the software.

Chapter 1 Introduction

1.1 Pavement Types

Historically, pavements have been divided into two broad categories. The flexible pavement system may consist of a relatively thin wearing surface built over a base course and subbase course, and they rest upon the compacted subgrade. In contrast, rigid pavements are two types, Jointed Plain Concrete Pavements (JPCP) and Continuously Reinforced Concrete Pavements (CRCP) and both the rigid pavement types are made up of Portland Cement Concrete (PCC) and may or may not have a base course between the pavement and subgrade [1]. Illustration of possible rigid and flexible pavements is shown in Figures 1.1 and 1.2. The essential difference between the two types of the pavements, flexible and rigid, is the manner in which they distribute the load over the subgrade.

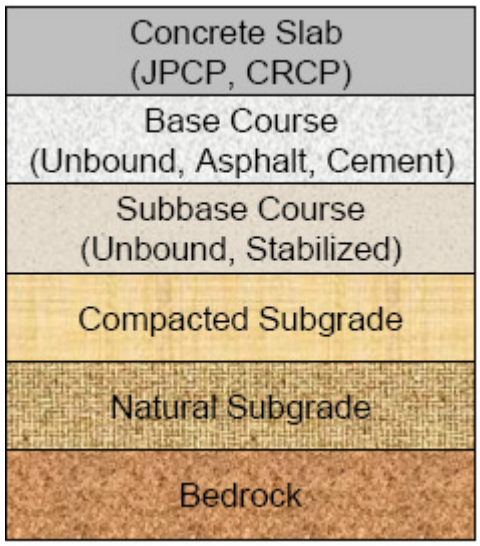

Figure 1.1 Illustration of possible rigid pavement layered system [5]

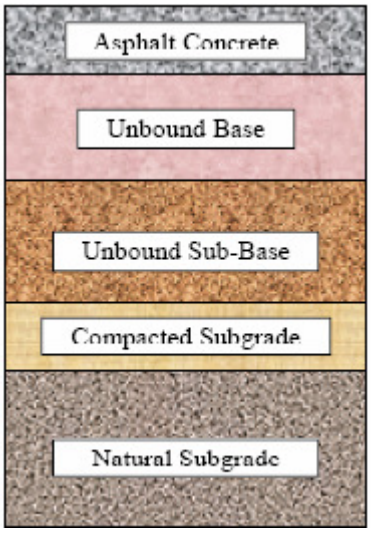

Figure 1.2 Illustration of possible conventional flexible pavement layered system [4]

The rigid pavement, because of its rigidity and high modulus of elasticity, tends to distribute the load over a relatively wide area of soil; thus, a major portion of the structure capacity is supplied by the slab itself. The major factor considered in the design of rigid pavements is the structural strength of the concrete. For this reason, minor variations in subgrade strength have little influence upon the structural capacity of the pavement. It should be noted that the definitions “flexible and rigid” are arbitrary and were established in an attempt to distinguish between asphalt and Portland cement concrete pavements [1]. This report talks about the sensitivity analysis of thermal properties on performance of both flexible and rigid pavement systems.

1.2 Pavement Distress

Distress of pavements can be due to many causes. The first is deterioration or deficiency of the pavement itself. This deterioration might be brought about by freezing and thawing, use of non-durable materials, unfavorable reactions, scaling resulting from use of salts for ice

removal, contraction and expansion stresses, and a variety of other causes. The other category deals with structural adequacy of the pavement-base-subgrade structure [1]. The present report talks about alligator cracking, longitudinal cracking, rutting and thermal cracking in flexible pavements, transverse cracking, joint faulting and IRI in JPCP's and punchouts and IRI in CRCP's.

1.3 Thermal Properties of Pavement Materials

Thermal properties of pavement materials have a great impact on design and performance of rigid and flexible pavement structures. These properties control the flow of heat through the pavement, thus affecting the distribution of temperature and moisture profiles within the pavement system. In the mechanistic-empirical pavement design guide (MEPDG), the thermal parameters constitute the primary inputs to the Enhanced Integrated Climatic Model (EICM), and include parameters such as the coefficient of thermal expansion, drying shrinkage, mix coefficient of thermal contraction, heat capacity, thermal conductivity, and surface shortwave absorptivity [2]. The present study deals with the effect of these properties on the performance of the pavements.

1.4 Mechanistic Empirical Pavement Design Guide (MEPDG)

The overall objective of the guide for the Mechanistic-Empirical Design of New and Rehabilitated Pavement Structures (referred to hereinafter as Design Guide) is to provide the highway community with a state-of-the-practice tool for the design of new and rehabilitated pavement structures, based on mechanistic-empirical principles [3]. The American Association of State Highway and Transportation Officials (AASHTO) Guide for Design of

Pavement Structures is the primary document used to design new and rehabilitated highway pavements.

The Federal Highway Administration's (FHWA) 1995-1997 National Pavement Design Review found that some 80 percent of states use the 1972, 1986, or 1993 AASHTO Guides [3]. All those versions are empirically based on performance equations developed using 1950's AASHO Road Test Data. The various versions of AASHTO Guide for Design of Pavement Structures have served well for several decades; nevertheless, many serious limitations exist for their continued use as the nation's primary pavement design procedures. For example, climatic affects deficiencies. Because the AASHTO Road Test was conducted at one specific geographic location, it is impossible to address the effects of different climatic conditions on pavement performance. Similarly, there are deficiencies in subgrade materials, surfacing materials, traffic loading, base course materials etc. In order to overcome these deficiencies a more robust design guide is to be developed which encompasses different parameters to better predict the performance of the pavements under these conditions.

During the development of the 1986 AASHTO Guide, it was recognized that future pavement design procedures would be based on mechanistic-empirical (M-E) principles. The M-E format of the design guide provides a framework for future continuous improvement to keep up with changes in trucking, materials, construction, climate, design concepts, computers and so on.

1.5 Objectives of Thesis

The objectives of the study presented herein are

1. Evaluate the reasonableness of sensitivity of thermal properties of pavement materials on flexible and rigid pavement design models in MEPDG Version 1.0 for Minneapolis and Phoenix climatic conditions.
2. Identify any problems or bugs evident in the software.

1.6 Scope of the Report

In Chapter 2, various types of pavement distresses and discussion about how and what leads to more distress are discussed. Chapter 2 also talks about the mechanistic-empirical design guide and also results from the previous studies using MEPDG. Chapter 3 talks about the experiment design for the sensitivity analysis, the various types of inputs used in the analysis. The results of the sensitivity analysis using MEPDG Version 1.0 are discussed in Chapter 4. Various plots summarizing the effects of different variables on different performance predictions are presented. This chapter also describes cases in the sensitivity analysis where results disagree with the prevailing knowledge in pavement engineering. Chapter 4 also discusses the heat transfer in pavements using finite element method by considering thermal properties of the constituent materials. Chapter 5.concludes the study, provides recommendations and talks about the future work.

Chapter 2 Literature Review

2.1 Distress in Pavements

2.1.1 Flexible Pavement Distress

The most important distresses in flexible pavements are discussed in this section.

Bottom-Up Fatigue Cracking

Cracking occurs in areas subjected to repeated traffic loadings (wheel paths). It can be a series of interconnected cracks in early stages of development. Basically, the pavement and Hot Mix Asphalt (HMA) layer deflects under wheel loads that result in tensile strains and stresses at the bottom of the layer. With continued bending, the tensile stresses and strains cause cracks to initiate at the bottom of the layer and then propagate to the surface [4]. The mechanism is shown in the Figure 2.1.

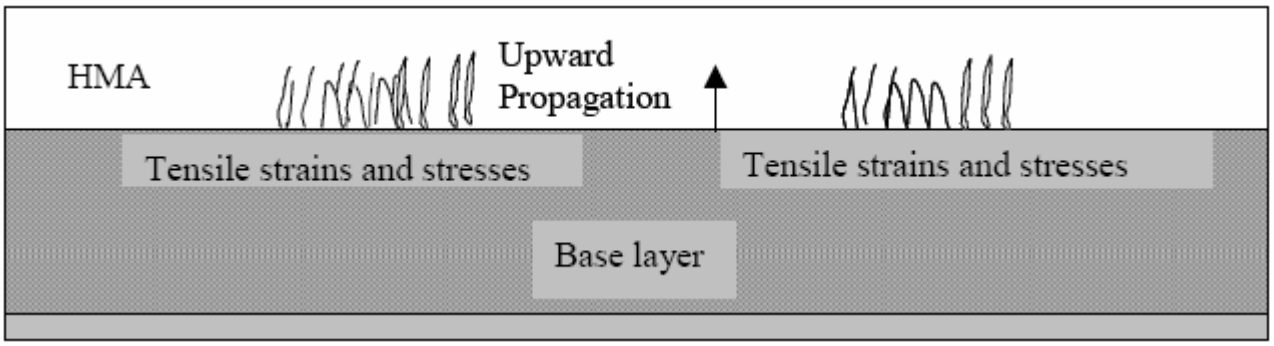

Figure 2.1 Bottom-up fatigue cracking [4]

Figure 2.2 High severity fatigue cracking [6]

Surface-Down Fatigue Cracking or Longitudinal Cracking

Most fatigue related cracks initiate at the bottom of the HMA layer and propagate to the surface. However there is increasing evidence that suggests load related cracks some times do initiate at surface and propagate downward. Wheel load induced tensile stresses and strains that occur at surface cause cracks to initiate at the surface and propagate downward. The mechanism is shown in the figure. Longitudinal cracks are predominantly parallel to pavement centerline. Location within the lane (wheel path versus non-wheel path) is significant [4].

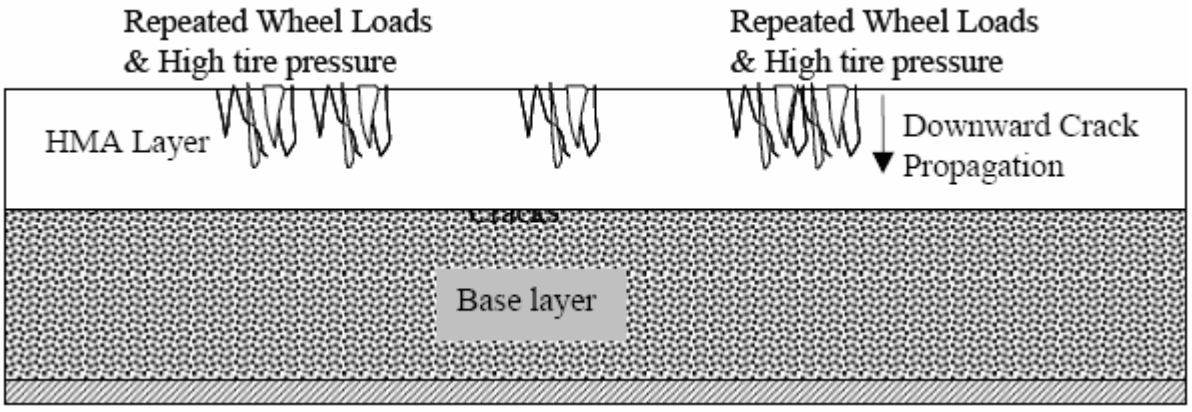

Figure 2.3 Top-down fatigue cracking [4]

Figure 2.4High severity longitudinal cracking [6]

Permanent Deformation or Rutting

Rutting is a surface depression in the wheel paths caused by inelastic or plastic deformations in any or all of the pavement layers and subgrade [4]. These plastic deformations are typically the result of: 1) densification or one dimensional compression and consolidation and 2) lateral movements or plastic flow of materials (HMA, aggregate base and subgrade soils) from wheel loads.

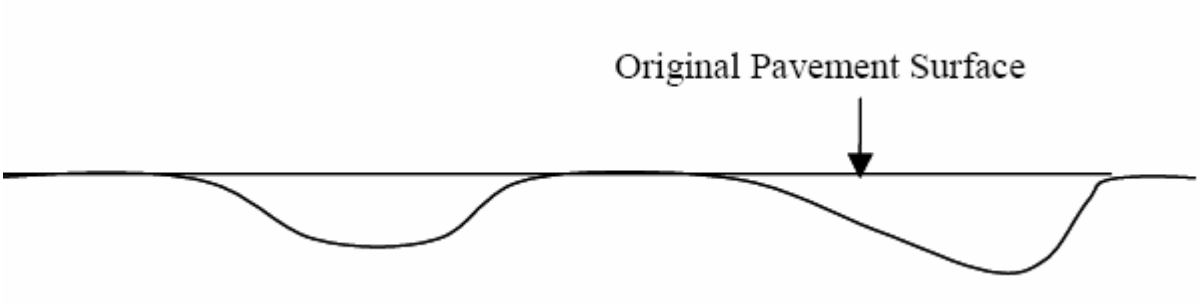

(a) One dimensional densification or vertical compression

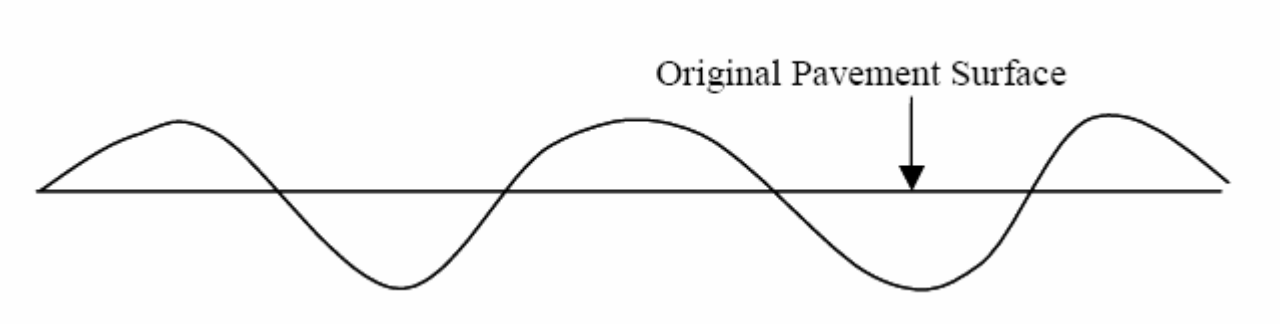

(b) Lateral displacement or two dimensional plastic movements

Figure 2.5 Types and mechanisms of rutting in flexible pavements [4]

Figure 2.6 High severity rut [6]

Thermal Cracking or Transverse Cracking

Cracking in flexible pavements due to cold temperatures or temperature cycling is commonly referred to as thermal cracking [4]. Thermal cracks typically appear as transverse cracks on the pavement surface which are predominantly perpendicular to pavement centerline.

Figure 2.7 High severity transverse cracking [6]

2.1.2 Rigid Pavement Distress

Rigid pavements are further classified into Continuously Reinforced Concrete Pavements (CRCP) and Jointed Plain Concrete Pavements (JPCP). CRCP is a Portland cement concrete (PCC) pavement that has continuous longitudinal steel reinforcement and no intermediate transverse expansion or contraction joints. The pavement is allowed to crack in a random transverse cracking pattern and the cracks are held tightly together by the continuous steel reinforcement. On the contrary, JPCP uses contraction joints to control cracking and does not use any reinforcing steel. Common distresses among these pavements are given below.

Bottom-Up Transverse Cracking (JPCP)

As shown in Figure 2.8 and Figure 2.9, when the truck axles are near the longitudinal edge of the slab, midway between the transverse joints, a critical tensile bending stress occurs at the bottom of the slab as shown in the figure. This stress increases greatly when there is a high positive temperature gradient through the slab (the top of the slab is warmer than the bottom of the slab). Repeated loadings of heavy axles under those conditions result in fatigue damage along the bottom edge of the slab, which eventually result in a transverse crack that propagates to the surface of the pavement [5].

Top-Down Transverse Cracking (JPCP)

Repeated loading by heavy truck tractors with certain axle spacing when the pavement is exposed to high negative temperature gradients (the top of the slab is cooler than the bottom of the slab) result in fatigue damage at the top of the slab, which eventually results in a transverse or diagonal crack that is initiated on the surface of the pavement as shown in Figure 2.10. The critical loading condition for top-down cracking involves a combination of axles that loads the opposite ends of a slab simultaneously. In the presence of a high

temperature gradient, such load combinations cause a high tensile stress at the top surface of the slab near the critical edge as shown in the figure. Typical values of allowable cracking range from 10 to 45 percent [5].

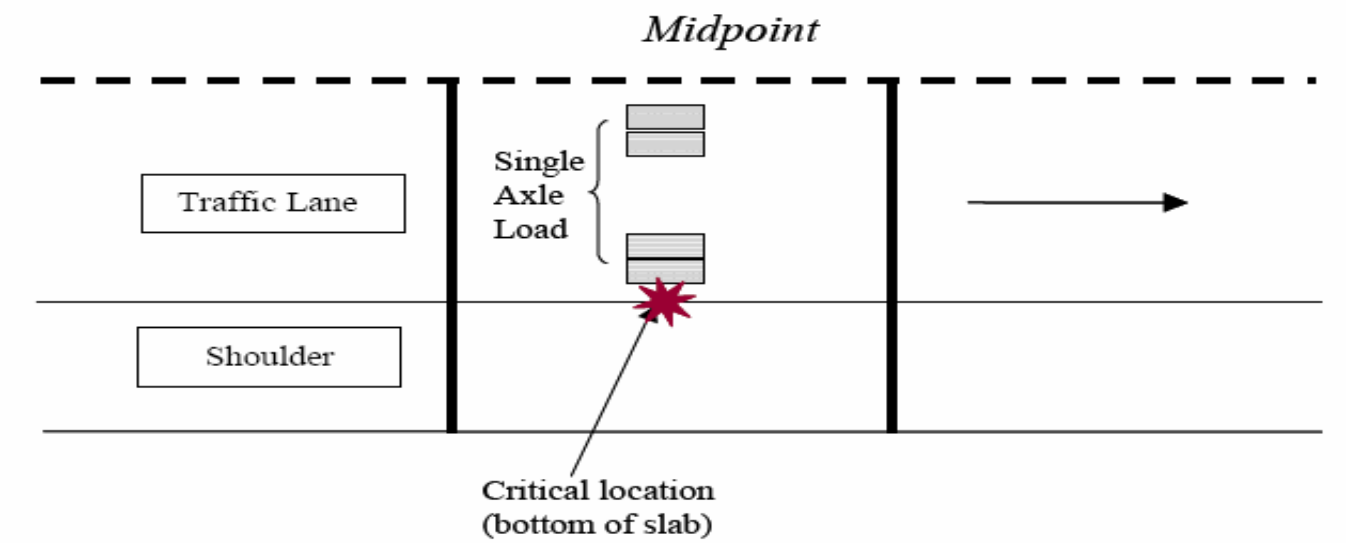

Figure 2.8 Critical location in bottom-up transverse cracking in JPCP [5]

Figure 2.9 High severity transverse cracking [6]

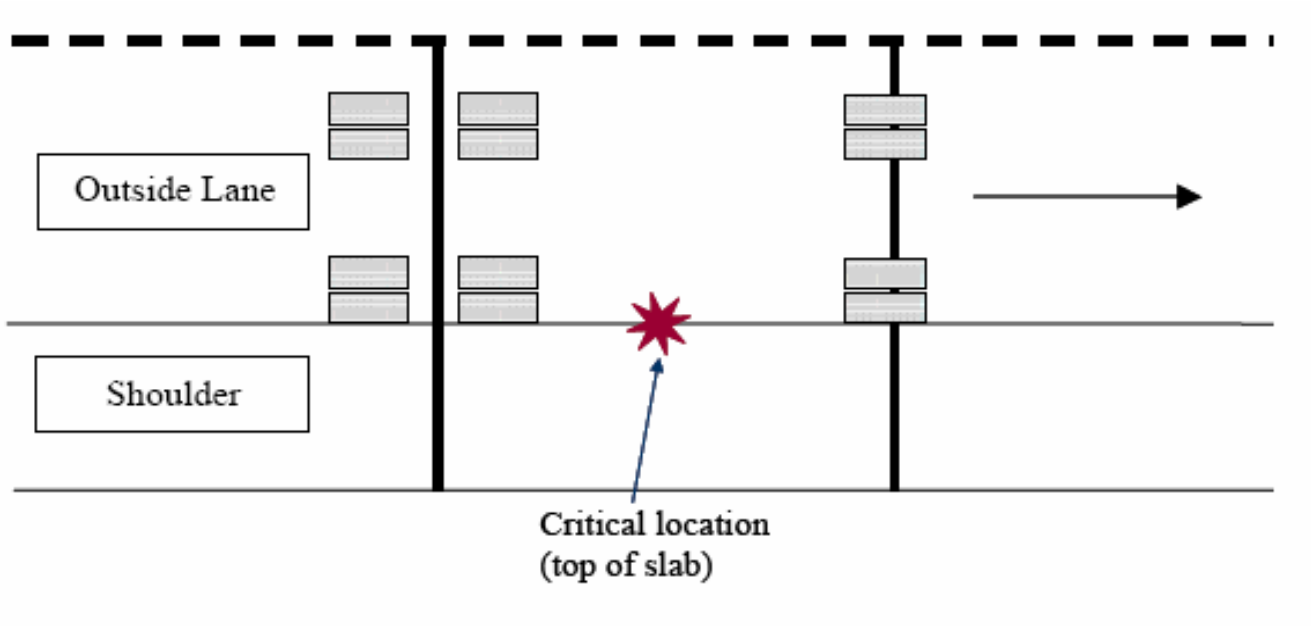

Figure 2.10 Critical location in top-down transverse cracking in JPCP [5]

Joint Faulting (JPCP)

Repeated heavy axle loads crossing transverse joints creates the potential for joint faulting as shown in Figure 2.11 and 2.12. Faulting can become severe for several reasons

1. Presence of free moisture under the joint
2. Presence of pumpable fines beneath the joint-an erodible base, subbase or subgrade.
3. Poor joint load transfer efficiency
4. Repeated heavy axle loads

Typical values of allowable JPCP mean faulting range from 0.1in to 0.2in [5].

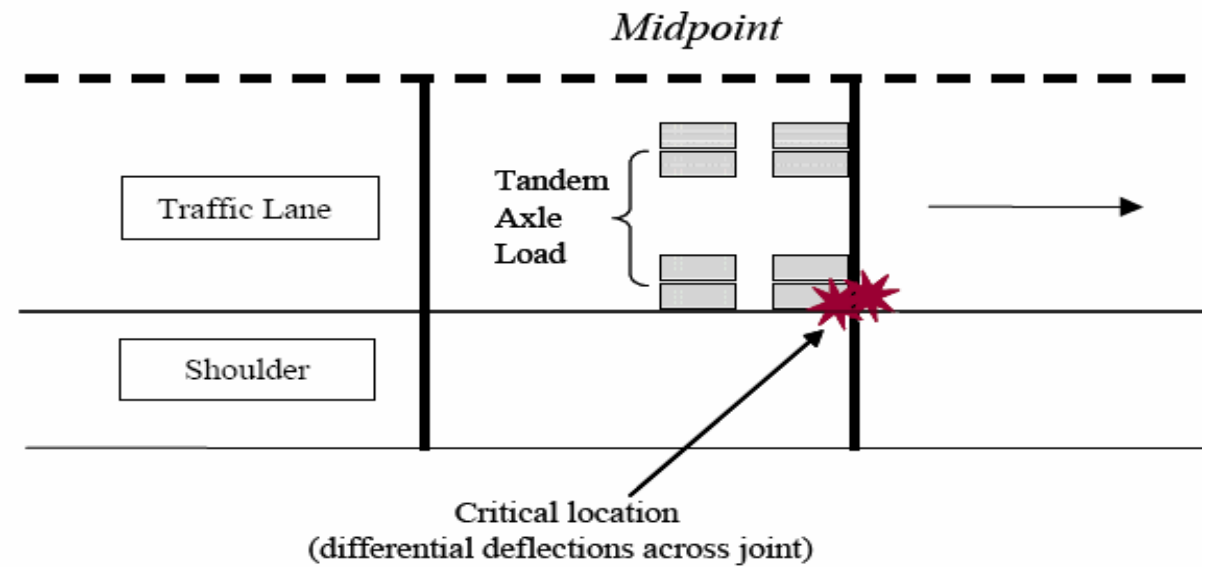

Figure 2.11 Critical location in faulting [5]

Figure 2.12 High severity faulting [6]

Punchouts (CRCP)

When truck axles pass along near the longitudinal edge of the slab between two closely spaced transverse cracks , a high tensile stress occurs at the top of the slab, some distance from the edge (say from 40 to 60 in from the edge), transversely across the pavement as shown in Figure 2.13 [5]. This stress increases greatly when there is loss of load transfer

across the transverse cracks or loss of support along the edge of the slab. Typical values of allowable CRCP punchouts range from 10 to 20 per mile (all severities) [5].

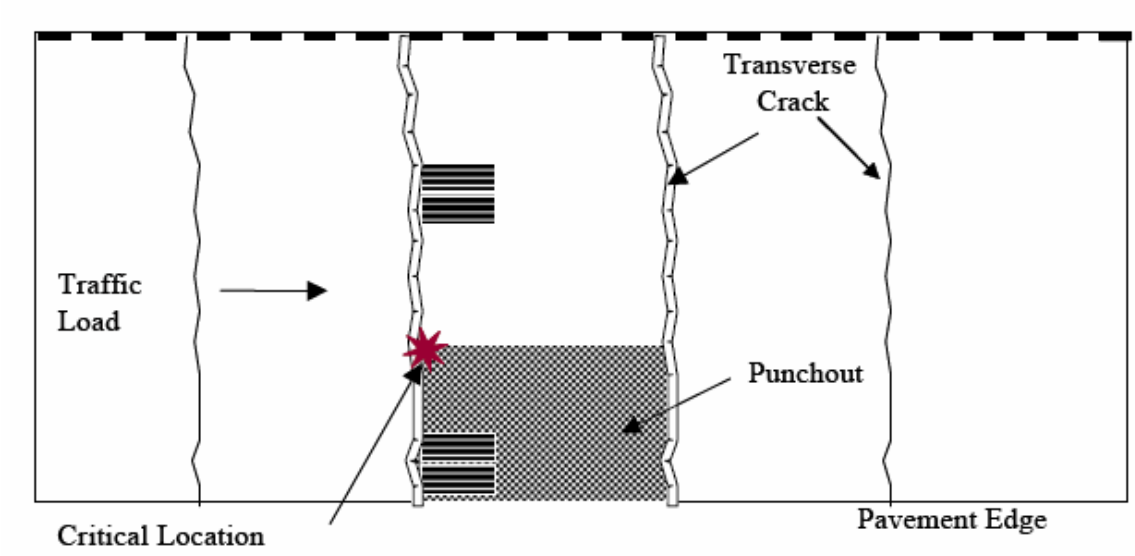

Figure 2.13 Critical location in punchouts [5]

Figure 2.14 High severity punchout [6]

Smoothness (HMA, JPCP and CRCP)

Functional adequacy is quantified most often by pavement smoothness. Rough roads not only lead to user discomfort but also to increased travel times and higher vehicle operating costs.

Although the structural performance of a pavement, in terms of pavement distress, is important the public complaints generated by rough roads often contribute to a large part of the rehabilitation decisions that are made by state highway agencies. Smoothness is defined as “the variation in surface elevation that induces vibrations in traversing vehicles” [5]. IRI is the most common way of measuring smoothness in managing pavements. Typical values in the range of 150 to 200 in/mile are used for terminal IRI.

2.2 MEPDG

The MEPDG is intended to be user-friendly software for analysis and design of new, reconstructed and rehabilitated flexible, rigid and composite pavements. The design guide represents a major change in the way the design of pavements is performed. The design approach consists of three main stages. Stage 1 consists of the development of the input variables for the trial design. During this stage, foundation analysis, pavement material characterization, traffic input and climatic input data are developed. Stage 2 consists of analyzing the trial design incrementally over time using the pavement response and distress models and the outputs of the analysis are the accumulated damage, the expected amount of distress and smoothness over time. Stage 3 is to check if the trial design meets the performance criteria or not, if not, modifications are made and the analysis re-run until a satisfactory result is obtained. The three stage process explained above can be shown by a simple flow chart as shown in Figure 2.15. Several sensitivity studies using MEPDG exist which mainly concentrate on the effect of non-thermal input parameters on the pavement performance predictions. Kannekanti [7] in his sensitivity study on Jointed Plain Concrete Pavements in California showed that dowels, traffic volume, joint spacing, PCC thickness,

climate zone, and shoulder type have a significant effect on IRI, faulting and cracking. Moreover the study was carried out using the older version of the software which has significant software problems.

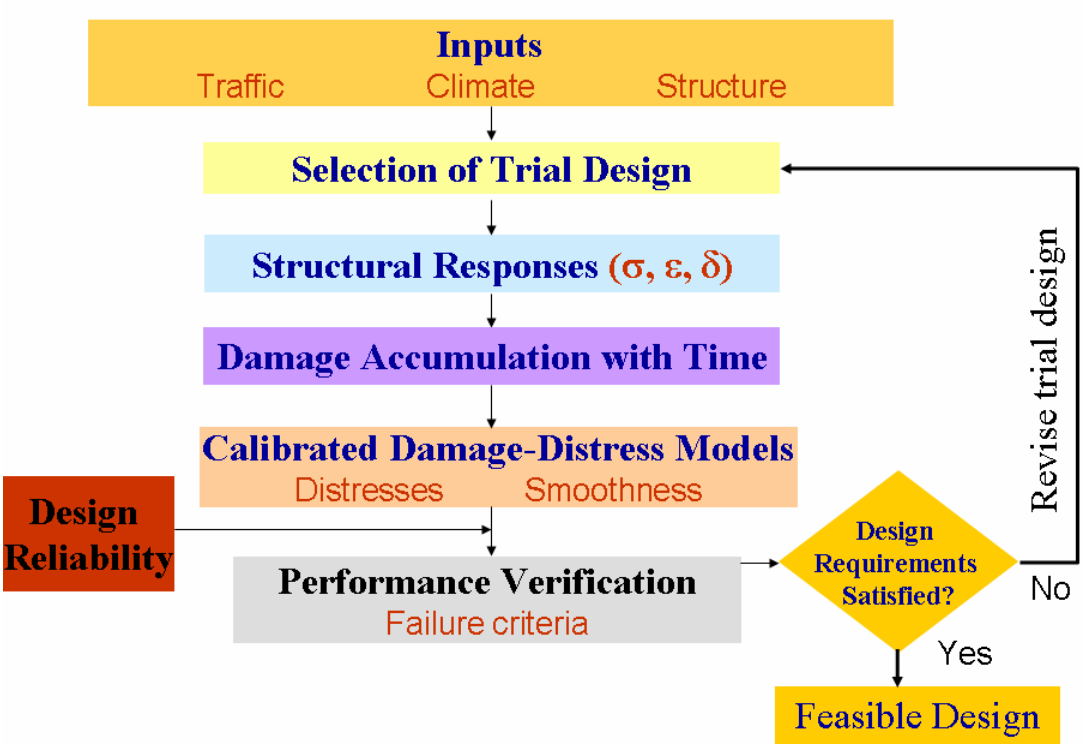

Figure 2.15 Flow chart explaining the three stage design process

For example, Kannekanti [7] found that MEPDG version 0.7 has reproducibility problems. This occurred when two input files containing the same data produced totally different outputs. Fortunately, in his study it was easy to identify such cases because they predicted 0% cracking when they were expected to crack substantially and there were very few such cases. He also reported some specific cases for which the models predict results that do not agree with accepted pavement knowledge. Other problems reported were PCC properties like

coefficient of thermal expansion are not changed automatically when the user changes aggregate type, making it a redundant variable, also the software occasionally crashes and needs to generally be more robust.

Guclu [8] in his JPCP sensitivity study for pavements in Iowa using version 0.7 found out that coefficient of thermal expansion and thermal conductivity were extremely sensitive to transverse cracking and sensitive to faulting. Similarly, Sunghwan [9] in his sensitivity study for flexible pavements in Iowa found out that heat capacity and thermal conductivity is less sensitive to cracking and rutting. All the previous studies were carried out using the older versions and the older version has significant software problems, very few data for determining the calibration constants and many more draw backs. The MEPDG version 1.0 was released in 2007 and it has been corrected for all the software bugs and also it includes more climate data for newer calibration constants. The present study is carried out using the version 1.0 MEPDG and since from the preliminary studies it has been found out that the thermal properties have an important role in the performance of the flexible and rigid pavements and since there are no significant studies on the effect of thermal properties of the pavement materials on the pavement performance, the main focus of this study is to identify the sensitivity of thermal input parameters needed to design the flexible and rigid pavements.

2.3 Thermal Properties of Pavement Materials

Mix Coefficient of Thermal Contraction (HMA)

There are no current American Association of State Highway and Transportation Officials (AASHTO) or ASTM standard tests for determining the coefficient of thermal contraction

(CTC) of HMA materials. The design guide computes CTC internally using the HMA volumetric properties and thermal contraction coefficient for the aggregates [2].

Coefficient of Thermal Expansion (PCC)

All materials expand and contract to some extent as their temperatures rise or fall. The coefficient of thermal expansion (CTE) is a measure of a material's expansion or contraction with temperature. Because the length changes associated with thermal expansion are very small, the CTE is usually expressed in microstrains per unit temperature change. The magnitude of curling stress (caused by differences in temperature through slab thickness) is very sensitive to CTE. Under certain exposure conditions, curling stresses comprise 50 percent or more of the critical stress experienced by a loaded slab and thus greatly affects slab cracking and CRCP punchouts [5]. Thus CTE plays an important role in optimizing JPCP joint design, CRCP reinforcement, and in accurately calculating pavement stresses and joint and crack load transfer efficiency over the design life which is critical to faulting.

Drying Shrinkage (PCC)

Drying shrinkage of hardened concrete is an important factor affecting the performance of PCC pavements. Drying shrinkage affects crack development in CRCP as well as long term performance of load transfer across the cracks. For JPCP, the principal affect of drying shrinkage is PCC warping caused by differential shrinkage due to through-thickness variation in moisture conditions leading to increases cracking susceptibility. For JPCP faulting, both slab warping and magnitude of shrinkage strains are important for joint opening [5]. Drying shrinkage related input in this guide is ultimate shrinkage strain which is measured in microstrains.

Surface Shortwave Absorptivity (HMA and PCC)

Surface shortwave absorptivity is the amount of available solar energy that is absorbed by the pavement surface. SSA of a given layer depends on its composition, color and texture. Generally lighter and more reflective surfaces tend to have lower SSA and viceversa. There are no current AASHTO standards for estimating the SSA of pavements.

Thermal Conductivity and Heat Capacity (HMA and PCC)

Thermal conductivity, K, is the quantity of heat that flows normally across a surface of unit area per unit of time and per unit of temperature gradient. In Asphalt concrete, the moisture content has an influence upon the thermal conductivity. Only when moisture content is high, does the thermal conductivity vary substantially [4]. Heat capacity is the actual amount of heat energy Q necessary to change the temperature of a unit mass by one degree. Thermal conductivity and heat capacity are key inputs in MEPDG and are used for estimating temperature and moisture profiles in the pavement structure and subgrade over the design life of a pavement and since these profiles are very important in performance predictions, these properties are very important for designing pavements.

Chapter 3 Sensitivity of Thermal Properties on Performance

3.1 Experiment Design

The very first part of this project involved extensive data collection. Two types of rigid pavement sections, Jointed Plain Concrete Pavement (JPCP) and Continuous Reinforced Concrete Pavement (CRCP) and one type of Hot Mix Asphalt (HMA) Pavement (Flexible Pavement) were selected. Some important thermal properties which affect the pavement design software were selected and the software was run for several factor levels for the selected properties. The variables selected for the rigid and flexible pavement sensitivity study and the factor levels used are shown in Table 3.1.

Table 3.1 Variables and factor levels used for sensitivity analysis

Type	Variable		Factor Levels
JPCP & CRCP	1	Co-efficient of Thermal Expansion	2×10^{-6}, 4×10^{-6}, 6×10^{-6}, 8×10^{-6}, 9×10^{-6} (Per F^0)
	2	Thermal Conductivity	0.2,0.5,1.0,1.5,2.0 ($BTU/hr-ft-F^0$)
	4	Heat Capacity	0.2,0.3,0.4,0.5 ($BTU/lb-F^0$)
	5	Surface Shortwave Absorptivity	0.5,0.6,0.7,0.8,0.9,1.0
	6	Drying Shrinkage	300,600,1000
HMA	1	Thermal Conductivity	0.5, 0.6, 0.7, 0.8, 0.9, 1.0 ($BTU/hr-ft-F^0$)
	2	Heat Capacity	0.2,0.3,0.4,0.5 ($BTU/lb-F^0$)
	3	Surface Shortwave Absorptivity	0.5,0.6,0.7,0.8,0.9,1.0
	4	Mix Co-efficient of Thermal Contraction	0.0001, 1e-005, 1e-006, 1e-007 (in/in/F^0)
	5	Air-Void Content	0 %, 8.5 %, 20%

All cases were run with a reliability level of 90% and a design life of 20 years. A detailed discussion of inputs and the source of inputs are presented in the next section. Level 1 inputs yield accurate results, but the inputs require lot of lab and field testing and consume more time and resources. Level 2 inputs are obtained from agency databases or estimated through correlations. Level 3 inputs are default values or typical averages for the project location and materials used. Since there are no known standard tests for some of the thermal properties, level 3 inputs are selected for the present study.

3.2 Traffic Inputs

Since the present study focuses on the effect of thermal properties on the pavement performance, default values for traffic have been selected. The MEPDG software requires the following inputs for the traffic. These default input values have been kept constant in each of the pavement types and sensitivity analysis to essentially look at the effect of only thermal properties of the pavement material.

3.2.1 Two-way Annual Average Daily Truck Traffic (AADTT)

Minneapolis, MN and Phoenix, AZ are urban locations, so an initial two way AADTT of 4563 is selected and an expected growth rate of 4 % is selected in the present study. The screen shots of the inputs used are shown in Appendix A.

3.2.2Traffic Volume Adjustment Factors

Traffic volume adjustment factors are used to determine AADTT within each hour of the day for each month and for each truck class. This determination requires the following:

• Hourly truck distribution factors

• Vehicle class distribution factors

• Monthly adjustment factors

Default values have been used for all these inputs. The screen shots of the inputs used are shown in Appendix A.

3.2.3 Axle Load Distribution Factors

Default values for the axle load distribution factors have been used for single axles, tandem axles, tridem axles, and quad axles. The screen shots of the inputs used are shown in Appendix A.

3.2.4 General Traffic Inputs

This category of inputs include information like mean wheel location, traffic wander standard deviation, design lane width, wheel base information, tire dimensions, and tire inflation pressures. Default values have been used for all of the general traffic inputs. The screen shots of the inputs used are shown in Appendix A. Other information in this category includes the number of axle types per truck class and axle configuration, which were obtained from WIM data and are also presented in Appendix A.

3.3 Climate

The Long-term Pavement Program (LTPP) subdivided the country into four environmental regions: Wet-Freeze, Wet-Nonfreeze, Dry-Freeze, and Dry-Nonfreeze as shown in Figure 3.1.Two different climatic stations, Minneapolis (Wet-Freeze) and Phoenix (Dry-Nonfreeze) have been selected for the present analysis. In MEPDG, all of the necessary climate information at any given location can be generated by simply selecting the weather station near the location of the pavement construction. All the three different pavement systems, namely, JPCP, CRCP and HMA pavements have been analyzed at each of these locations.

The idea behind two climatic zones is to see whether climatic conditions or the thermal properties play an important role in pavement performance prediction using MEPDG version 1.0.

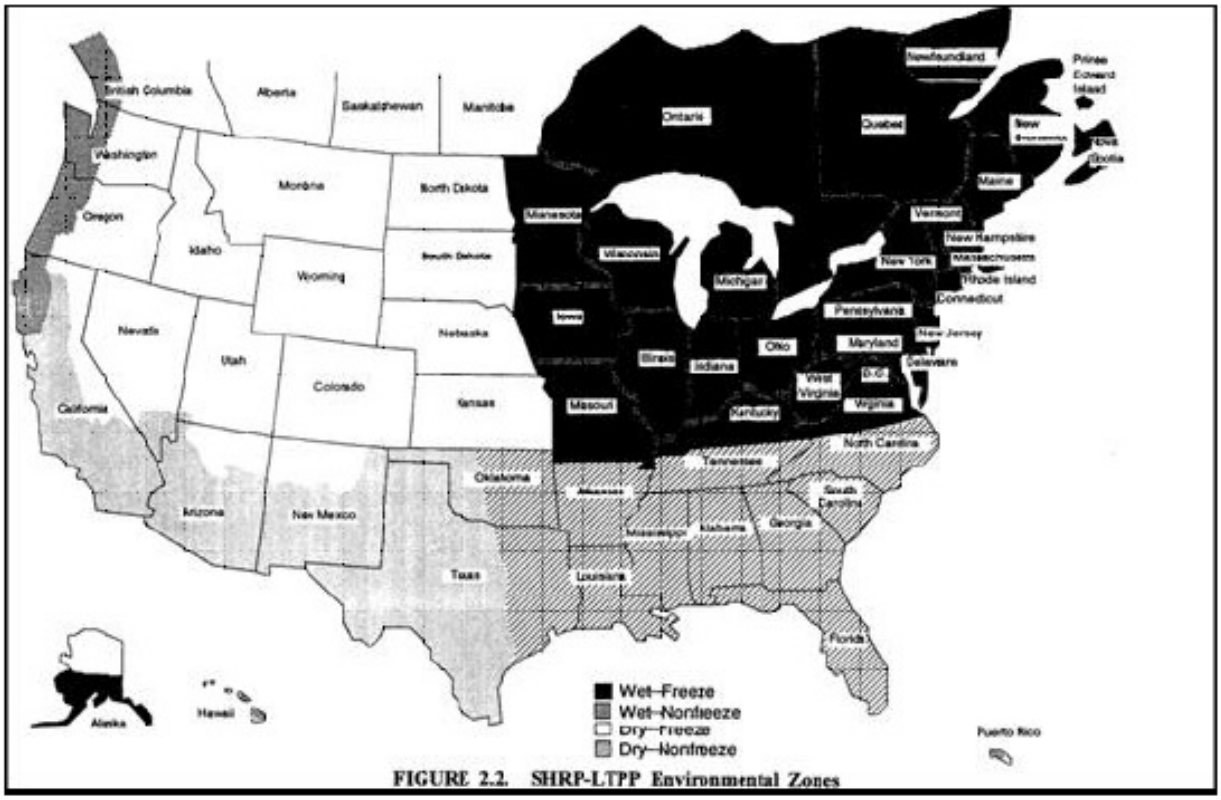

Figure 3.1 Climatic regions as defined by Long-Term Pavement Program (LTPP) [10]

The mean daily average temperature variation throughout the country is presented in Figure 3.2. Zone 1 exhibits the largest variation in temperature varying from less than 32°F to over 70°F, Zones 2, 5, and 6 exhibits a more modest variation in temperature, Zone 4 exhibits the least variation, and Zone 3 is the warmest. In the present study Minneapolis comes under zone 5 which exhibits modest variation and Phoenix comes under zone 1 which exhibits the

largest variation in temperature. Table 3.2 shows the differences in temperatures and precipitation for the two climate regions. One other climate input required for analysis is the depth of the water table. A default value of 10 ft is assumed for the two regions.

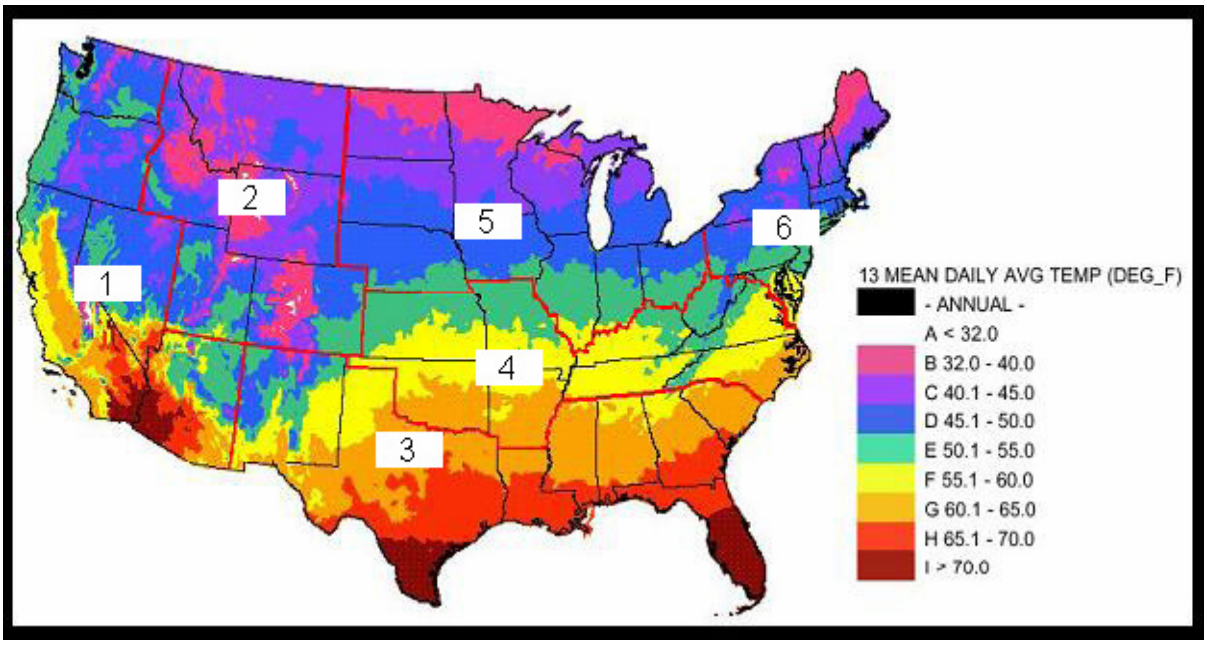

Figure 3.2 Mean daily average temperature [10].

Table 3.2 Annual average weather data for the two climate regions used in the study [10]

Weather Data\Climate Region	Minneapolis, MN	Phoenix, AZ
Mean Daily Average Temperature(^0F)	40-45	65-70
Mean Annual Snowfall, inches	45 to 60	5-6
Mean Yearly Precipitation, inches	28.32	7.66

3.4 Pavement Design Features

3.4.1 Rigid Pavement Features

JPCP design features include joint spacing, load transfer efficiency, and PCC-base interface. Default values for these features are selected and are shown in Table 3.3. A screen shot of the JPCP design features input window is shown in Appendix A.

Table 3.3 JPCP design features

Structure – Design Features	
Permanent curl/warp effective temperature difference (°F):	-10
Joint Design	
Joint spacing (ft):	15
Sealant type:	Liquid
Dowel diameter (in):	1
Dowel bar spacing (in):	12
Edge Support	None
Long-term LTE(%):	n/a
Widened Slab (ft):	n/a
Base Properties	
Base type:	Granular
Erodibility index:	Erosion Resistant (3)
PCC-Base Interface	Full friction contact
Loss of full friction (age in months):	245

CRCP design features include percentage steel use, steel diameter, steel depth, crack spacing and base properties. Default values for these features are selected and are shown in Table 3.4. A screen shot of the CRCP design features input window is shown in Appendix A.

Table 3.4 CRCP design features

Structure – Design Features	
Permanent curl/warp effective temperature difference (°F):	-10
Shoulder Type	Asphalt
Steel Reinforcement	
Percent steel (%):	0.7
Bar diameter (in):	0.625
Steel depth (in):	4
Base Properties	
Base type:	Granular
Base/slab friction coefficient:	2.5
Crack Spacing	
Cracking Model	Generate using model

3.4.2 Flexible Pavement Features

MEPDG default values are selected for the flexible pavement structure design features and the values are shown in Table 3.5. A screen shot of the HMA design features input window is shown in Appendix A.

Table 3.5 HMA design features

Structure-Design Features	
HMA E* Predictive Model:	NCHRP 1-37A viscosity based model.
HMA Rutting Model coefficients:	NCHRP 1-37A coefficients
Endurance Limit (microstrain):	None (0 microstrain)

3.5 Drainage and Surface Properties

This category of inputs includes surface shortwave absorptivity, infiltration, drainage path length, and pavement cross slope. Surface shortwave absorptivity is an important surface property which has been found to affect the performance of the pavements significantly. So

the present study focuses on the sensitivity of this property by varying it from 0.5 to 1.0 at 0.1 incremental intervals. Default values are used for drainage parameters.

3.6 Pavement Structure

3.6.1 Rigid Pavement

The assumed JPCP and CRCP pavement structure is a PCC slab of 10 inch thickness, 5 inches of crushed gravel base and A-5 subgrade. Figure 3.3 below shows the pavement structure used for the study.

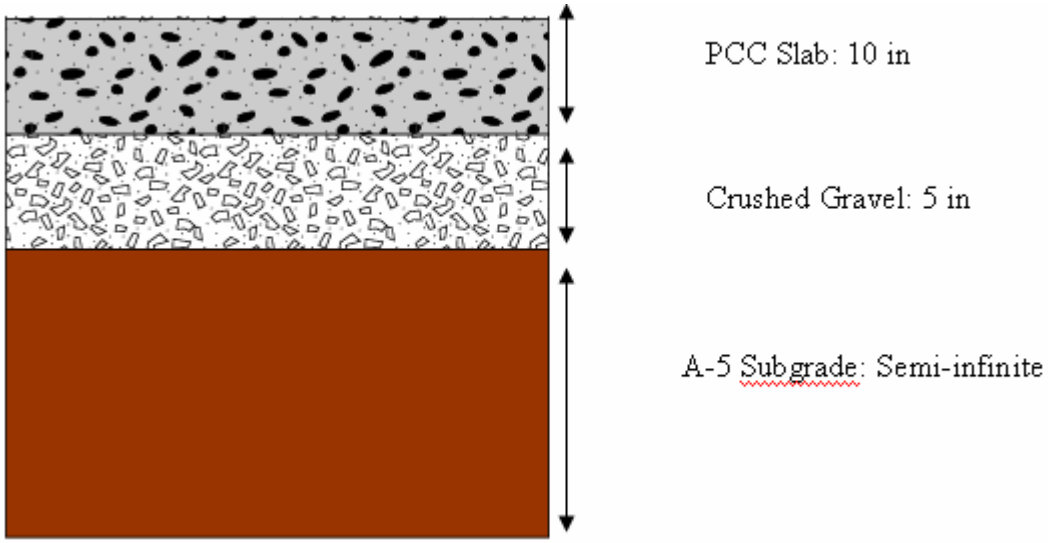

Figure 3.3 PCC pavement structure used in the sensitivity analysis

3.6.2 Flexible Pavement

The assumed HMA structure is an HMA layer of 4 inches, 6 inches of crushed stone base and A-5 subgrade. Figure 3.4 below shows the pavement structure used for the study. Even though the structure used is same in both the climate zones, the HMA binders used in Phoenix and Minneapolis are different.

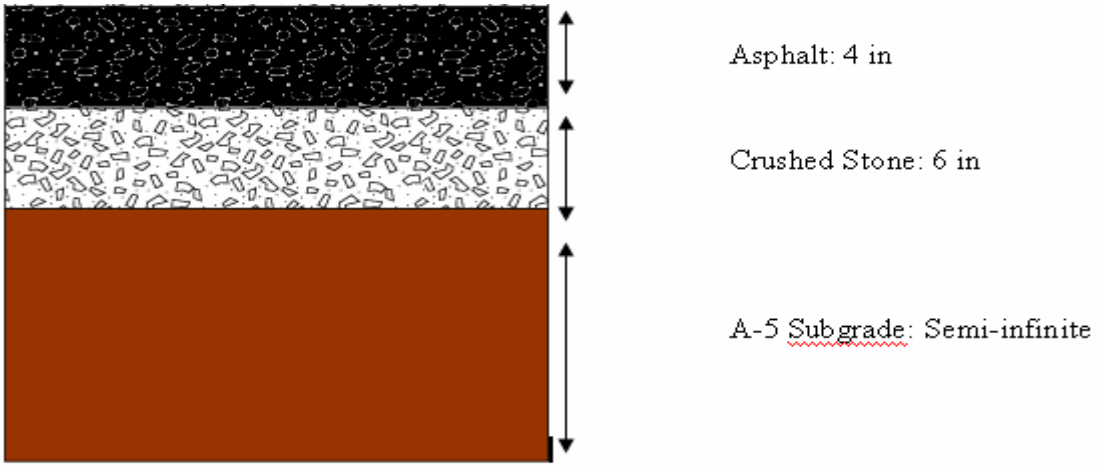

Figure 3.4 HMA pavement structure used in the sensitivity analysis

3.7 Layer Properties

3.7.1 Rigid Pavement Layer Properties

PCC Slab (CRCP & JPCP)

The unit weight of PCC used in both JPCP and CRCP is 150 pcf. Thermal properties and aggregate type were varied at different factor levels as shown in Table 3.1. Type I cement is used with a cement content of 600 lb/cu. yd. and a water-to-cement ratio of 0.42. Default values were used for shrinkage parameters. Level 3 input values were used for strength properties. Screen shots of the PCC thermal, mix, and strength input windows are shown in Appendix A.

Aggregate Base

Level 3 inputs for crushed gravel are used for the base properties. Modulus of 25,000 psi is assumed. Screen shots of base properties input windows are shown in Appendix A.

Subgrade

Level 3 inputs are used for the subgrade. Default modulus of 8,000 psi is assumed for A-5 subgrade. Screen shots of subgrade properties input windows are shown in Appendix A.

3.7.2 HMA Pavement Layer Properties

HMA Slab

The total unit weight of HMA used is 148 pcf. Superpave binders PG 58-22 and PG 70-10 are used for Minneapolis and Phoenix respectively. These binders are chosen according to the climatic conditions of the two locations. Thermal properties and air-void content of the HMA layer were varied at different factor levels as shown on Table 3.1. Screen shots of asphalt mix, binder and general properties (including aggregate gradation) input windows are shown in Appendix A for both the locations.

Aggregate Base

Level 3 inputs for crushed stone are used for the base properties. Modulus of 30,000 psi is assumed. Screen shots of base properties input windows are shown in Appendix A.

Subgrade

Level 3 inputs are used for the subgrade. Default modulus of 15,500 psi is assumed for A-5 subgrade. Screen shots of subgrade properties input windows are shown in Appendix A.

Chapter 4 Sensitivity Results

All the variables and factor levels in Table 3.1 were run using MEPDG Version1.0 software and the results loaded into a database. The software was run in batch mode for which the models for two different climatic stations need to be run separately.

Sensitivity analysis was initially carried out using Version 0.7 of MEPDG. After the official release of Version 1.0 of MEPDG, some sensitivity cases were re-run to see if there was significant difference in the results from Version 0.7 and Version 1.0 and it was evident that the results were significantly different because in the latest version, more bugs were fixed, more extensive data for climate and traffic were used for calculating the calibration constants. So all the sensitivity cases were re-run using the Version 1.0 and this chapter analyzes the results from Version 1.0.The results from the cases run enabled the isolation of the effect of various variables on rigid and flexible pavement performance prediction and are discussed in the following sections. In the plots presented in the following sections, the results from the cases were compared to the acceptable values for each of the performance predictions.

4.1 Effect of Variables on JPCP Performance

4.1.1 Effect of Variables on Transverse Cracking in JPCP

The transverse cracking model in MEPDG predicts transverse cracking as percent of slabs cracked. Jointed plain concrete pavements crack because of various parameters like traffic, climate, construction practices, nature of materials and several other reasons. The main objective of this section is to see the affect of thermal properties of the pavement materials on

cracking in JPCP. The effects of different variables in the sensitivity study on transverse cracking, as predicted by the MEPDG Version 1.0, are presented in the following sections.

Effect of Thermal Conductivity on Transverse Cracking

The results from the sensitivity analysis show a dramatic difference in cracking between structures with thermal conductivity of 0.2 BTU/hr-ft-0F versus 2.0 BTU/hr-ft-0F. Thermal conductivity of 0.2 BTU/hr-ft-0F is very detrimental to JPCP pavements .Figure 4.1 shows that JPCP mix with lower thermal conductivity, crack more compared to mix with higher thermal conductivity. Cracking at higher thermal conductivity is also below the acceptable cracking values. It also shows that at lower thermal conductivities, pavements in phoenix crack more when compared to pavements in Minneapolis for the same given thermal conductivity. This justifies the fact that, as thermal conductivity of a mix decreases, its ability to conduct heat in to the pavement decreases and since phoenix has more number of days with sun radiation exposure when compared to Minneapolis, the pavements in phoenix get more hotter and at low thermal conductivities the upper surface of the pavement becomes more hotter making it vulnerable to cracking.

Effect of Heat Capacity on Transverse Cracking

The allowable range for heat capacity of a PCC mix in MEPDG is from 0.1 BTU/lb-0F to 0.5 BTU/lb-0F. MEPDG failed to run stating stability problems with a heat capacity value of 0.1 BTU/lb-0F. So the heat capacity was varied from 0.2 to 0.5 BTU/lb-0F. Figure 4.2 shows the effect of heat capacity on cracking. Heat capacity does not have much effect on cracking. Even though pavements cracked, these values are well below the acceptable cracking values. Pavements in Phoenix cracked a little more when compared to pavements in Minneapolis.

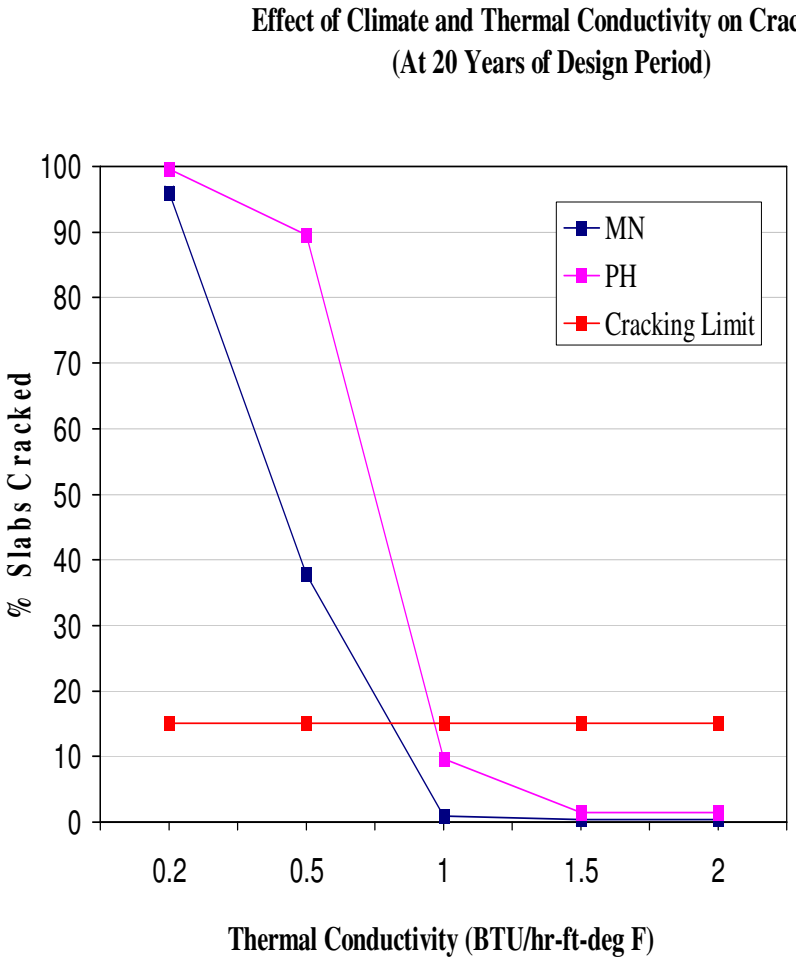

Figure 4.1 Effect of thermal conductivity on JPCP transverse cracking

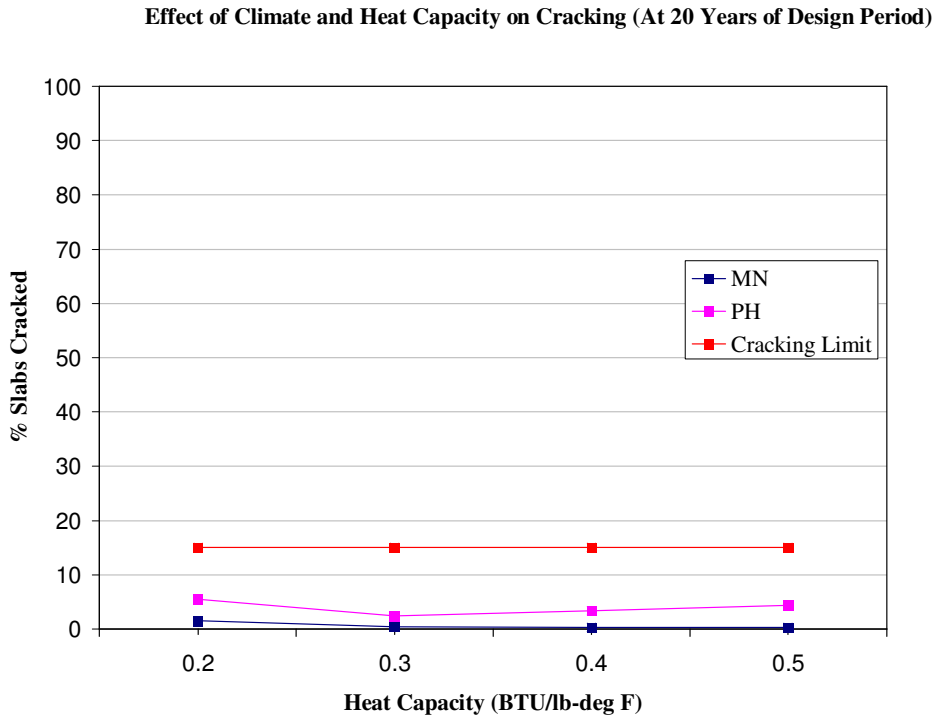

Figure 4.2 Effect of heat capacity on JPCP transverse cracking

Effect of Co-efficient of Thermal Expansion (CTE) on Transverse Cracking

The allowable range for CTE of PCC mix in MEPDG is from 2×10^{-6} /^{0}F to 10×10^{-6} /^{0}F. Figure 4.3 shows that CTE of PCC mix significantly affects cracking and higher the CTE, higher is the percent slabs cracked. Cracking at lower CTE is approximately zero and as CTE increases, cracking increases beyond acceptable cracking values. A CTE value of 10×10^{-6} /^{0}F is very detrimental to pavements. The plot shows that climate also plays an important role and pavements in phoenix crack more compared to pavements in Minneapolis for the same CTE value and higher CTE has more affect in phoenix than Minneapolis. The above conclusions can be explained through curling behavior of concrete pavements which basically depend on temperature gradients and material thermal properties.

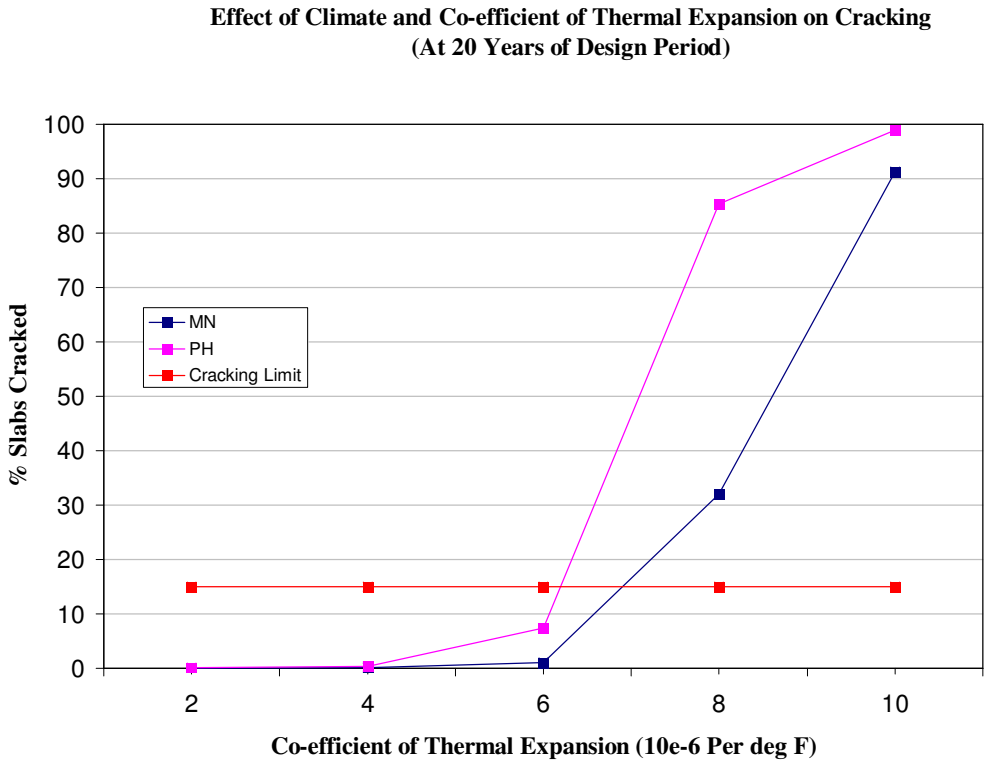

Figure 4.3 Effect of CTE on JPCP transverse cracking

The PCC pavement response to temperature differences through the slab thickness has been recognized as curling. As shown in Figure 4.4, a positive temperature difference between the top and the bottom surfaces of the concrete slab during daytime causes the slab corners to curl downwards, while a negative temperature difference during nighttime results in the upward curling of slab corners. For the same temperature gradient through PCC slab, the curling behavior increases as the CTE value of the PCC mix increases leading to more curvature. Because self weight of the slab resists slab curling and because other factors cause the slab to curl upward, actual voids do no exist beneath the center of the slab [5]. However, any forces (including self weight) that restrain free slab movements cause stress, and in

downward curling case, the restraint to slab curling results in increased tensile stress at the slab bottom. Under traffic loads, any actual loss of support due to temperature differences further increases the critical tensile stresses at the slab bottom. In upward curling case, it is equivalent to having voids beneath the edges of the slab, which when combined with traffic load, increases tensile stress at the top that can lead to fatigue cracking initiating from top down. These stresses when combined with increase in CTE leads to significant cracking.

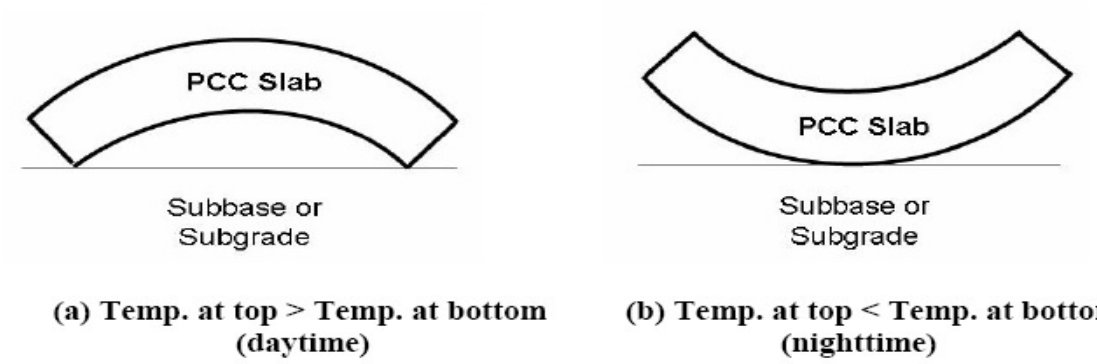

Figure 4.4 Typical curling behavior [11]

Effect of Surface Shortwave Absorptivity (SSA) on Transverse Cracking

As seen from Figure 4.5, as SSA increases, cracking increases in Phoenix and SSA has no affect on cracking in Minneapolis. The above result is in agreement with the actual definition of SSA which is defined as the amount of solar radiation absorbed by the pavement surface. Thermo technologies [12] quotes annual average total solar radiation for Pheonix to be 5,694,742 BTU's per square meter and for Minneapolis it is 3,613,690 BTU's per square meter. So clearly phoenix pavements are exposed to more radiation compared to Minneapolis

pavements. And hence the result is logical. But since the distress is well below the acceptable value, one can conclude that SSA is insensitive to cracking in JPCP.

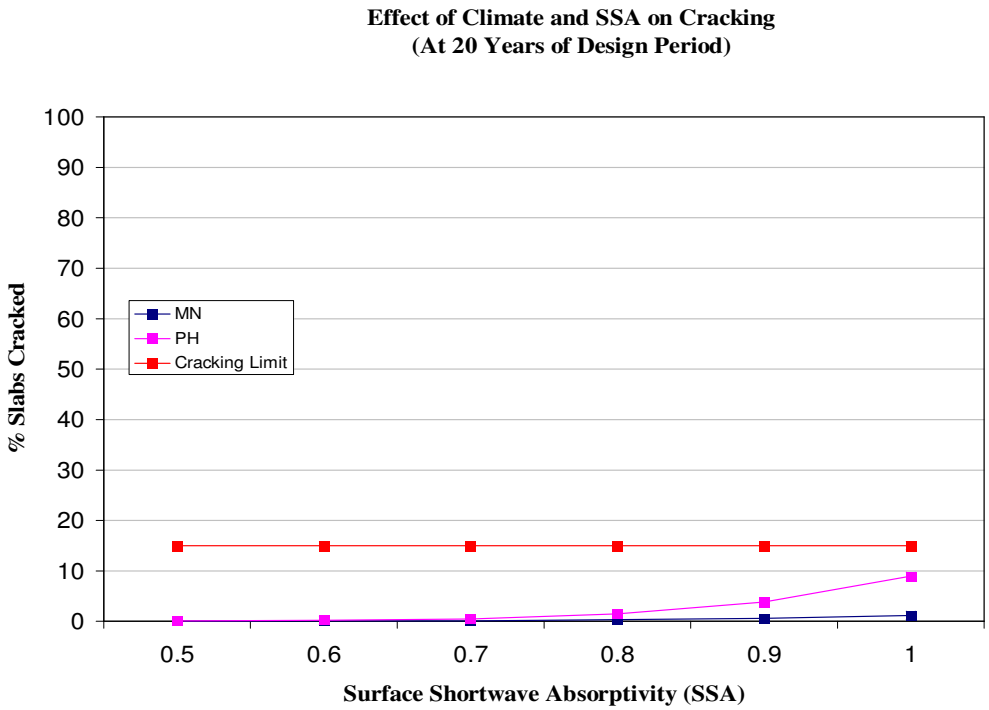

Figure 4.5 Effect of SSA on JPCP transverse cracking

Effect of Ultimate Shrinkage on Transverse Cracking

As seen from Figure 4.6, as ultimate shrinkage increases, according to MEPDG, there is no effect on transverse cracking which seems unreasonable. As ultimate shrinkage strain increases, PCC slab warping (explained in detail below) also increases leading to more cracking. The moisture gradient through the depth of PCC affects the reversible shrinkage which is recognized as warping. The moisture gradient is influenced by the daily and

seasonal weather conditions and the pavement material, such as permeable base and poor drainage soils [13].

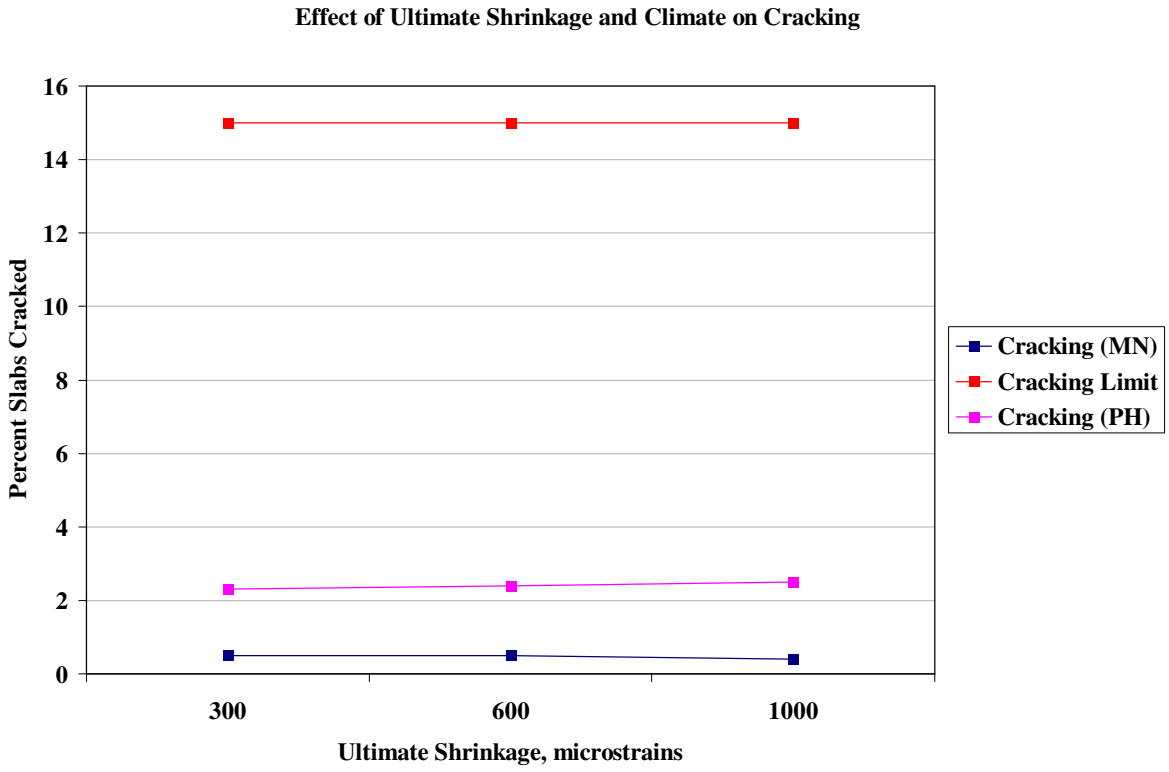

Figure 4.6 Effect of ultimate shrinkage strain on JPCP transverse cracking

As shown in Figure 4.7, a positive moisture difference between the top and the bottom surfaces of the concrete slab causes the slab corners to warp downwards while a negative moisture difference results in the upward warp of PCC slab. However, even in very dry area, the surface of the slab is typically only partially saturated while the bottom is usually completely saturated [14]. Therefore, upward warp of PCC slab caused by negative moisture difference, as shown in Figure 4.7(b), is usually more obvious than the downward warp as

shown in Figure 4.7(a). As the negative moisture difference increases combined with increase in ultimate shrinkage (in the present case, phoenix is more dry and Minneapolis is more wet) upward warping also increases leading to more distress in Phoenix compared to Minneapolis. Even though MEPDG is able to capture the effect of climate, it's not able to capture the shrinkage effect which seems like an anomaly.

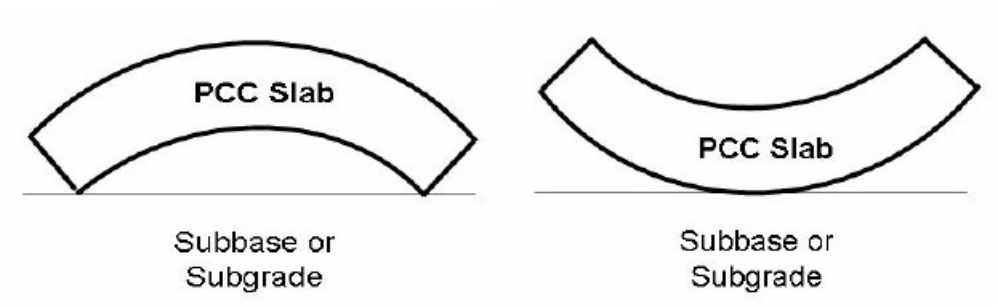

(a) Moisture at top > moisture at bottom **(b) Moisture at top < moisture at bottom**

Figure 4.7 Typical warping behavior [11]

Relative Effect of All Variables on Transverse Cracking

Six different variables have been used for the sensitivity analysis to analyze the affect of these variables on transverse cracking. Figure 4.8 summarize the effect of all these different variables on transverse cracking and their relative importance in controlling cracking. The plot shows the cracking at the end of 20 years of design life for each factor level of all the variables. Among the variables that a designer can control co-efficient of thermal expansion and thermal conductivity have significant effect on transverse cracking.

It can be seen from Figure 4.8 that co-efficient of thermal expansion and thermal conductivity affect transverse cracking the most compared to other variables. And also the

damage caused by other parameters other than CTE and thermal conductivity are well within the accepted cracking value of 10%. One more important conclusion that can be drawn is that cracking due to all the thermal parameters is more in Phoenix when compared to Minneapolis. In general, model predictions for different factor levels of all the variables agree with prevailing knowledge in pavement engineering.

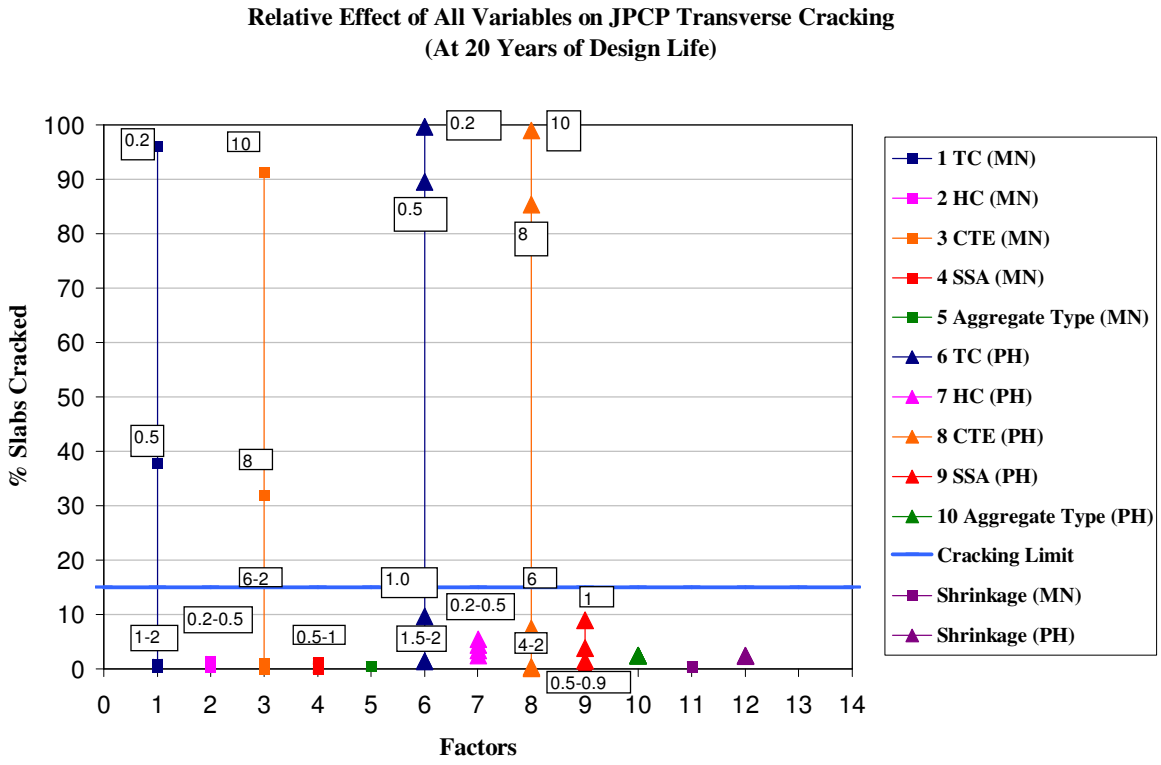

Figure 4.8 Relative effect of all variables on JPCP transverse cracking

4.1.2 Effect of Variables on Faulting

Faulting as defined in the first chapter is the differential deflection across a transverse joint and the acceptable faulting value implemented in the present study is 0.12 inches. The

development of faulting is often attributed to a combination of repeated heavy axle loads, insufficient load transfer between the adjacent slabs, free moisture in the pavement structure, and erodible base or subgrade material [5]. In the present section, the effect of thermal properties of PCC mix, subgrade type and load transfer efficiency on faulting is presented.

Effect of Thermal Conductivity on Faulting

It should be noted from the Figure 4.9 that for all thermal conductivity values of the PCC mix, the faulting is above the acceptable faulting value. This shows that thermal conductivity significantly affects faulting in JPCP's. It is evident from the figure that as thermal conductivity of the PCC mix increases, the faulting of the transverse joints decreases significantly. And also faulting in Minneapolis is more compared to faulting in Phoenix. So according to MEPDG, lower thermal conductivity of PCC mix is detrimental to pavements.

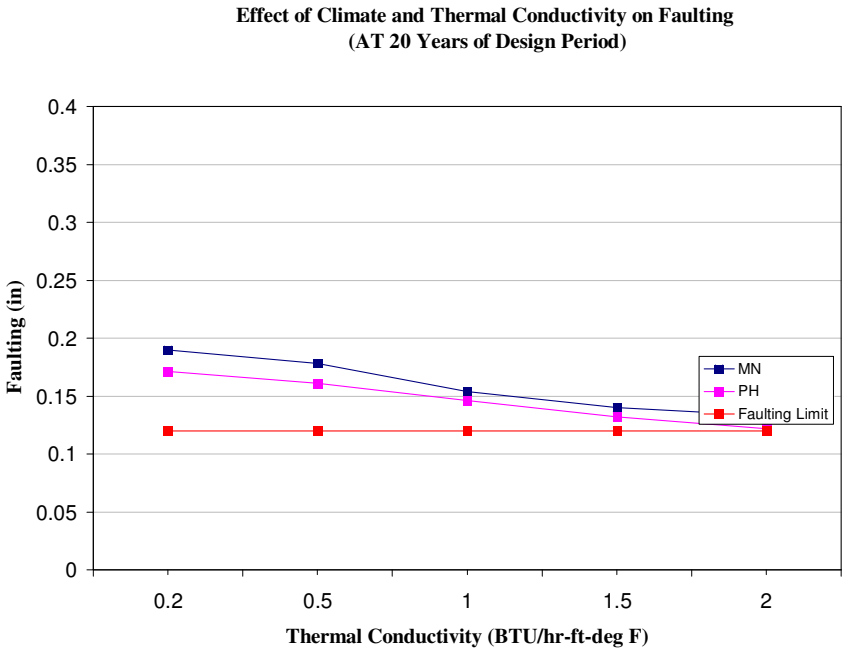

Figure 4.9 Effect of thermal conductivity on faulting

Effect of Heat Capacity on Faulting

As seen from the Figure 4.10, for all the heat capacities of PCC mix, the faulting is above the acceptable faulting value making it a significant factor in pavement performance prediction. As the heat capacity of PCC mix increases one can see that there is not much difference in faulting prediction, so according to MEPDG, heat capacity is not sensitive to faulting in JPCP's.

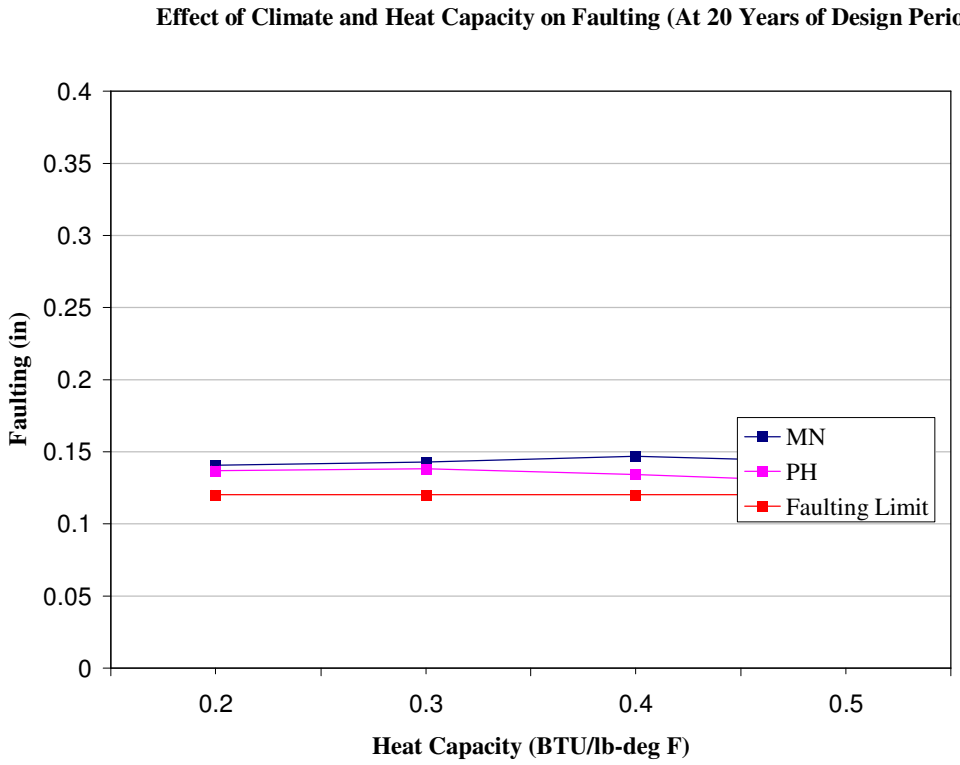

Figure 4.10 Effect of heat capacity on faulting

Effect of Co-efficient of Thermal Expansion (CTE) on Faulting

CTE as seen from the Figure 4.11 significantly affects faulting in JPCP's. As CTE of PCC mix increases faulting in JPCP's increases dramatically making it the most sensitive parameter which affects faulting. At lower CTE values the faulting is well below the acceptable faulting values and as CTE increases faulting increases above the acceptable values. At higher CTE values, faulting in Minneapolis is more compared to faulting in Phoenix.

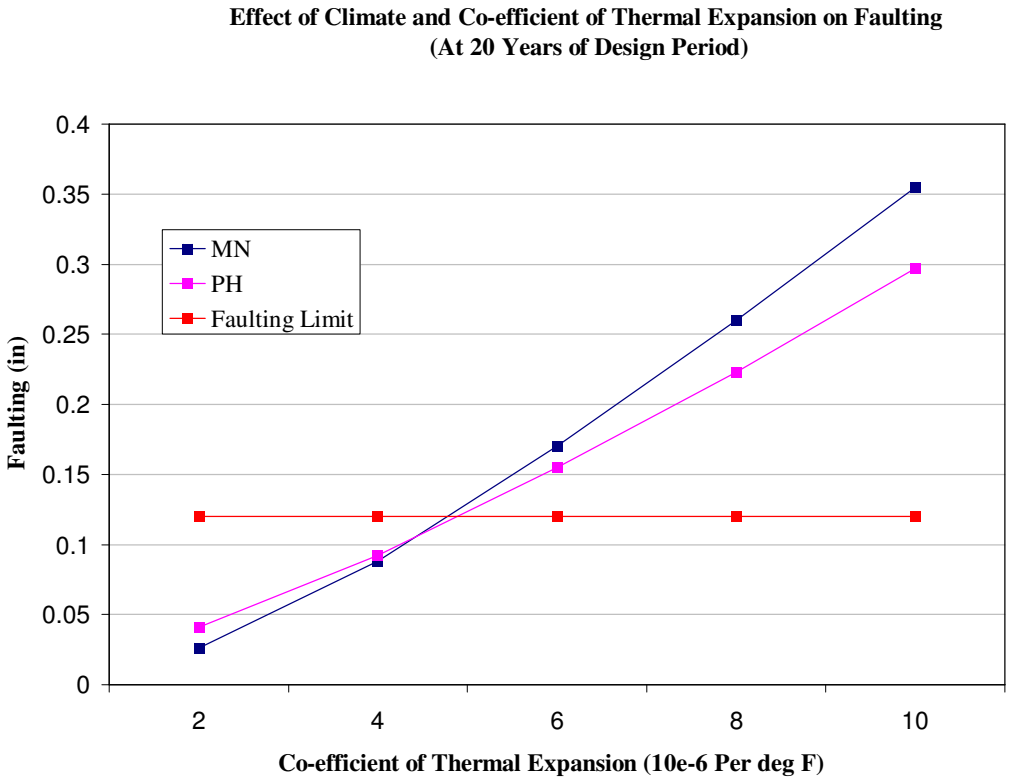

Figure 4.11 Effect of CTE on faulting

Effect of Surface Shortwave Absorptivity (SSA) on Faulting

As SSA increases, faulting of JPCP's also increases. As seen in the Figure 4.12, for all SSA's the faulting predicted is above the acceptable faulting values and hence SSA is an important design factor. The conclusion compliments the fact that as SSA increases, the ability of the pavements to absorb more sun radiation also increases making the pavements more vulnerable to faulting.

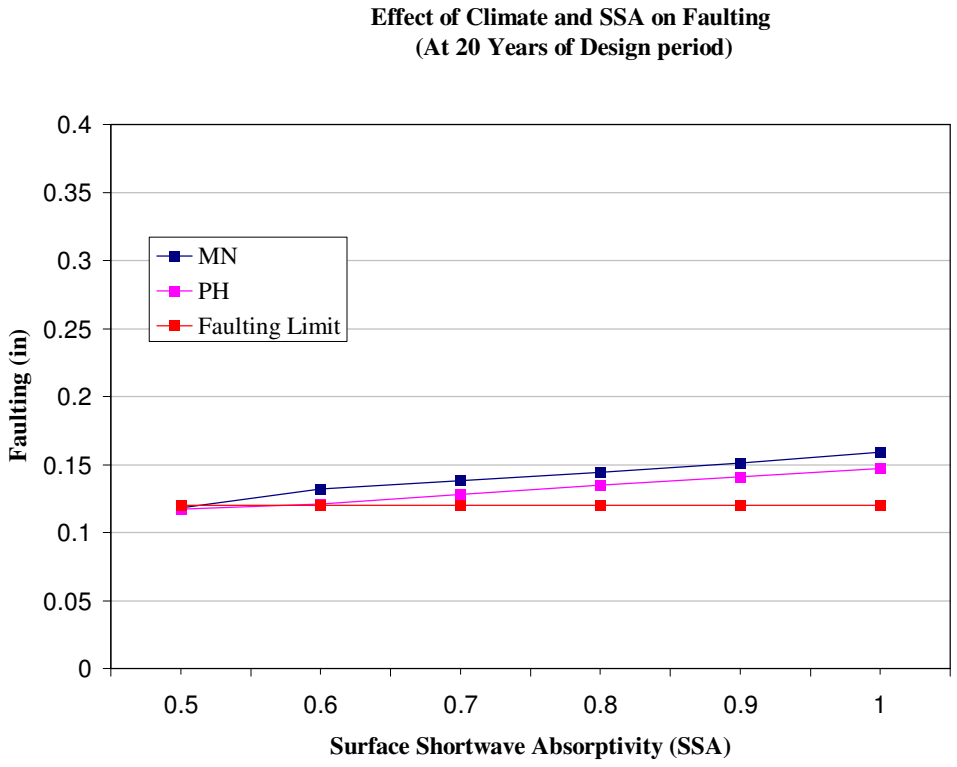

Figure 4.12 Effect of SSA on faulting

Effect of Ultimate Shrinkage on Faulting

As ultimate shrinkage strain increases, faulting of the slabs also increases as seen in Figure 4.13. As shrinkage increases, warping of the PCC slab and the JPCP joint opening increases leading to more faulting.

Relative Effect of All Variables on Faulting

Eight different variables have been considered for the sensitivity analysis. They are thermal conductivity, heat capacity, co-efficient of thermal expansion, ultimate shrinkage, surface shortwave absorptivity, aggregate type, subgrade type and doweled/undoweled joints. Previous studies have shown that faulting is mainly controlled by dowels [7]. Very few or no studies have evaluated the effect of thermal properties on faulting. So this section analyzes the relative effect of thermal properties and other parameters on faulting.

According to MEPDG, from Figure 4.14 one can conclude that co-efficient of thermal expansion of PCC mix effects faulting the most compared to any other variable making it the most sensitive parameter for faulting and most important design variable. As seen from the plot, lower CTE values tend to perform better and should be considered in the design of pavements. The second most sensitive variables which effect faulting are thermal conductivity of PCC mix and dowels. Both these variables seem to effect the faulting at the same sensitivity level. Third most sensitive parameter is surface shortwave absorptivity. The least sensitive of all the variables is heat capacity, subgrade type and shrinkage strains.

Climate also played an important role in the sensitivity analysis and it is seen that pavements in Minneapolis have more faulting compared to pavements in Phoenix and this can be attributed to availability of more free moisture in Minneapolis. When excess moisture exists in a pavement with an erodible base or underlying fine-grained subgrade material, repeated

vehicle loadings typically cause the mixture of water and fine material (fines) to be removed from beneath the leave slab corner and ejected to the surface through the transverse joint or along the shoulder. This process, commonly referred to as pumping, will eventually result in a void below the leave slab corner. In addition, some of the fines that are not ejected will be deposited under the approach slab corner, causing the approach slab to rise. This combination of a buildup of material beneath the approach corner and the loss of support resulting from a void under the leave corner can lead to significant faulting at the joint (especially for JPCP without dowels) [15] Hence pavements in Minneapolis have more faulting.

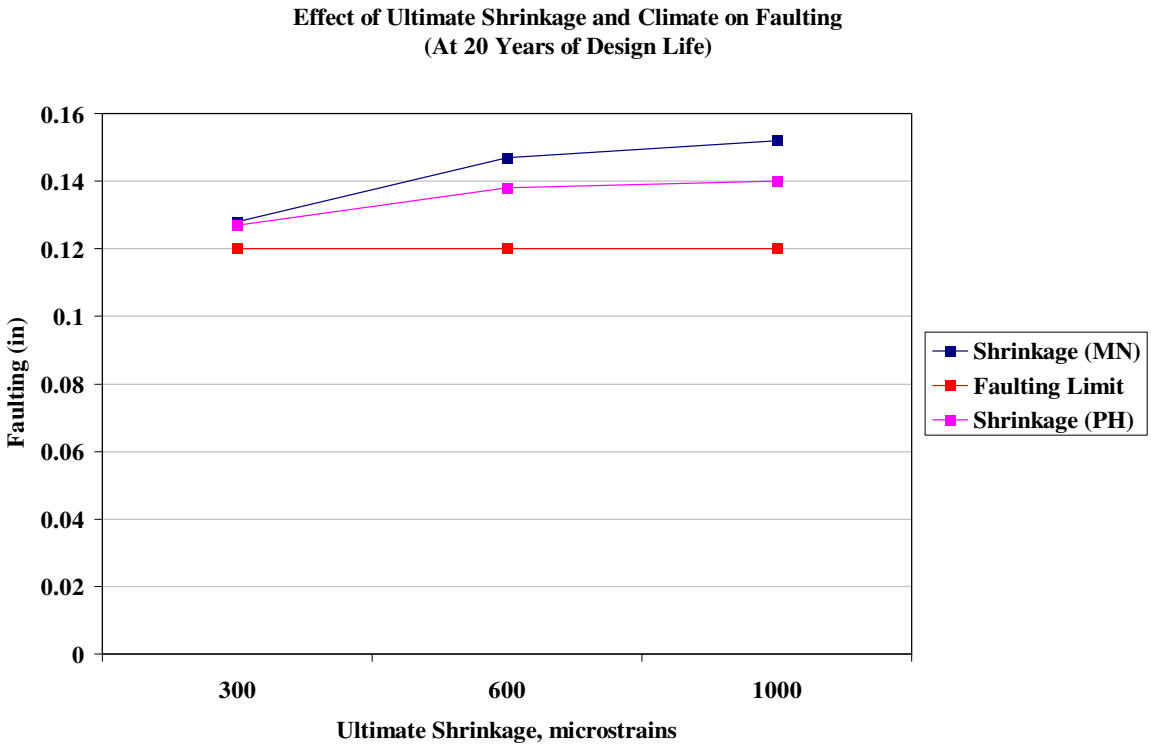

Figure 4.13 Effect of ultimate shrinkage strain on faulting

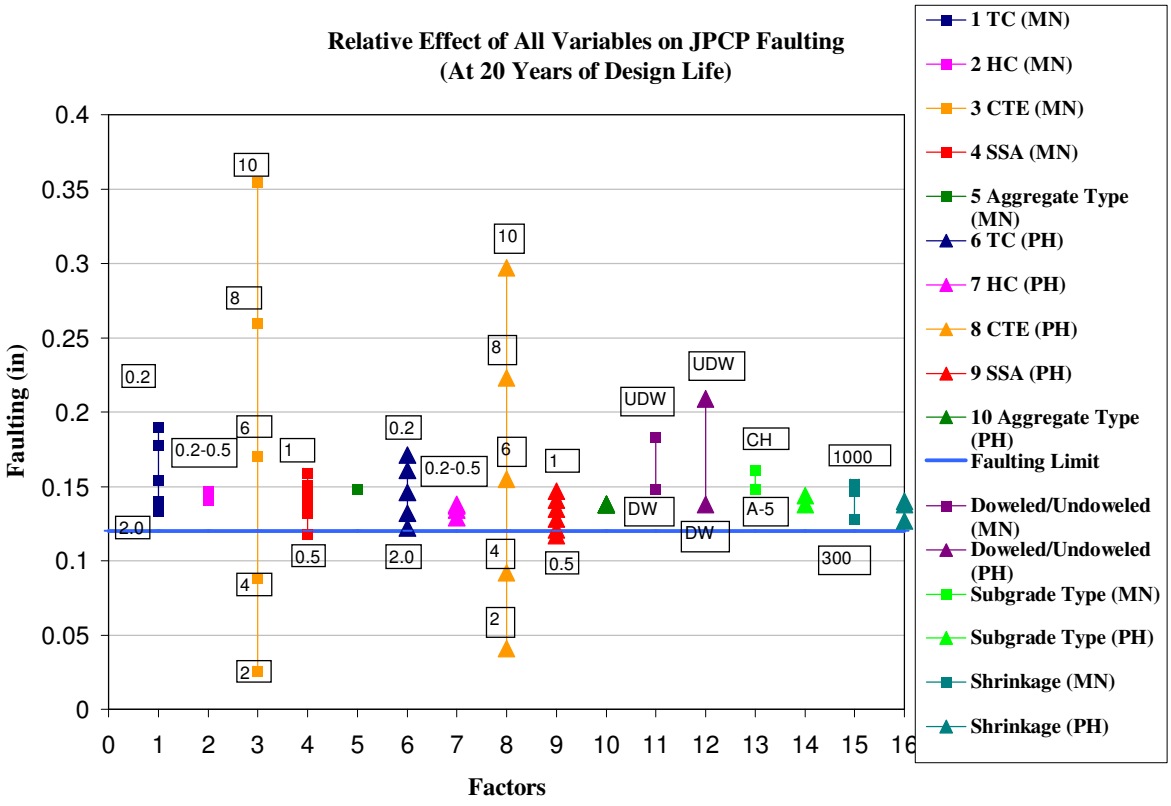

Figure 4.14 Relative effect of all variables on faulting

4.1.3 Effect of Variables on IRI (Smoothness)

Road smoothness can be defined as "the variation in surface elevation that induces vibrations in traversing vehicles." [16] Although there are various methods for measuring the smoothness of pavements, one of the most common indices used today is the International Roughness Index (IRI). A lower value of IRI indicates a smoother pavement

Effect of Thermal Conductivity on IRI

As seen from Figure 4.15, as thermal conductivity increases IRI decreases. For lower thermal conductivities, IRI values are above the acceptable values making lower thermal conductivities detrimental to pavements.

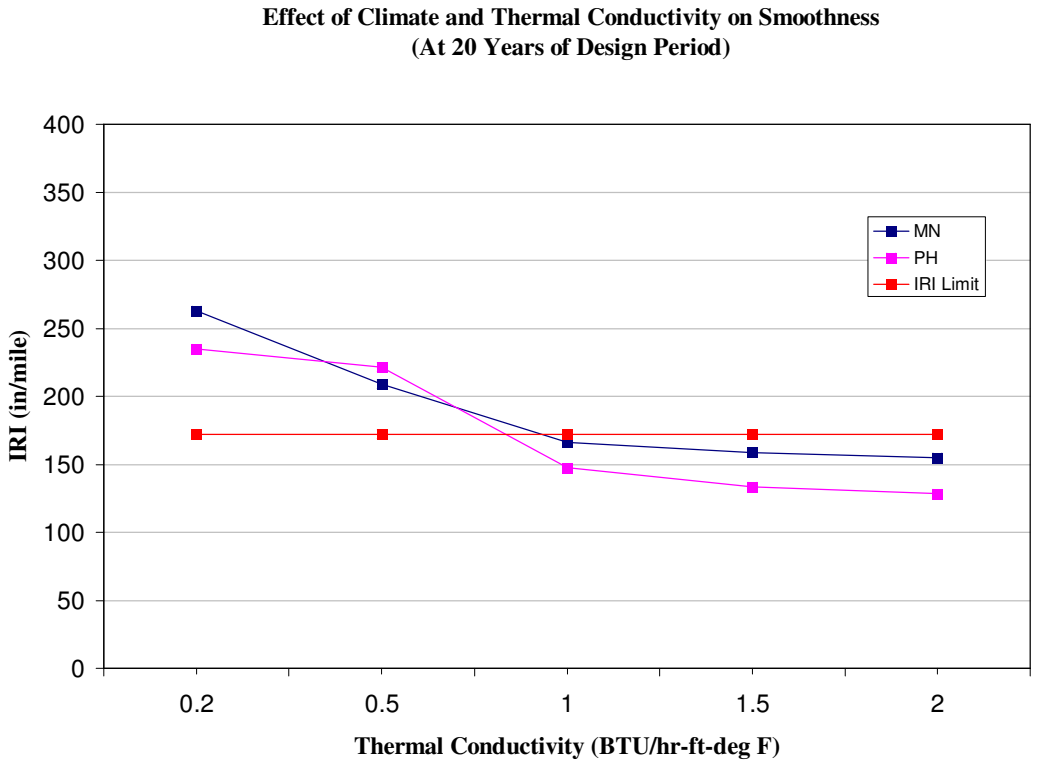

Figure 4.15 Effect of thermal conductivity on IRI

Effect of Heat Capacity on IRI

As seen from Figure 4.16, heat capacity of PCC mix has little or no effect on IRI making it insensitive. Also, the IRI predictions for all heat capacities are well below the acceptable IRI values making heat capacity a redundant variable for IRI prediction.

Effect of Co-efficient of Thermal Expansion on IRI

It was concluded from the previous sections that as CTE increases faulting and cracking increases, damaging the pavements, making them noisier and hence IRI also increases as CTE increases and this is effectively predicted by MEPDG as shown in the Figure 4.17 below.

Effect of Surface Shortwave Absorptivity (SSA) on IRI

As seen in Figure 4.18, SSA has little or no effect of IRI. And also the IRI predicted for all SSA's are well below the acceptable IRI values making it a redundant variable for IRI prediction.

Effect of Ultimate Shrinkage on IRI

As shrinkage strains increases, IRI also increases but these values are well below the acceptable values and hence IRI is insensitive to shrinkage strains as shown in Figure 4.19.

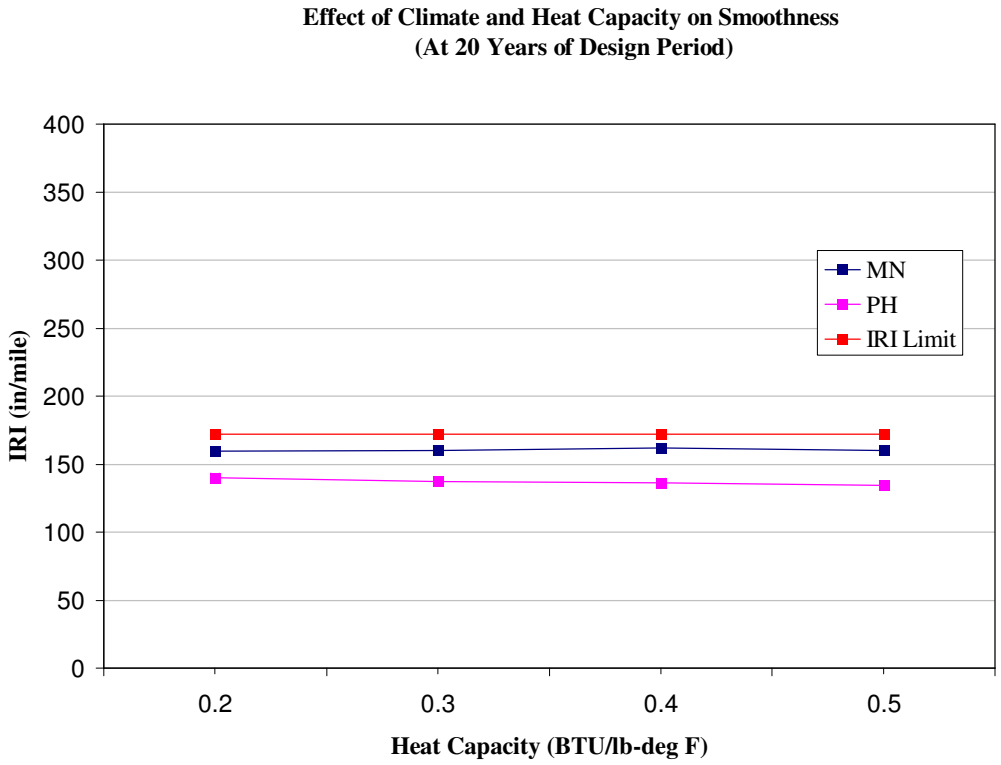

Figure 4.16 Effect of heat capacity on IRI

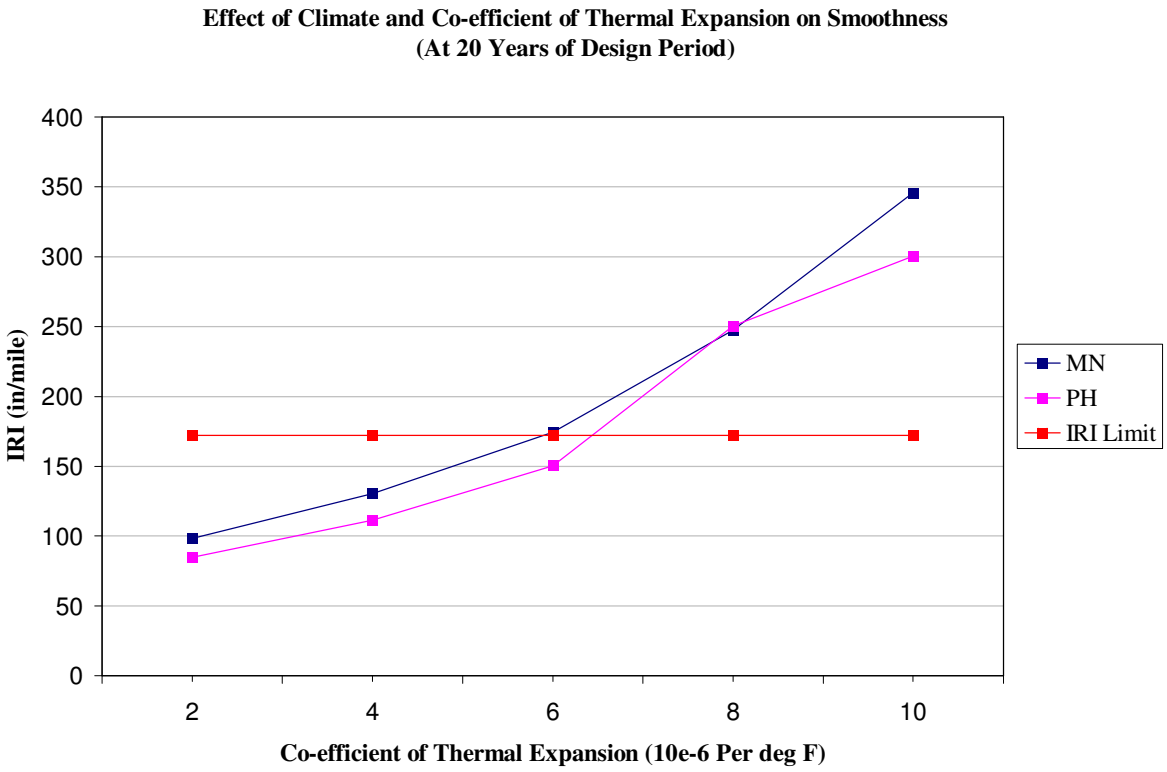

Figure 4.17 Effect of CTE on IRI

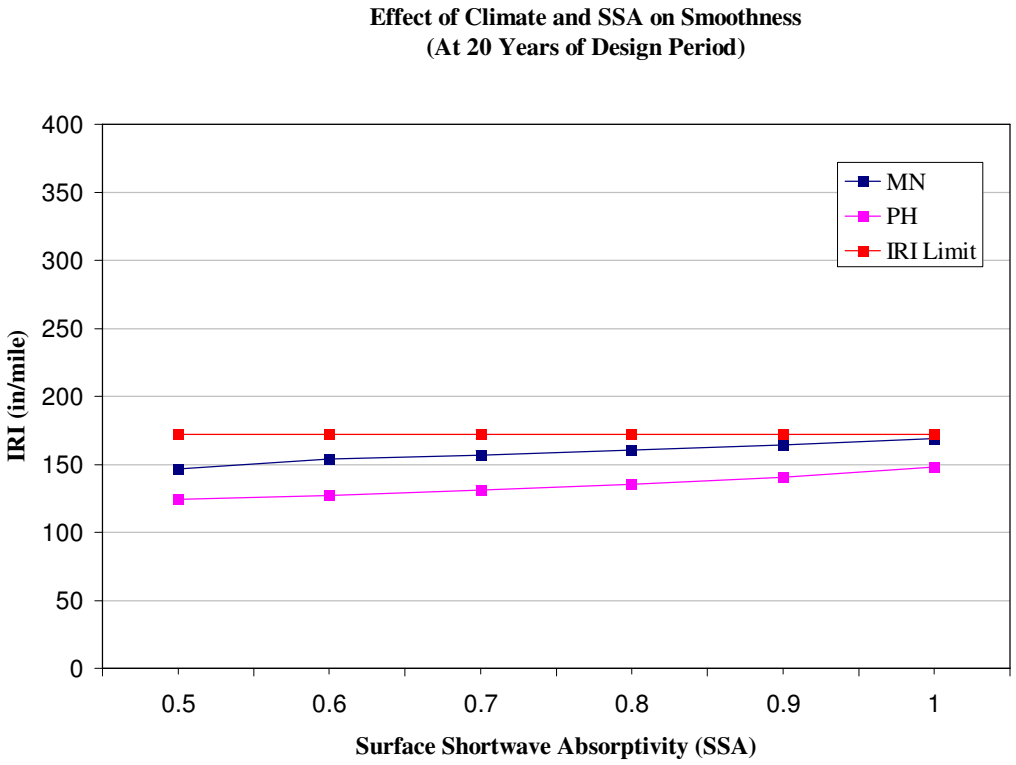

Figure 4.18 Effect of SSA on IRI

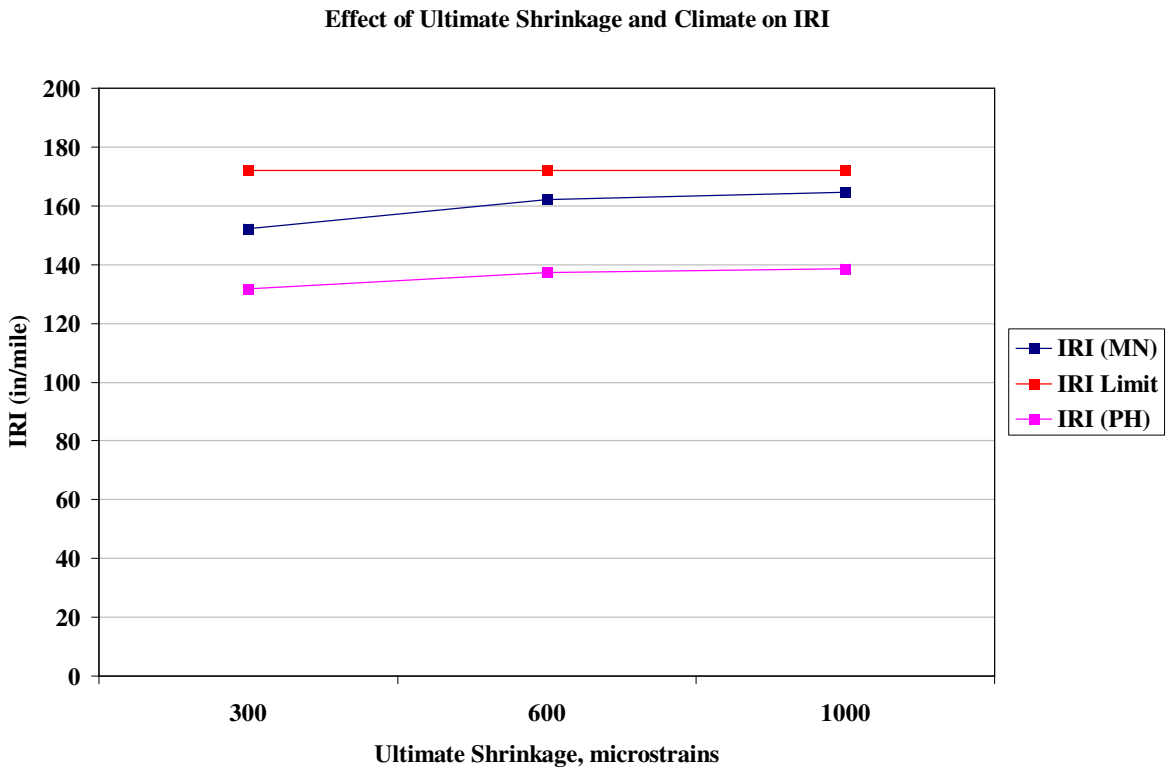

Figure 4.19 Effect of ultimate shrinkage strain on IRI

Relative Effect of All Variables on IRI

As seen from the Figure 4.20, according to MEPDG, CTE is the most sensitive parameter which effects IRI. Thermal conductivity is the second most sensitive parameter. Other variables are either less sensitive or insensitive to IRI predictions. Also climate played a sensitive role in IRI prediction, with Minneapolis having more rough roads compared to Phoenix for the same fixed input variable.

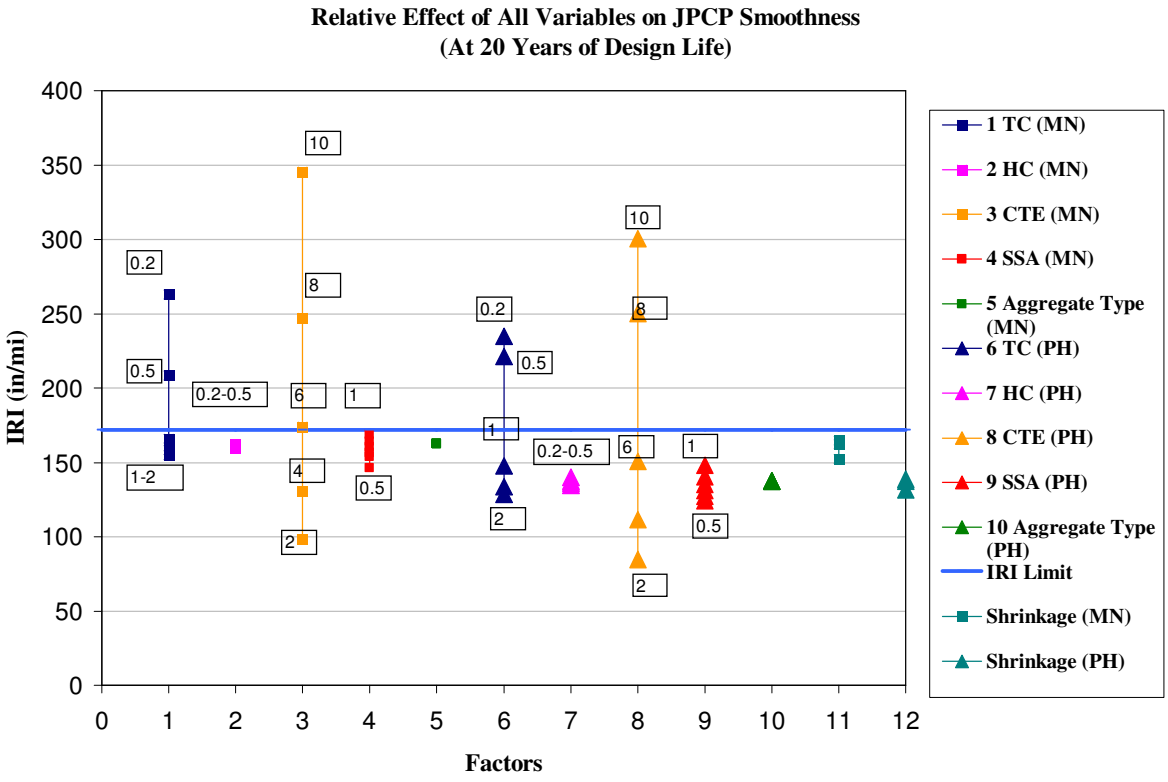

Figure 4.20 Relative effect of all variables on IRI

4.2 Effect of Variables on CRCP Performance

4.2.1 Effect of Variables on Punchouts

The causes and factors associated with CRCP punchouts have been the topic of many investigations. One of the first studies by LaCourserie and Darter [17, 18] in 1977 describes the mechanism of edge punchout based on the field investigations of punchout distress in CRCP in Illinois. This study showed the development of high tensile stress at the top of the slab about 1-2 m from the longitudinal edge of the slab as a result of poor load transfer at the surrounding transverse cracks. Crack spacing has also been shown to significantly affect the magnitude of the critical tensile lateral stresses on the top of the slab. Zollinger et al. [19]

reported that punchouts in field studies were invariably accompanied by severe base erosion and loss of support. However, there are no studies which show the effect of thermal properties of PCC mix on CRCP punchouts. The present section focuses on the effect of each of the thermal property on punchouts and the relative effect of all the variables on punchouts.

Effect of Thermal Conductivity on Punchouts

For any given thermal conductivity, the distress predicted is well above the acceptable punchout value. It can also be seen from Figure 4.21 that as thermal conductivity increases, CRCP punchouts in Minneapolis increases where as they remain constant in Phoenix.

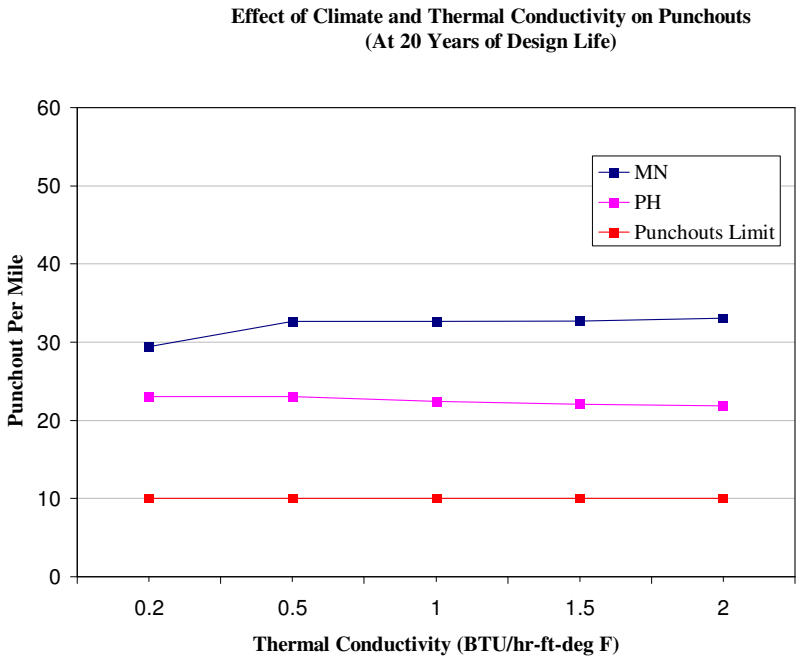

Figure 4.21 Effect of thermal conductivity on punchouts per mile

Effect of Heat Capacity on Punchouts

It is seen from the Figure 4.22 that as heat capacity increases, punchouts per mile remain constant making heat capacity insensitive to punchouts.

Effect of Co-efficient of Thermal Expansion on Punchouts

As seen from the Figure 4.23, as CTE increases punchouts also increases. This behavior is similar to the behavior which has been explained in the case of cracking. As CTE increases, pavements expand more leading to more curling of the slabs. Hence, it leads to more transverse cracks and punchouts.

Effect of Surface Shortwave Absorptivity on Punchouts

From Figure 4.24, as SSA increases, punchouts in Minneapolis decrease whereas in Phoneix they remain constant.

Effect of Ultimate Shrinkage on Punchouts

From Figure 4.25, as ultimate shrinkage strains increases, punchouts also increases dramatically. This is expected because as shrinkage strains increase, transverse cracks in CRCP increases leading to more punchouts.

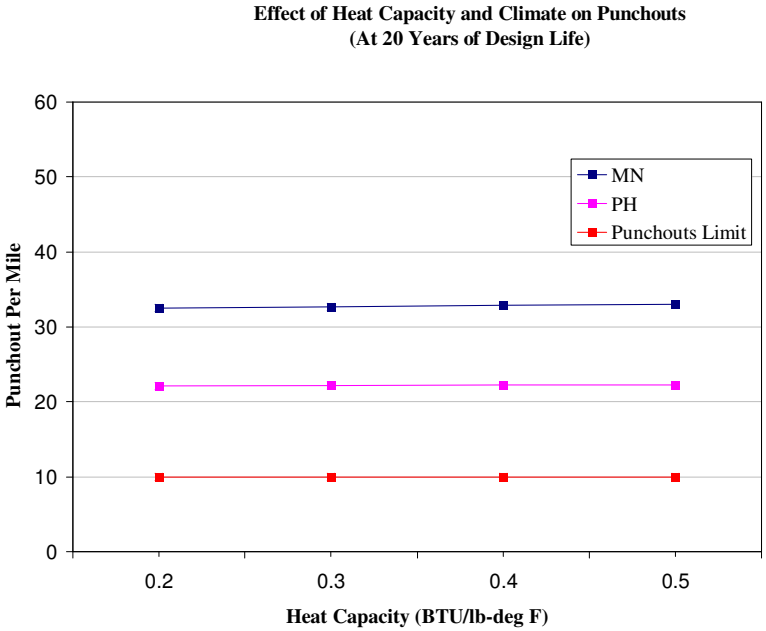

Figure 4.22 Effect of heat capacity on punchouts per mile

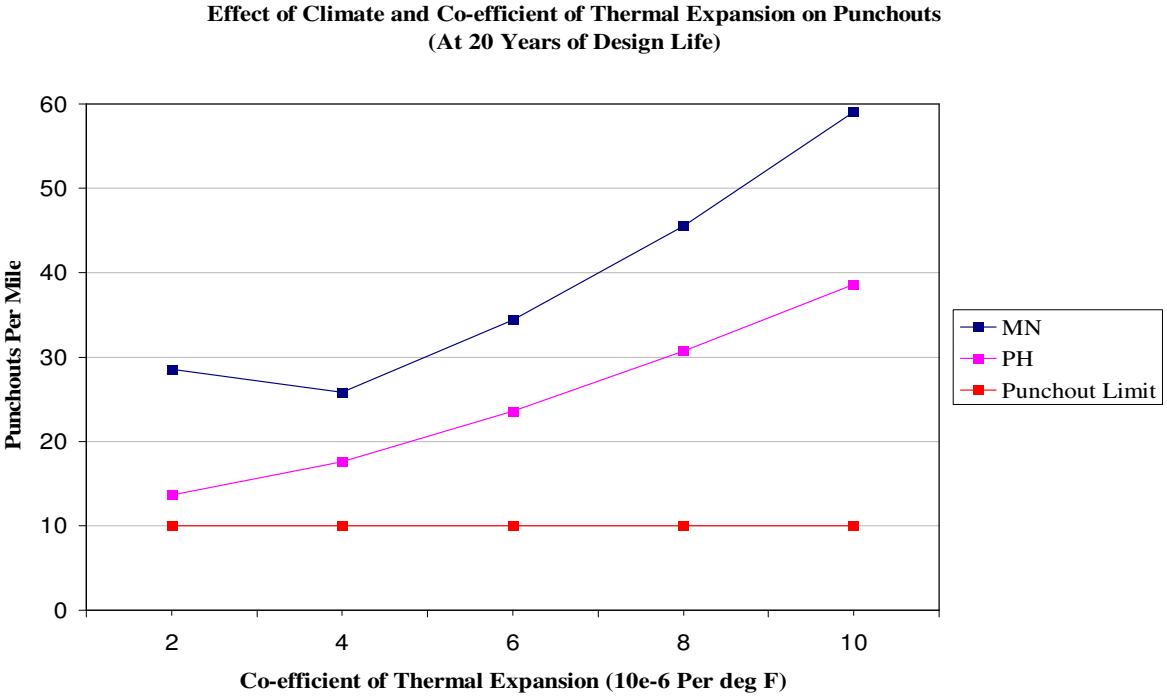

Figure 4.23 Effect of CTE on punchouts per mile

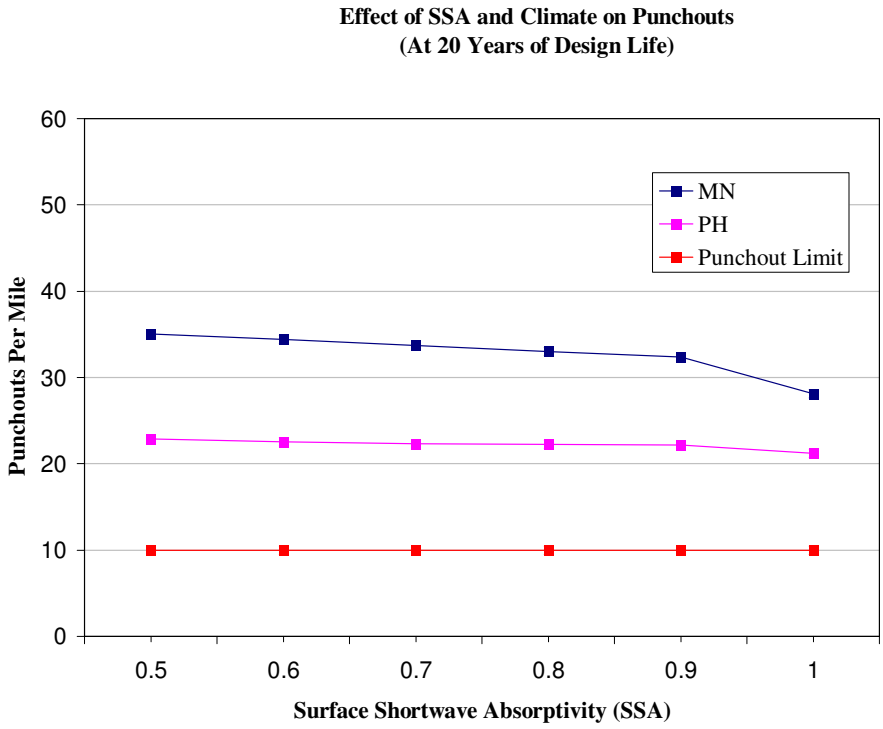

Figure 4.24 Effect of SSA on punchouts per mile

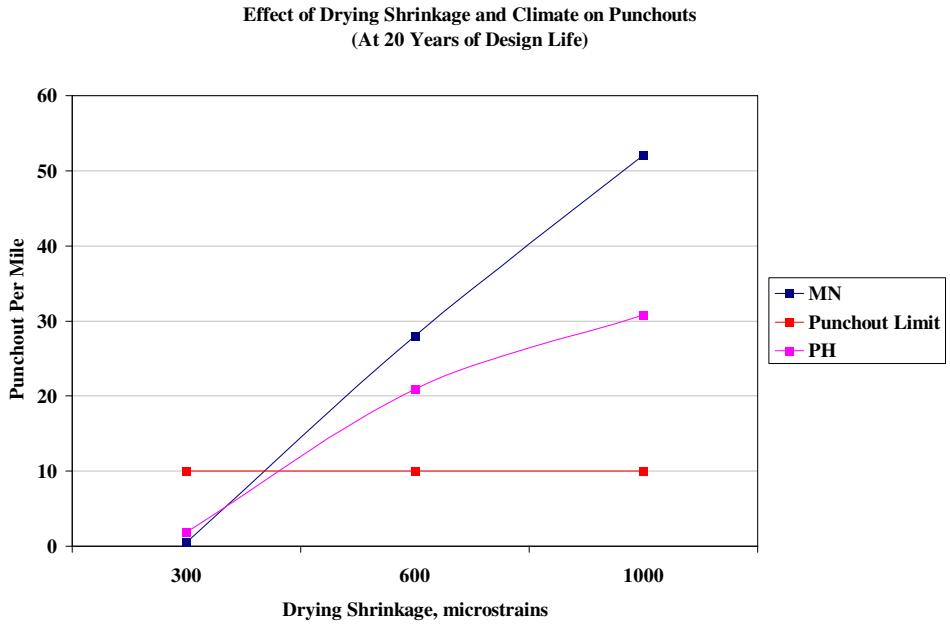

Figure 4.25 Effect of ultimate shrinkage strain on punchouts per mile

Relative Effect of All Variables on Punchouts

Previous studies have shown that base type and crack spacing play an important role in controlling punchouts [20]. In the present study, according to MEPDG, as seen from Figure 4.26 CTE is the most sensitive variable to punchouts among all the variables followed by crack spacing, shrinkage strain and climate zone. SSA and thermal conductivity are less sensitive and others are insensitive to punchouts. In all the cases, distress in Minneapolis is more compared to Phoenix. This can be attributed to availability of free moisture in Minneapolis which can lead to base and subgrade erosion which is the main cause for punchouts.

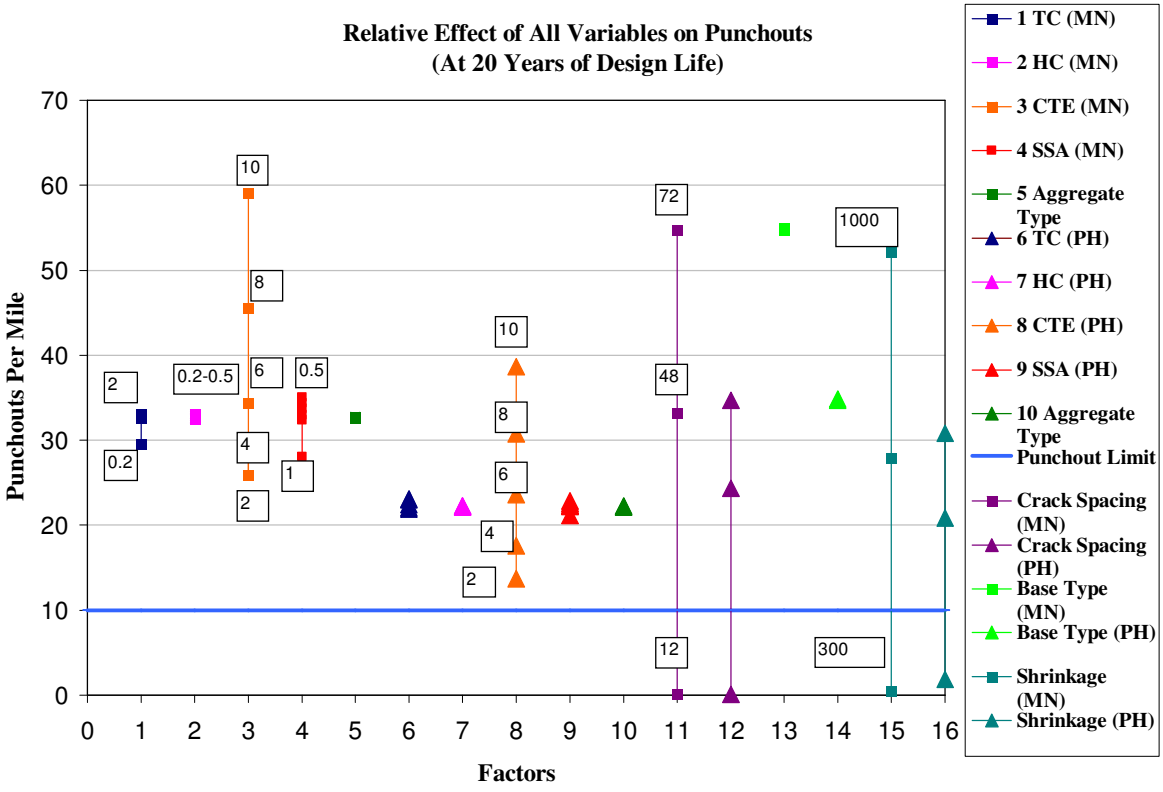

Figure 4.26 Relative effect of all variables on punchouts per mile

4.2.2 Effect of variables on IRI (Smoothness)

Effect of Thermal Conductivity on IRI

From Figure 4.27 for all thermal conductivity values, the IRI predicted is well below the acceptable values and also as the thermal conductivity increases, IRI remain constant. So, according to MEPDG, thermal conductivity is insensitive to IRI.

Effect of Heat Capacity on IRI

From Figure 4.28, heat capacity has a similar effect on IRI as thermal conductivity.

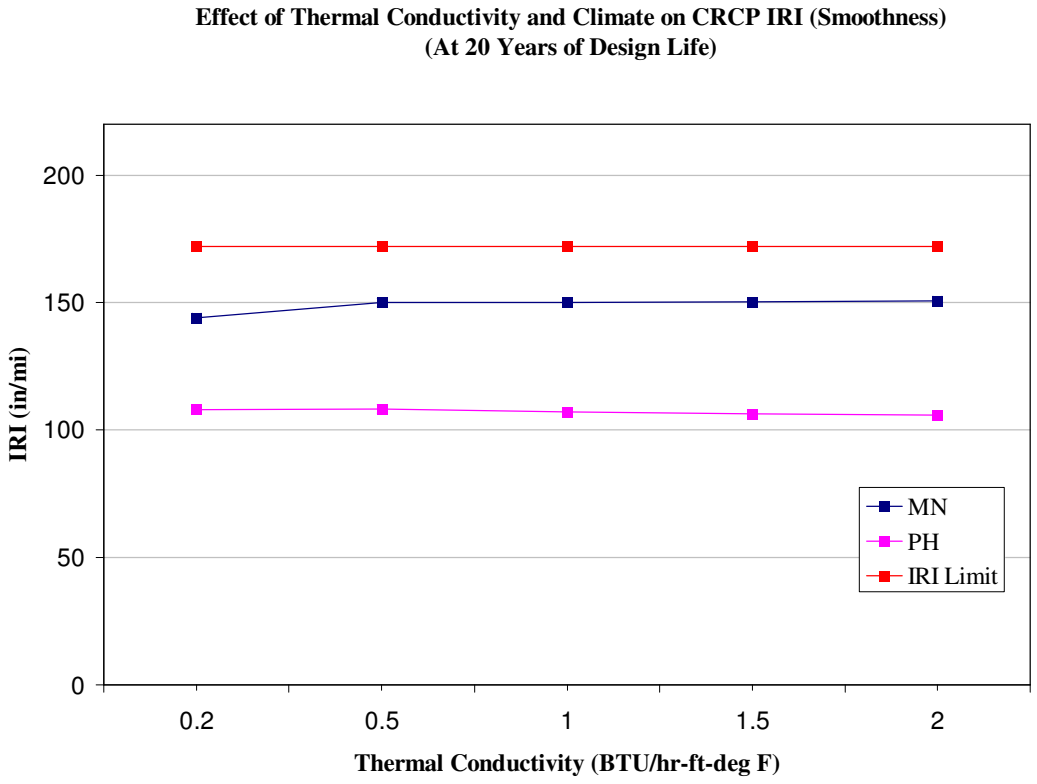

Figure 4.27 Effect of thermal conductivity on CRCP IRI

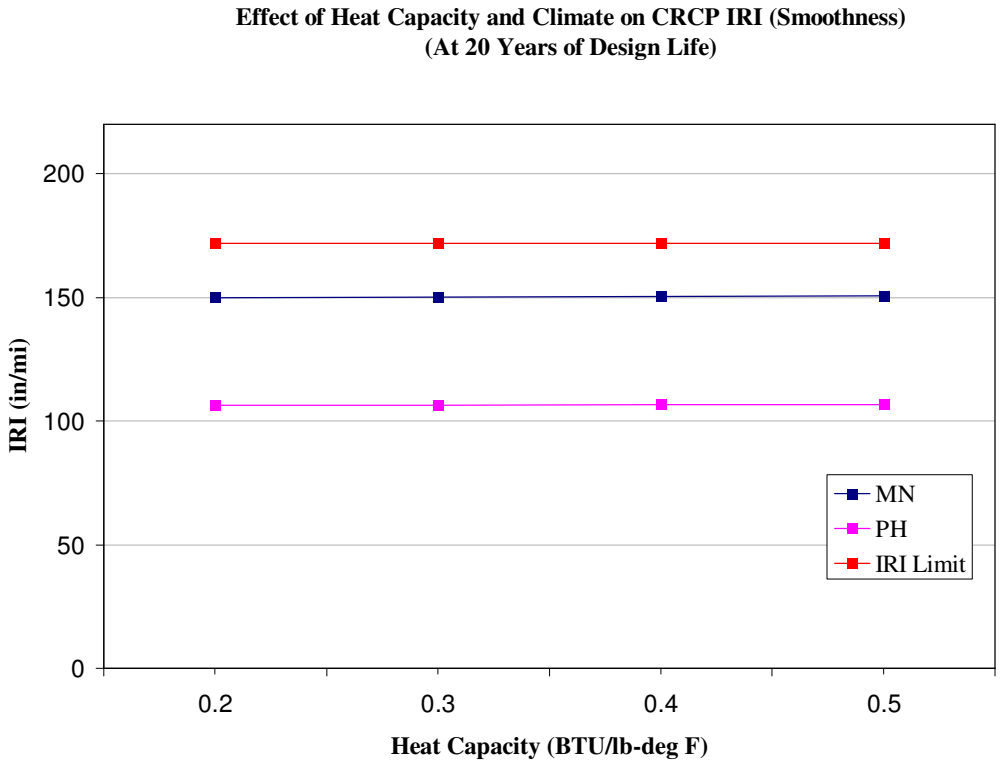

Figure 4.28 Effect of heat capacity on CRCP IRI

Effect of Co-efficient of Thermal Expansion on IRI

From the previous section we have noticed that as CTE increases, punchouts per mile increases and hence pavements become rougher. And this particular behavior is clearly captured by MEPDG as shown in Figure 4.29. As CTE increases IRI increases which means pavements become rougher.

Effect of Surface Shortwave Absorptivity on IRI

From Figure 4.30, SSA has similar effect on IRI as heat capacity and thermal conductivity.

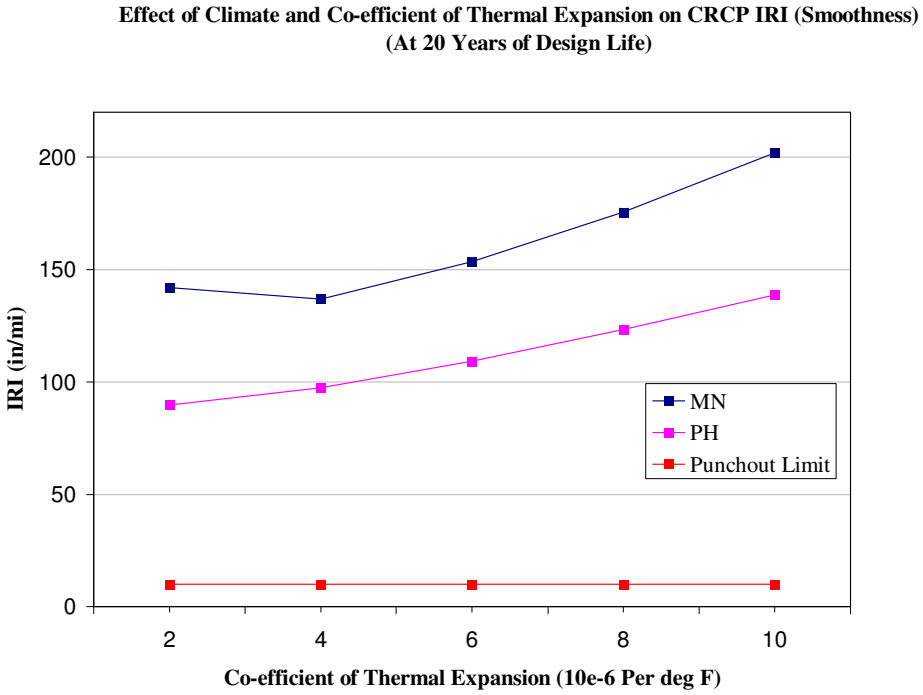

Figure 4.29 Effect of CTE on CRCP IRI

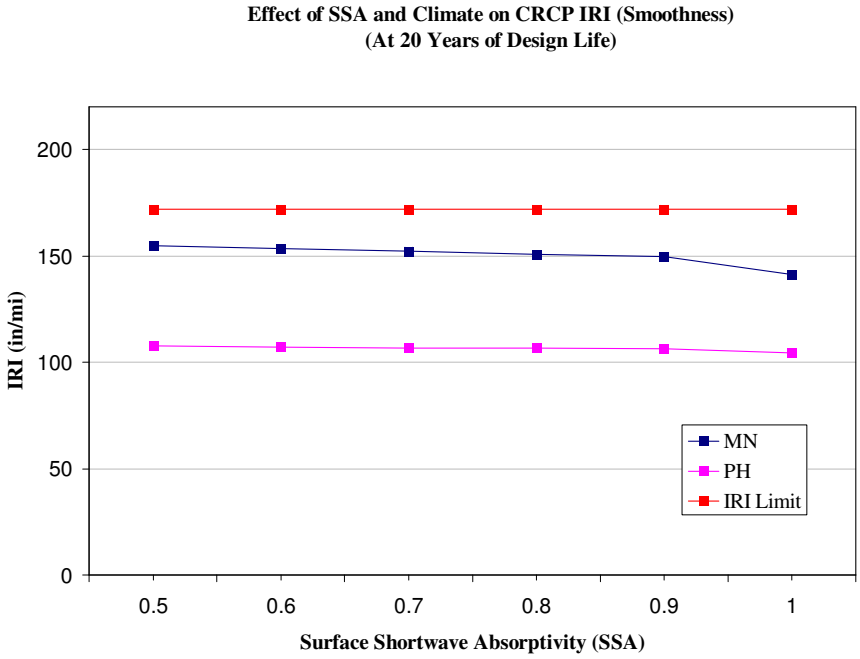

Figure 4.30 Effect of SSA on CRCP IRI

Effect of Ultimate Shrinkage on IRI

From Figure 4.31, as ultimate shrinkage strain increases, IRI also increases but the predicted values are well below the acceptable values. Hence IRI is insensitive to ultimate shrinkage strains.

Relative Effect of All Variables on IRI

As seen from Figure 4.32, CTE is the most sensitive variable to punchouts among all the variables followed by shrinkage strain. All other variables remain insensitive to IRI. Another conclusion from the results is pavements in Minneapolis are rougher than pavements in Phoenix.

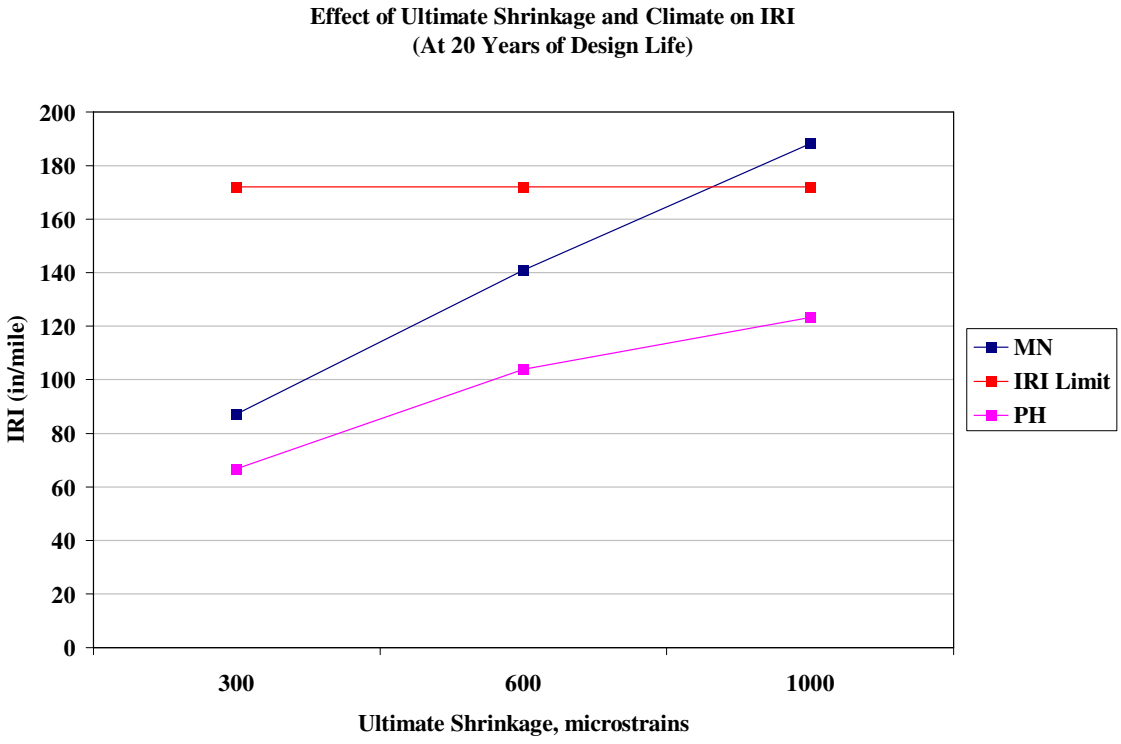

Figure 4.31 Effect of ultimate shrinkage strain on CRCP IRI

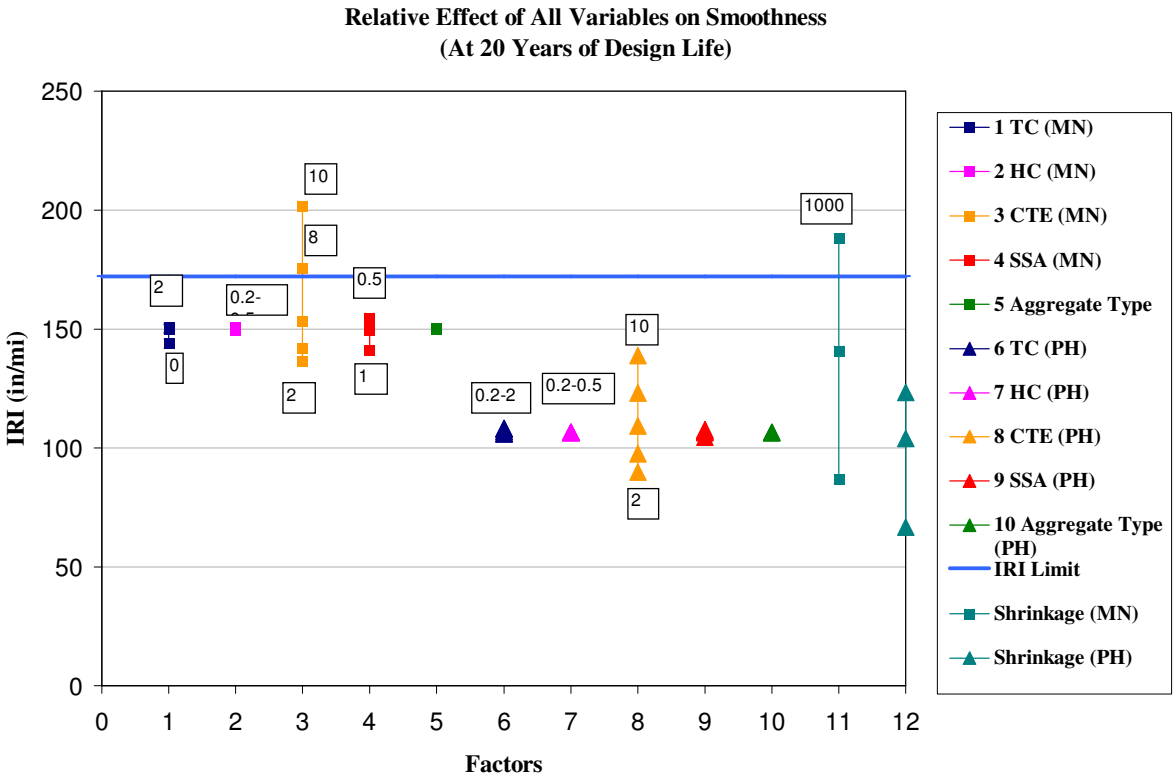

Figure 4.32 Relative effect of all variables on CRCP IRI

4.3 Effect of Variables on HMA Pavement Performance

4.3.1 Effect of Variables on Permanent Deformation (Rutting)

Previous sensitivity studies have associated rutting to load [21]. In this section sensitivity of thermal properties on rutting has been discussed in detail.

Effect of Thermal Conductivity on Rutting

As thermal conductivity of the asphalt material increases its ability to conduct heat increases and hence it would be able to drain the heat flow more quickly. So we expect more rutting for low thermal conductivity values. But according to MEPDG as shown in Figure 4.33,

predicts that thermal conductivity has no effect on rutting which seems unreasonable. Also, rutting is more in phoenix compared to Minneapolis for the same thermal conductivity.

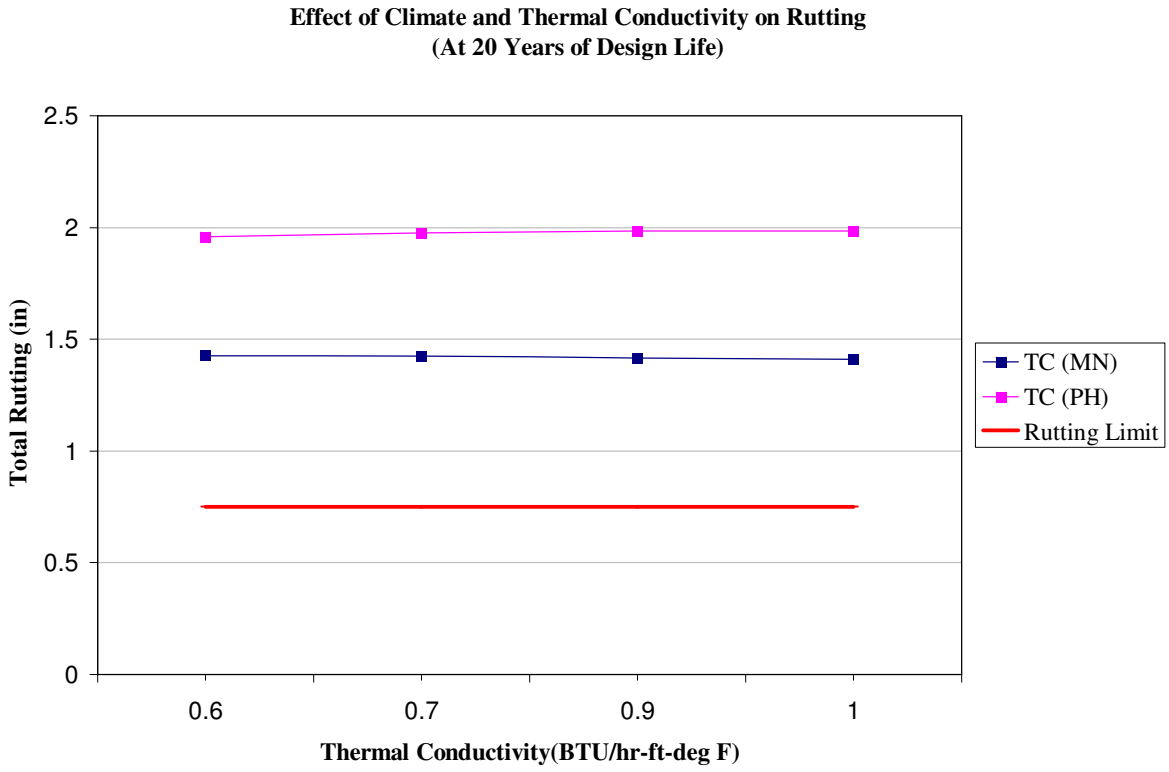

Figure 4.33 Effect of thermal conductivity on HMA rutting

Effect of Heat Capacity on Rutting

From Figure 4.34, as heat capacity increases, rutting decreases a little.

Effect of Surface Shortwave Absorptivity (SSA) on Rutting

From Figure 4.35, as SSA increases, rutting also increases.

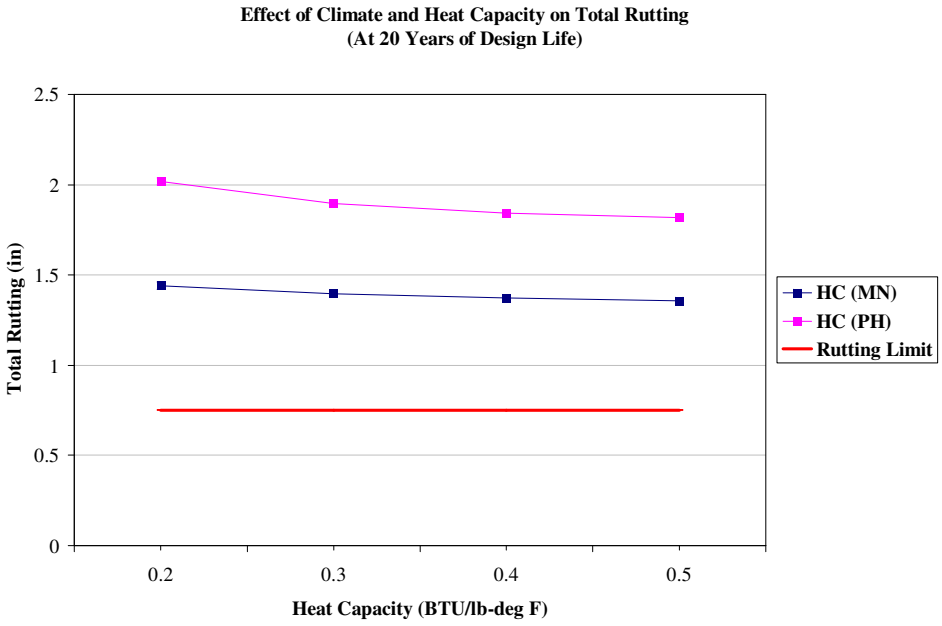

Figure 4.34 Effect of heat capacity on HMA rutting

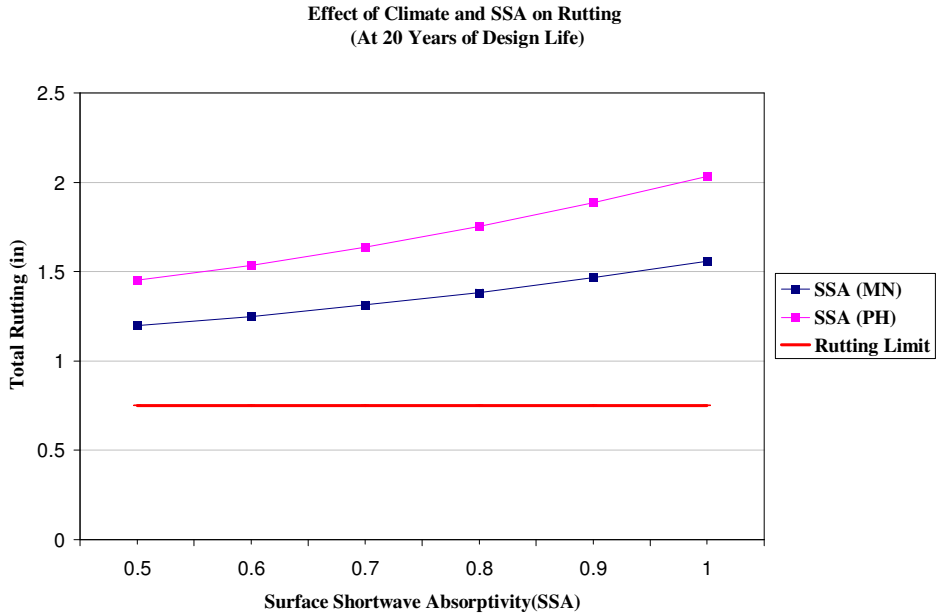

Figure 4.35 Effect of SSA on HMA rutting

Effect of Airvoid Content on Rutting

As airvoid content increases, rutting increases dramatically as seen from Figure 4.36. This can be attributed to following explanation. As airvoid content increases, the stiffness of the asphalt layer decreases and it becomes more vulnerable to damage due to load repetitions.

Effect of Mix Coefficient of Thermal Contraction on Rutting

As seen from Figure 4.37, change in mix co-efficient of thermal contraction has no effect in rutting predictions. It seems like an anomaly.

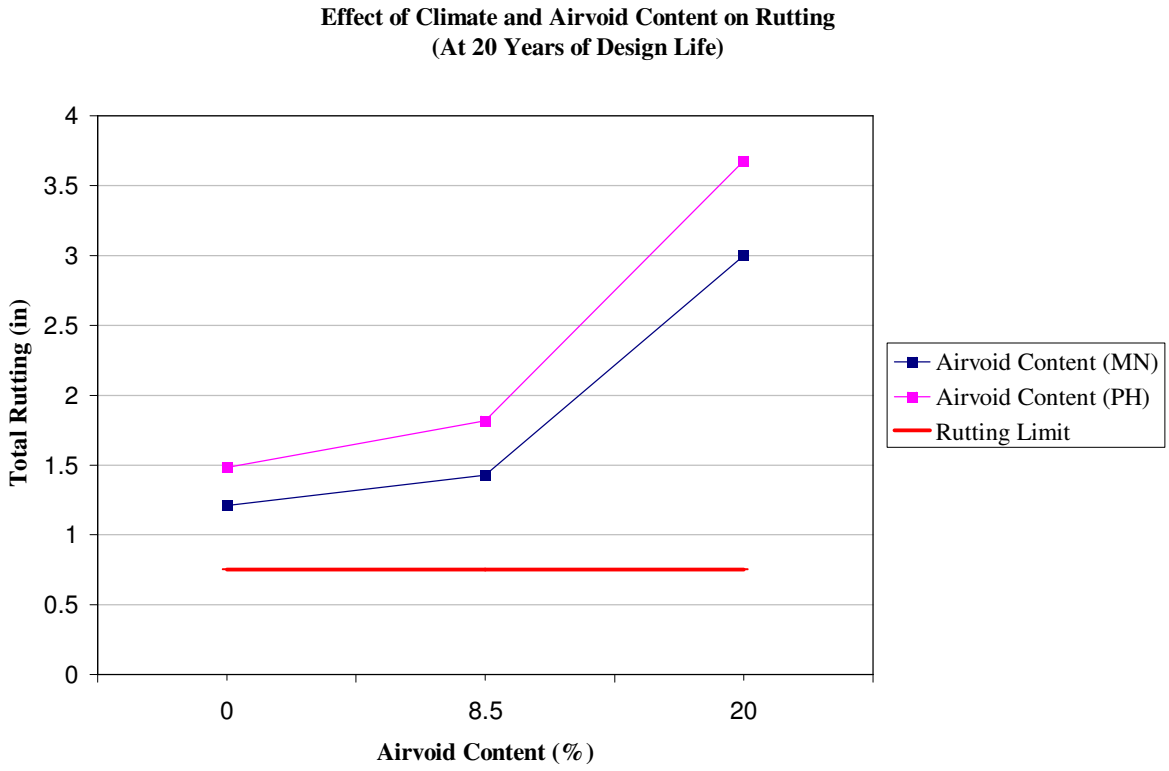

Figure 4.36 Effect of airvoid content on HMA rutting

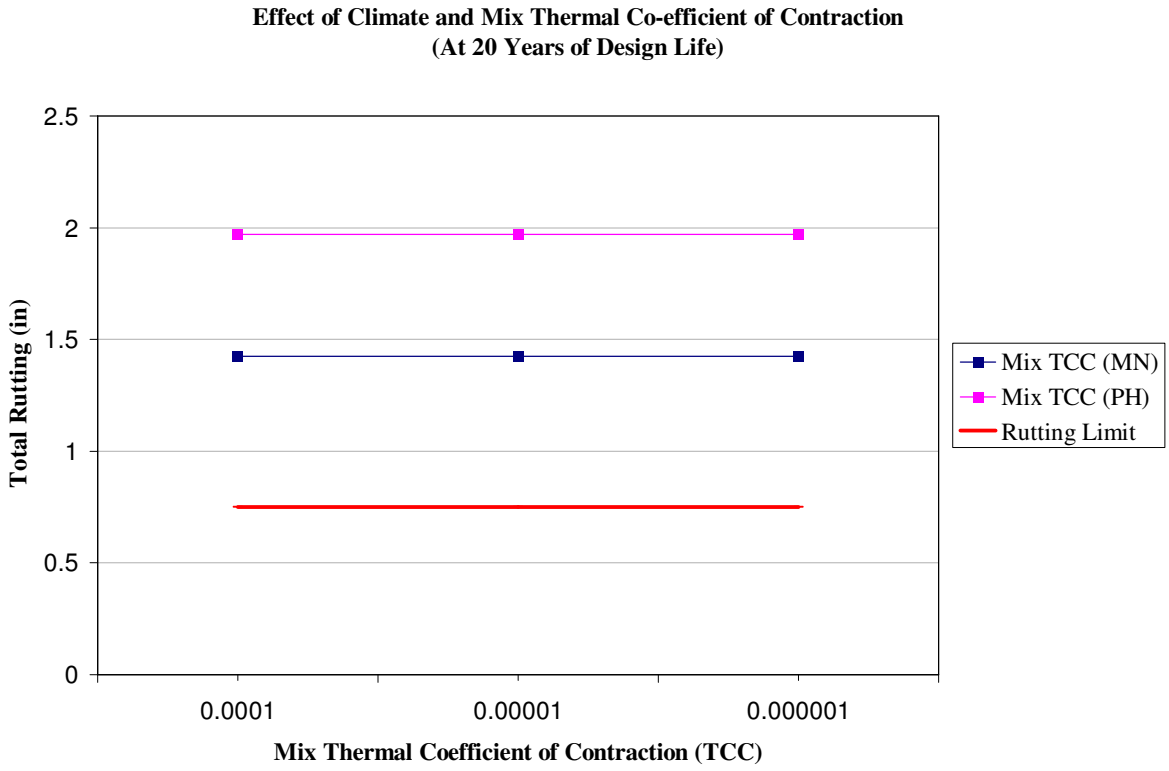

Figure 4.37 Effect of mix coefficient of thermal contraction HMA rutting

Relative Effect of All Variables on Rutting

As seen from Figure 4.38, airvoid content is the main important factor which controls rutting in HMA pavements followed by traffic and SSA. The effect caused by SSA is more than or equal to the effect caused by thickness, this shows that SSA is very important for HMA pavements. As SSA increases, the pavement absorbs more radiation and hence the layer becomes more plastic making it more susceptible to rutting. Heat capacity and thermal conductivity are insensitive to rutting. Also, rutting in Phoenix is more compared to rutting in Minneapolis for all variables. This shows that climate also plays an important role in rutting predictions.

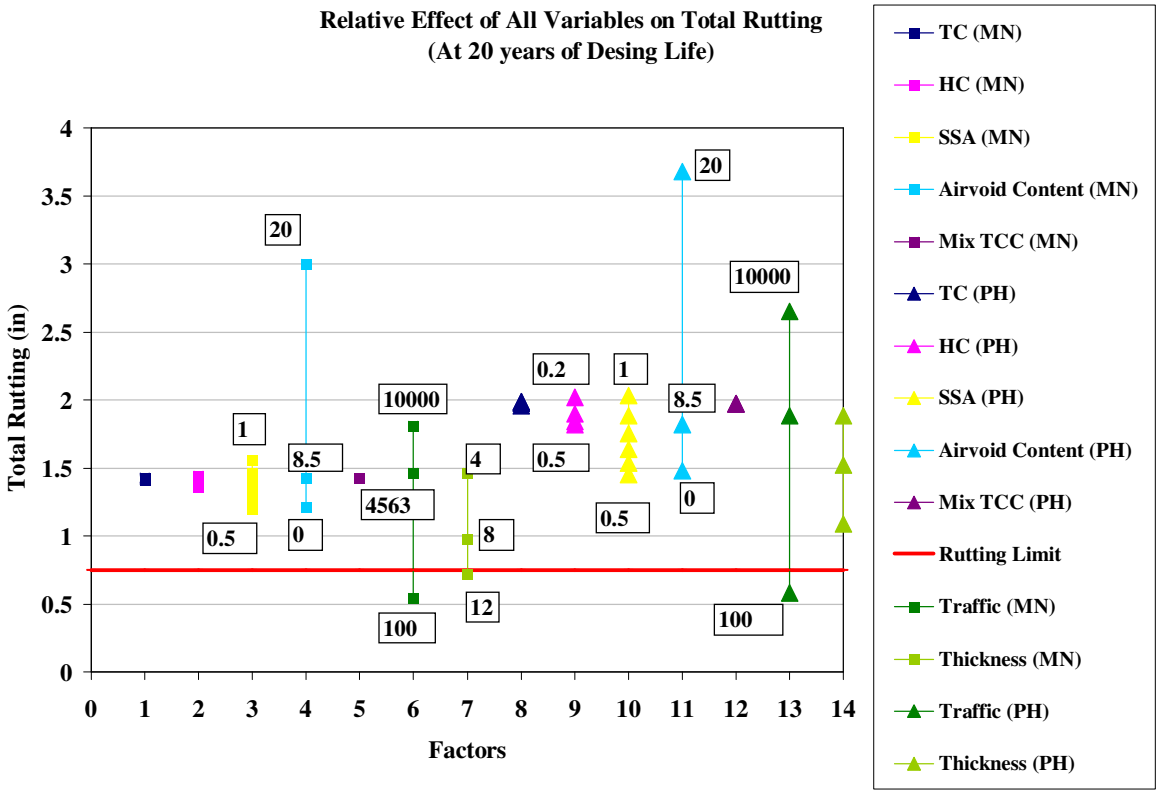

Figure 4.38 Relative effect of all variables on HMA rutting

4.3.2 Effect of Variables on Alligator Cracking

The fatigue cracking or alligator cracking in asphalt concrete mixture is influenced by many factors. Several key mix properties such as stiffness of the different layers, asphalt type, asphalt content and air-void content are well known to influence fatigue. Other factors such as temperature, frequency, and rest periods of the applied load also are known to influence fatigue life [22]. Other material properties also affect the fatigue life. Since stiffness of the layer system varies during different months depending on the weather, for example in Minneapolis in the winter season the stiffness of asphalt layer is as high as a Portland cement

concrete and during spring season it's as low as low stiffness soils, one would expect climate to play an important role in alligator cracking prediction. This section focuses on the affect of thermal properties and climate on fatigue cracking in asphalt pavements.

Effect of Thermal Conductivity on Alligator Cracking

As seen from Figure 4.39, as thermal conductivity (TC) increases alligator cracking remains constant, making TC insensitive to alligator cracking.

Effect of Heat Capacity on Alligator Cracking

From Figure 4.40, as heat capacity (HC) increases alligator cracking remains constant, making HC insensitive to alligator cracking.

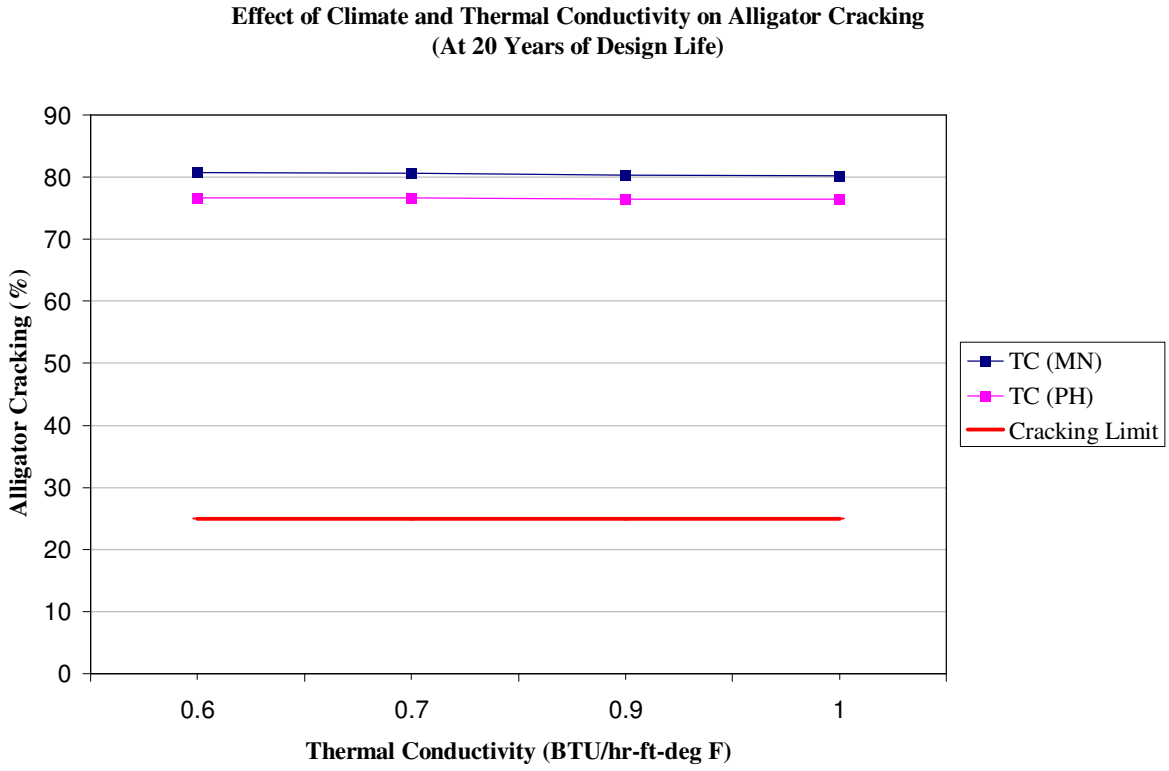

Figure 4.39 Effect of thermal conductivity on alligator cracking

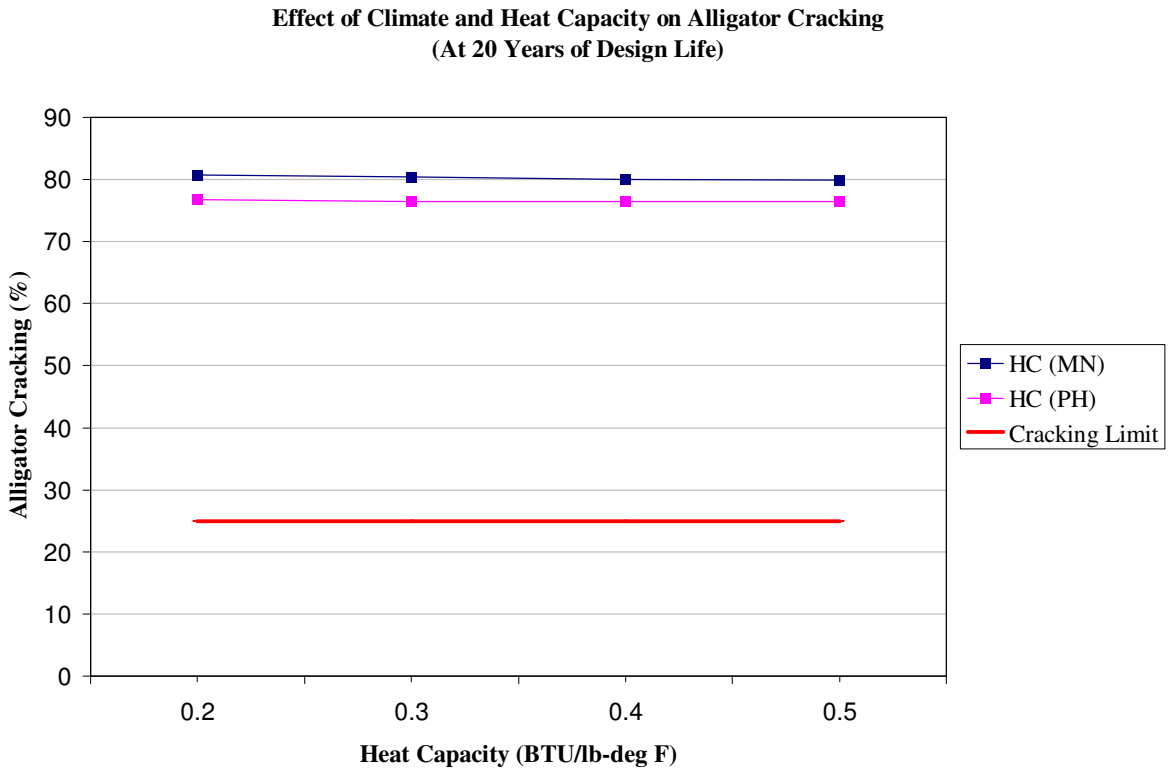

Figure 4.40 Effect of heat capacity on alligator cracking

Effect of Surface Shortwave Absorptivity (SSA) on Alligator Cracking

From Figure 4.41, as SSA increases, alligator cracking also increases.

Effect of Airvoid Content on Alligator Cracking

From Figure 4.42, airvoid content has a dramatic affect on alligator cracking. As airvoid content increases, alligator cracking increases dramatically. As the airvoid content increases, the stiffness of the mix decreases, at 0 % airvoid the stiffness is very high and at 20% airvoid the stiffness is very low and hence the result is a dramatic difference in cracking. And also as airvoid content increases, the thermal conductivity of the layer decreases because air does not conduct. This also aggravates the situation.

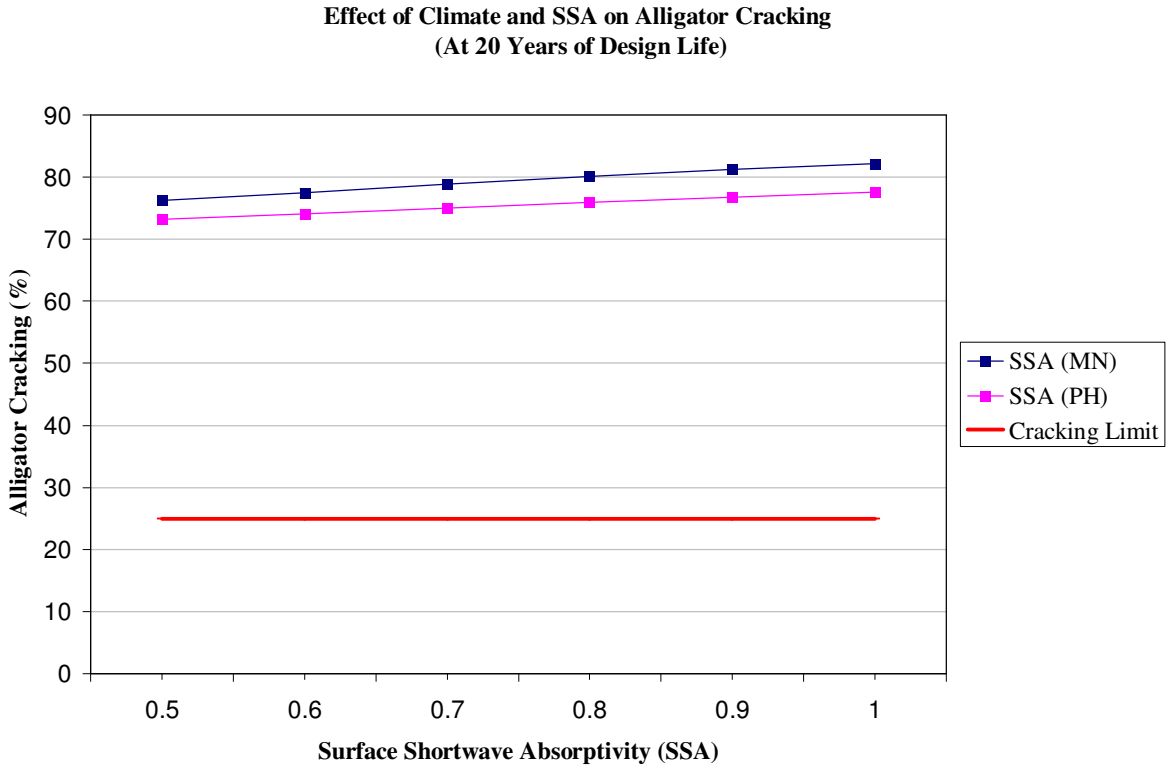

Figure 4.41 Effect of SSA on alligator cracking

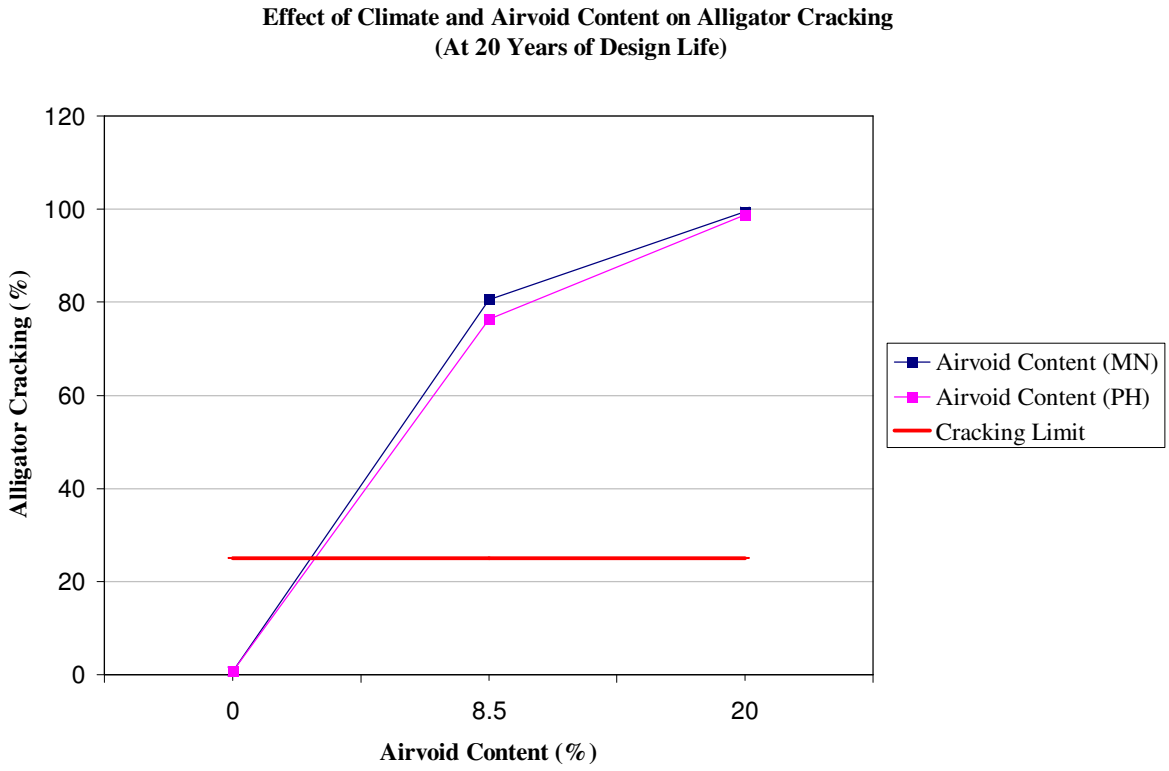

Figure 4.42 Effect of airvoid content on alligator cracking

Relative Effect of All Variables on Alligator Cracking

From Figure 4.43, airvoid content, traffic volume and thickness of the asphalt layer are the most important parameters controlling the alligator cracking. According to MEPDG, thermal properties of asphalt material seem to play little or no role in alligator cracking prediction. The most sensitive parameter to alligator cracking among the thermal properties is SSA. Also, climate has a little or no effect on alligator cracking prediction which seems unreasonable.

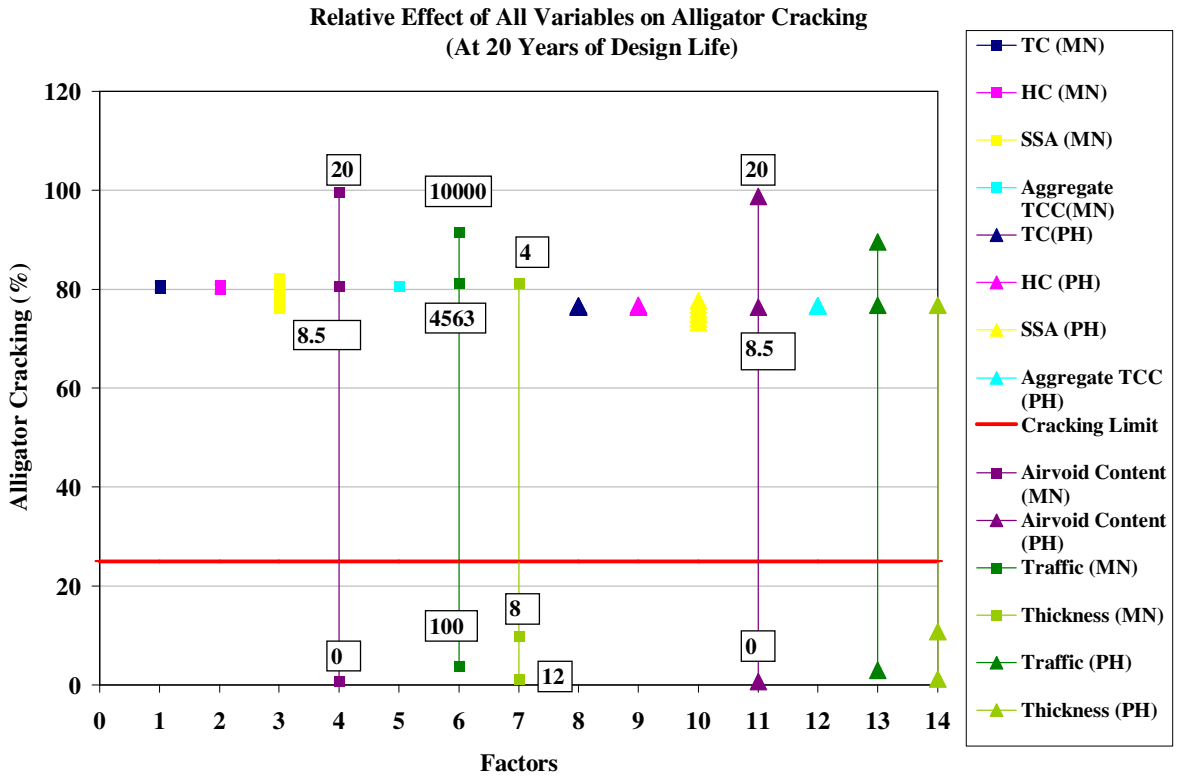

Figure 4.43 Relative effect of all variables on alligator cracking

4.3.3 Effect of Variables on Longitudinal Cracking

Thermal conductivity, heat capacity, surface shortwave absorptivity seems to have no effect on longitudinal cracking. This concludes that thermal properties have no effect on longitudinal cracking. Other parameters like airvoid content, traffic volume and thickness were also changed to see the relative effect of these parameters and thermal properties on longitudinal cracking. The results are shown below.

Effect of Airvoid Content on Longitudinal Cracking

From Figure 4.44, as airvoid content increases longitudinal cracking increases dramatically. Climate seems to have no effect on longitudinal cracking.

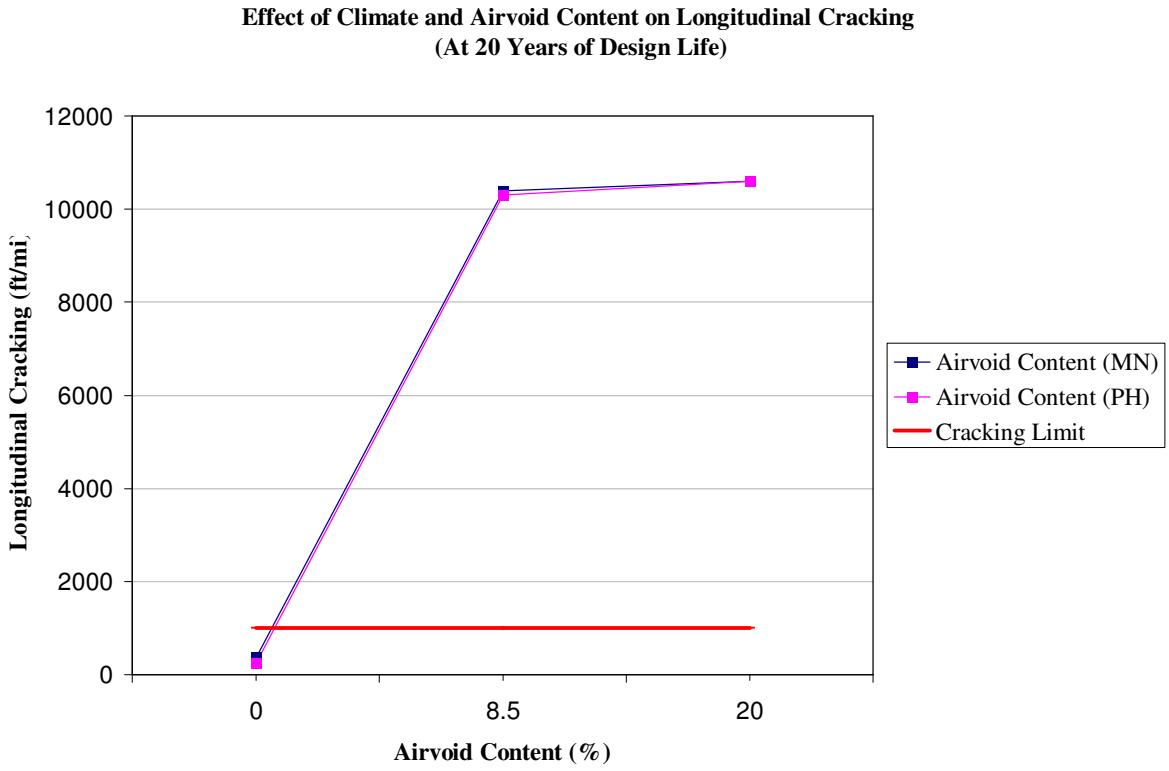

Figure 4.44 Effect of airvoid content on longitudinal cracking

Relative Effect of Variables on Longitudinal Cracking

According to MEPDG from Figure 4.45, airvoid content, traffic volume and thickness play major role in controlling longitudinal cracking. Thermal properties and climate have no effect on longitudinal cracking.

4.3.4 Effect of Variables on IRI

As seen from the Figures 4.46, 4.47, 4.48 and 4.49, thermal conductivity, heat capacity has no effect on smoothness. As surface shortwave absorptivity increases, IRI also increases. Change in airvoid void content has a dramatic effect on IRI.

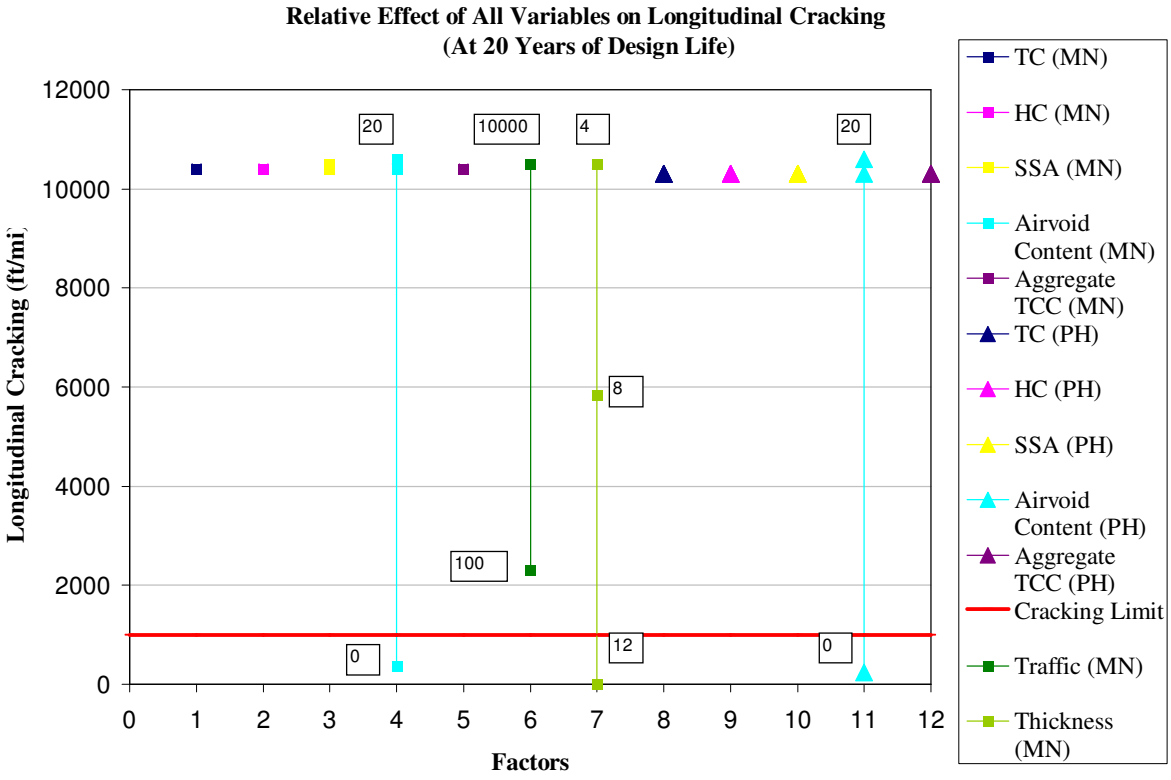

Figure 4.45 Relative effect of all variables on longitudinal cracking

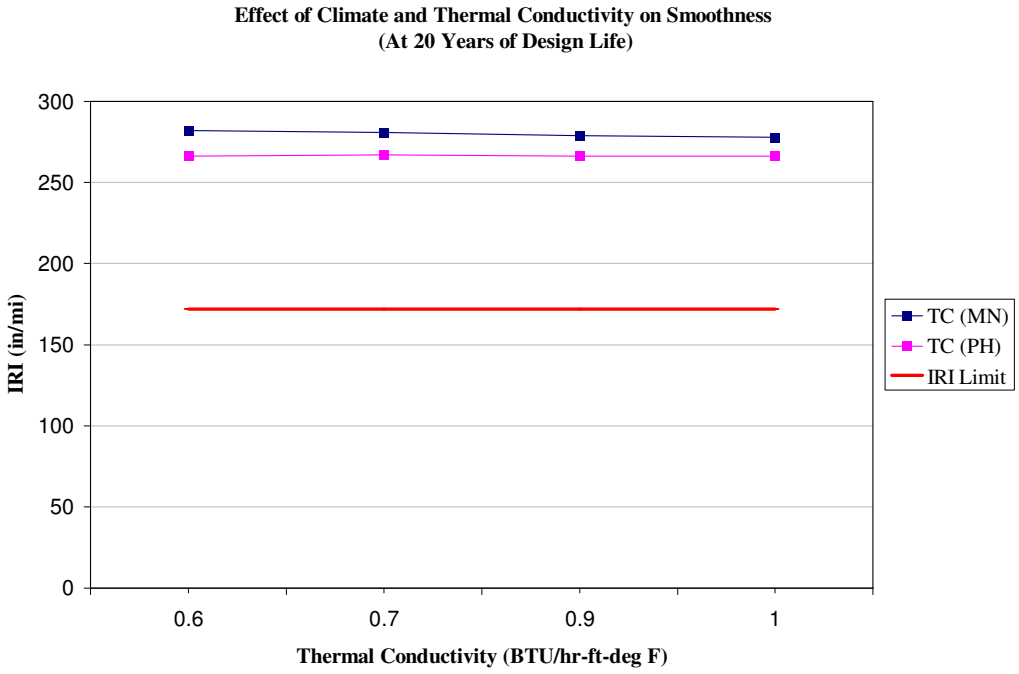

Figure 4.46 Effect of thermal conductivity on HMA IRI

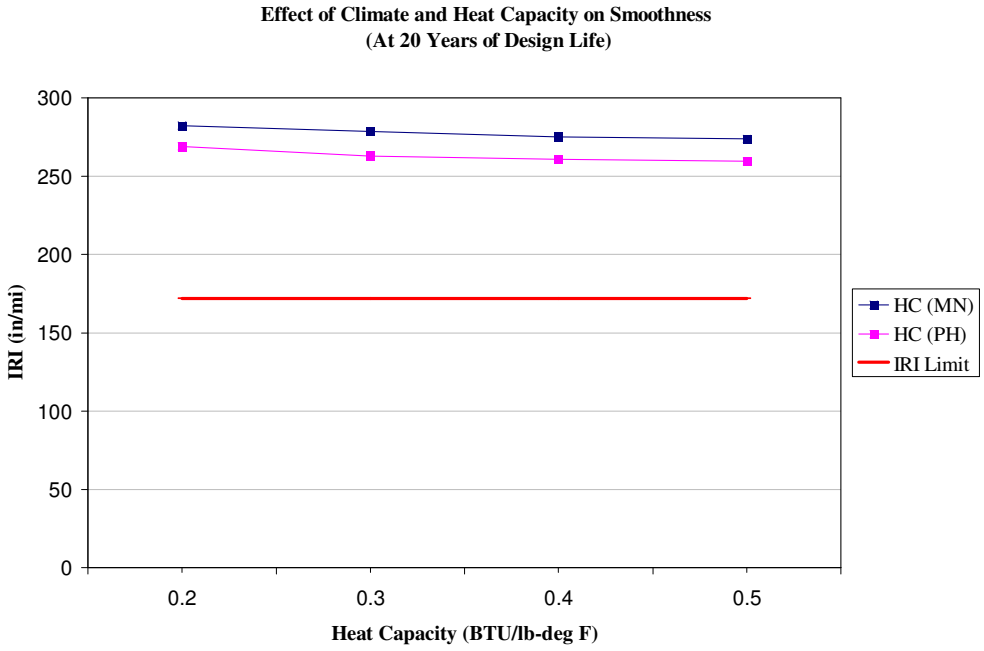

Figure 4.47 Effect of heat capacity on HMA IRI

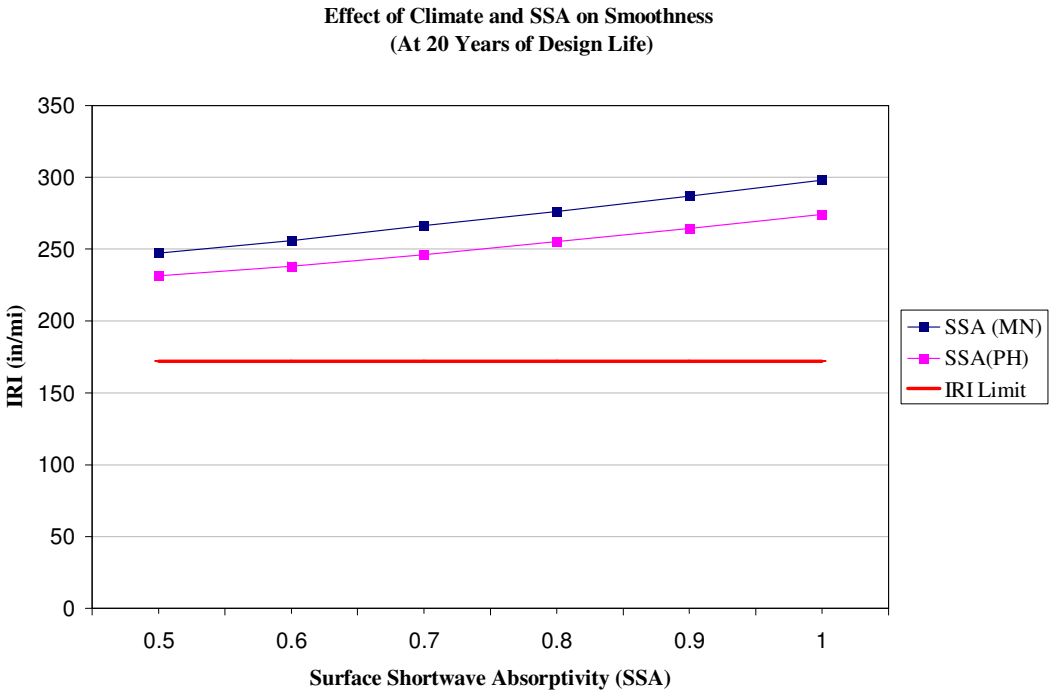

Figure 4.48 Effect of SSA on HMA IRI

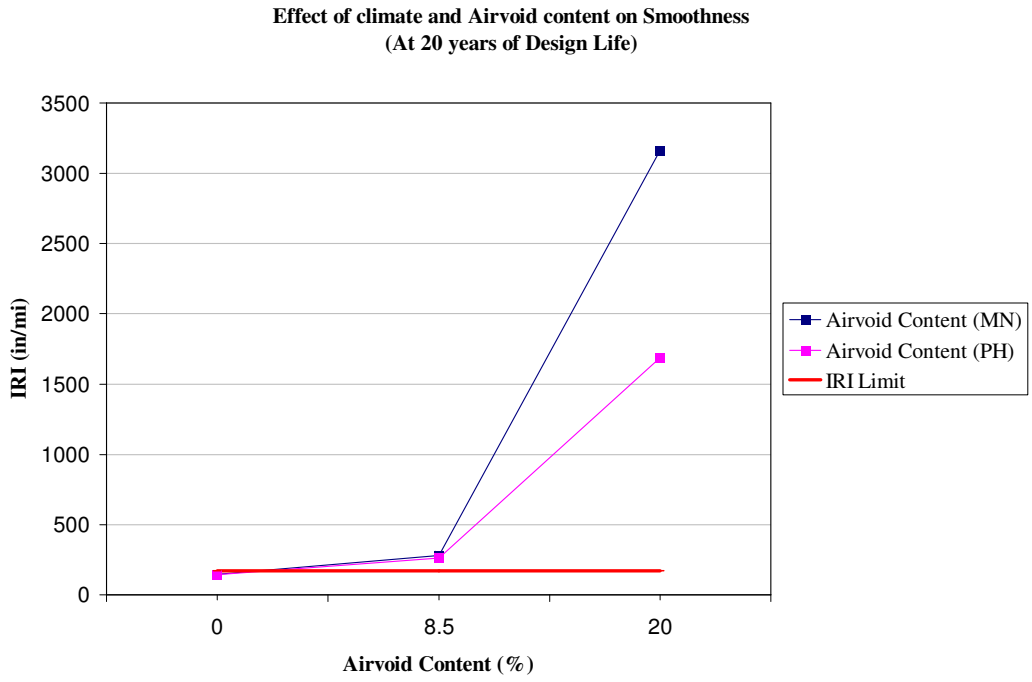

Figure 4.49Effect of airvoid content on HMA IRI

Relative Effect of All Variables on IRI

From Figure 4.50, Changes in airvoid content, thickness of the asphalt layer and traffic volume are the parameters which effect IRI the most. Thermal properties have no effect on IRI.

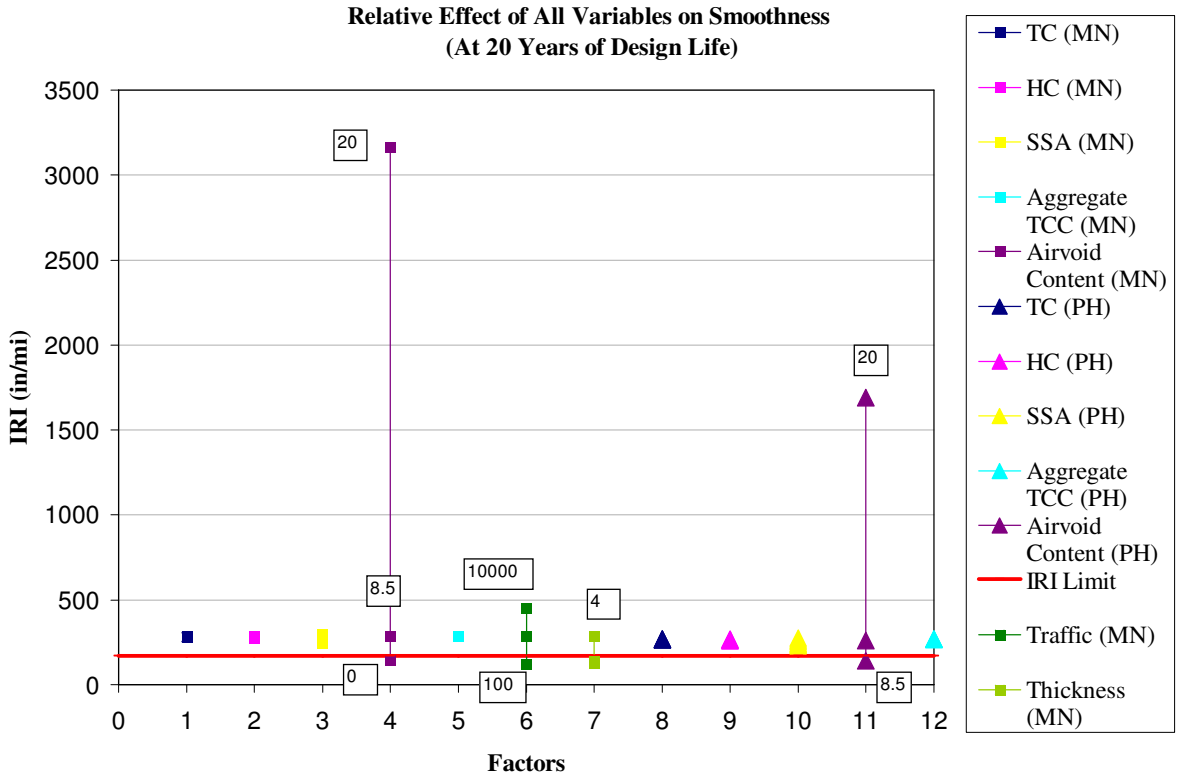

Figure 4.50 Relative effect of all variables on HMA IRI

4.3.5 Effect of Variables on Transverse Cracking in HMA pavements

One would expect thermal cracking to be more in colder regions [23] like Minneapolis. Thermal cracking model in MEPDG remain insensitive to all the thermal properties and also other parameters which were used in the sensitivity analyses which leads to a conclusion that

thermal cracking model in MEPDG may be having some problems or bugs which need to be fixed.

4.4 Relative Effect of All Thermal Properties on All Pavement Distress

In the previous sections, relative effect of different thermal properties and non thermal properties on each pavement distress has been discussed in detail. In this section, effect of each thermal property on different distresses has been discussed. For example, as thermal conductivity is changed from 0.2 to 2.0 BTU/hr-ft-^{0}F, JPCP faulting changes from 0.19 in to 0.133 in, cracking changes from 96.1 % to 0.4 % and IRI changes from 262.9 to 154.7 in/mi. The main objective of this section is to see which distress is affected more by thermal conductivity. To determine this, absolute percentage change for each distress has been calculated by the formula shown below.

$$\text{Absolute \% Change} = \frac{(fdv - idv)}{idv} \times 100 \tag{4.1}$$

where, fdv = final distress value, idv = initial distress value

The results obtained are discussed below.

4.4.1 Relative Effect of All Thermal Properties on JPCP Distress

As seen from the Figures 4.51, 4.52, 4.53, 4.54 and 4.55, thermal conductivity (TC), heat capacity (HC), surface shortwave absorptivity (SSA) and co-efficient of thermal expansion (CTE) affect transverse cracking the most compared to faulting and smoothness(IRI). This is logical because the stresses at the critical location as explained in the section, increases greatly with increase or decrease in temperature gradient through the slab. Since the temperature gradient in a slab is governed by TC, HC, SSA and CTE, these properties effect

cracking the most. However, ultimate shrinkage strain affects faulting the most. This is logical because, as shrinkage increases, the space between the transverse joints increases, which gives way to free moisture and water to seep into the pavement layers and make the base and subgrade more susceptible to erosion and hence more faulting.

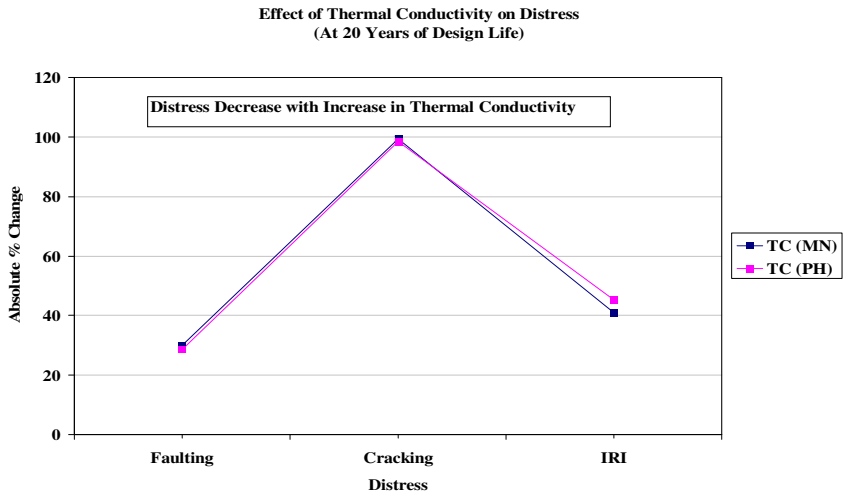

Figure 4.51 Effect of thermal conductivity on all JPCP distress

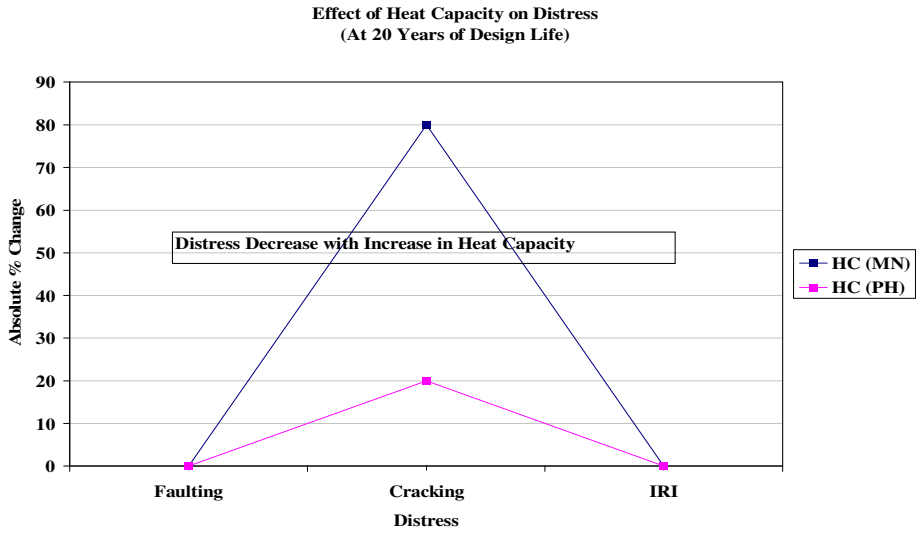

Figure 4.52Effect of heat capacity on all JPCP distress

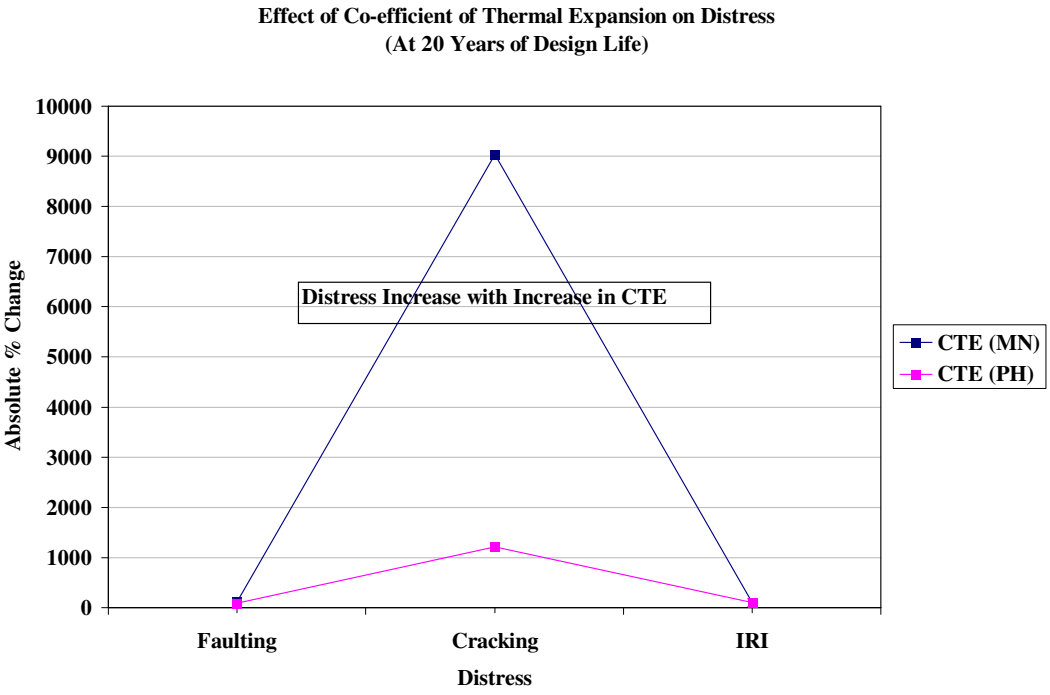

Figure 4.53 Effect of CTE on all JPCP distress

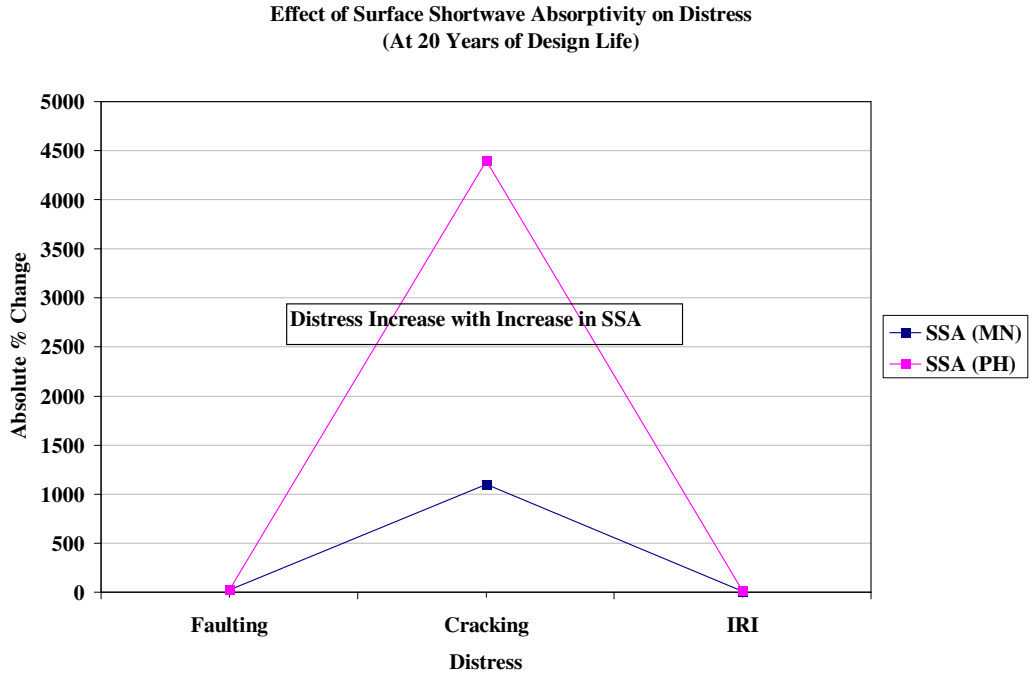

Figure 4.54 Effect of SSA on all JPCP distress

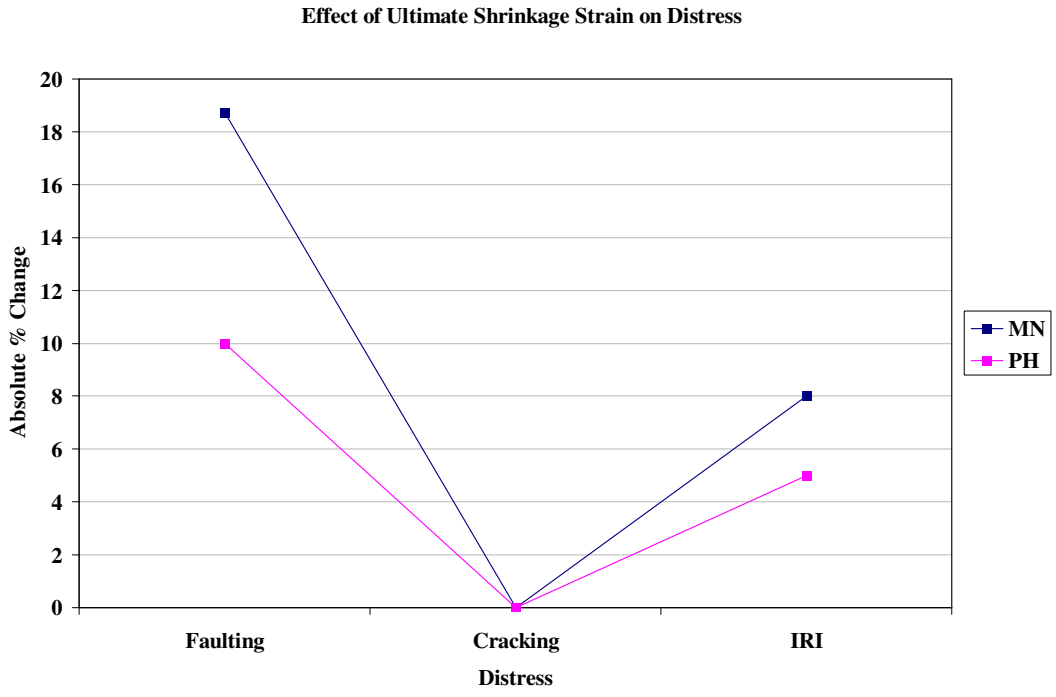

Figure 4.55 Effect of ultimate shrinkage strain on all JPCP distress

4.4.2 Relative Effect of All Thermal Properties on CRCP Distress

From Figures 4.56, 4.57, 4.58, 4.59 and 4.60 below, thermal conductivity (TC), heat capacity (HC), surface shortwave absorptivity (SSA), ultimate shrinkage strain (USS) and co-efficient of thermal expansion (CTE) affect punchouts the most. This is logical because, TC, HC, SSA and CTE affects the temperature gradients in the slab leading to more transverse cracks and USS increase the transverse crack space making way for free water to enter into the pavement layers and hence leading to punchouts which are caused mainly due to loss of crack load transfer efficiency and erosion.

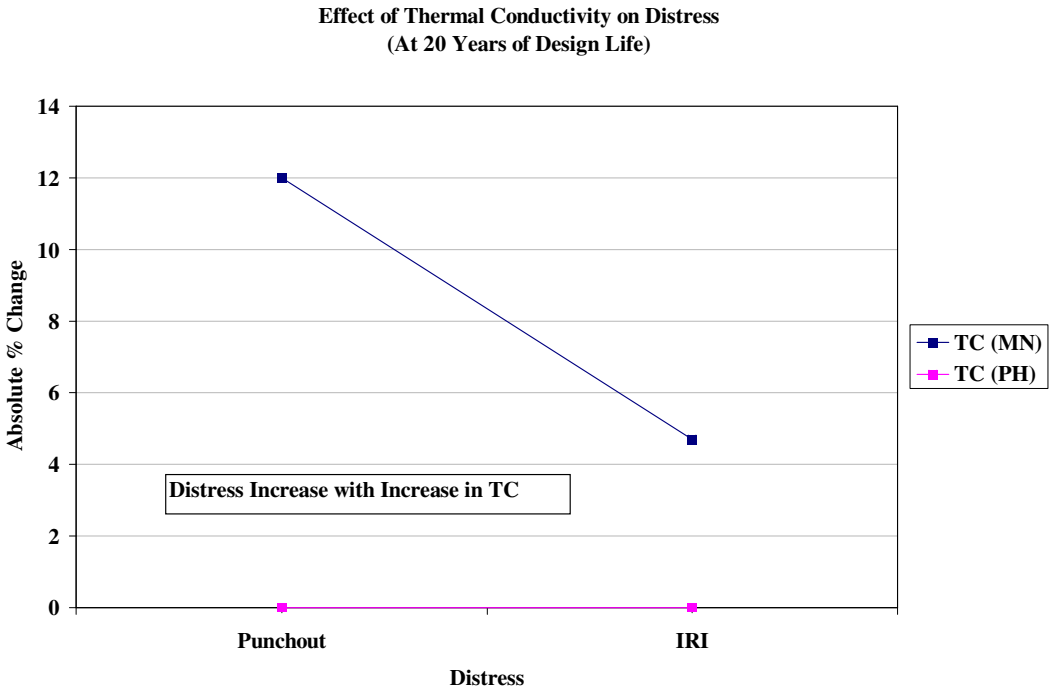

Figure 4.56 Effect of thermal conductivity on all CRCP distress

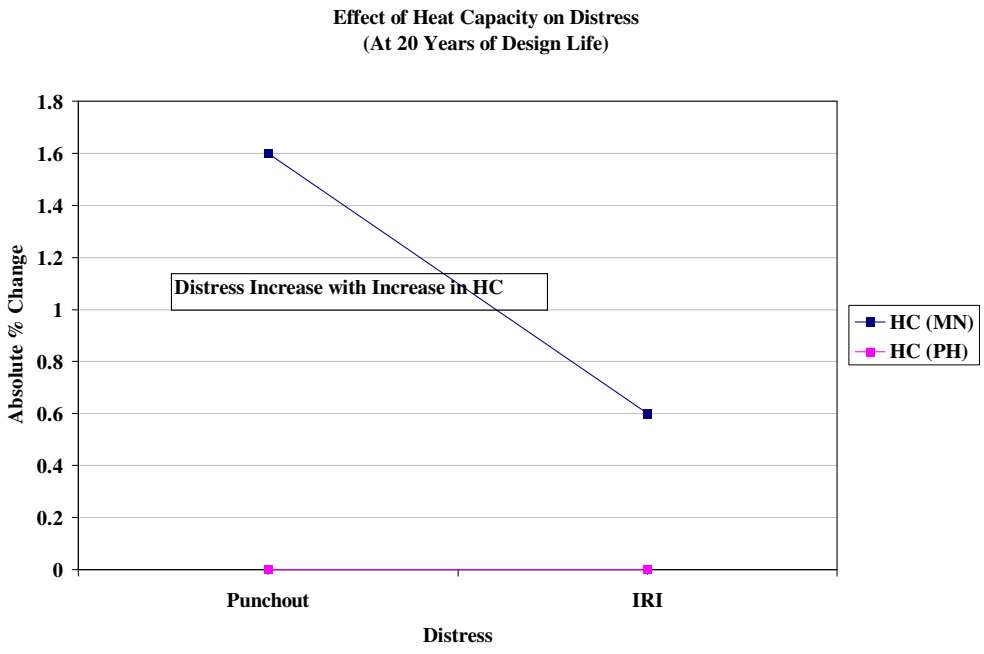

Figure 4.57 Effect of heat capacity on all CRCP distress

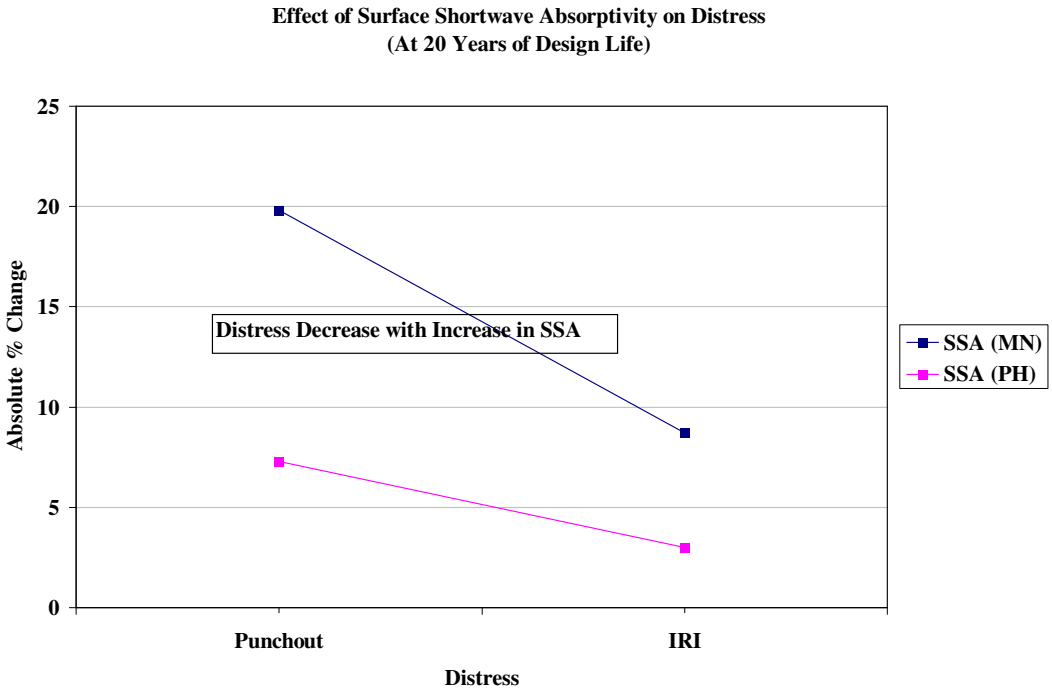

Figure 4.58 Effect of SSA on all CRCP distress

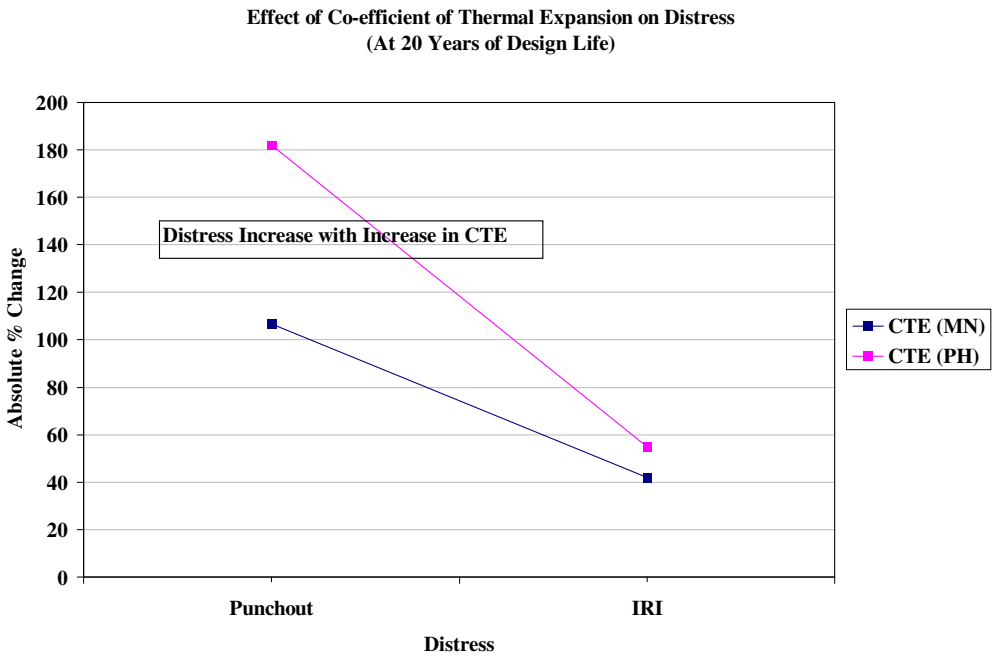

Figure 4.59 Effect of CTE on all CRCP distress

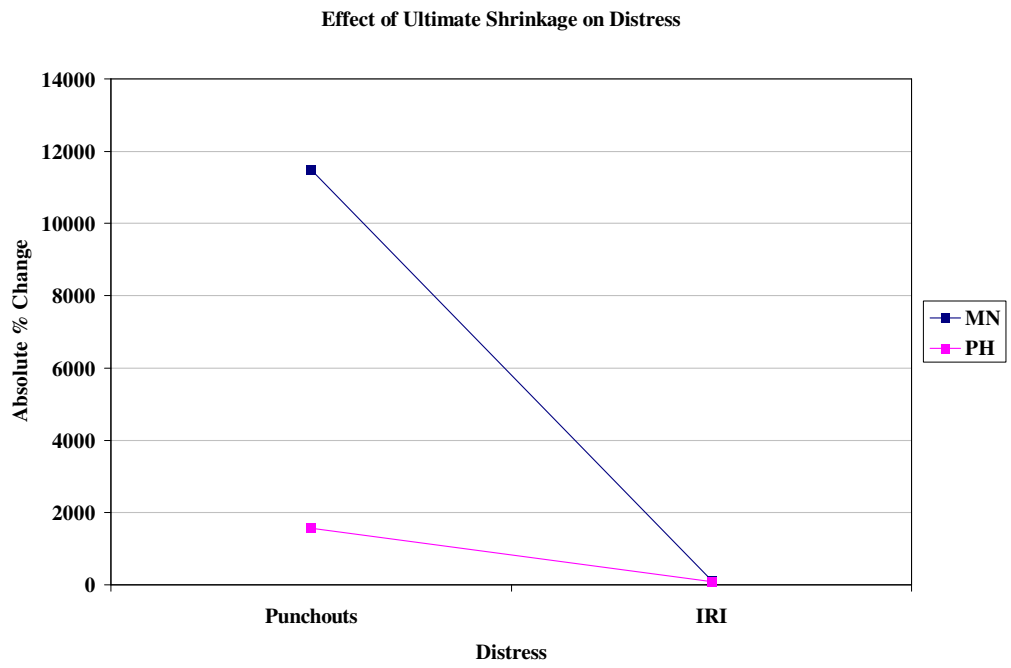

Figure 4.60 Effect of ultimate shrinkage strain on CRCP distress

4.4.3 Relative Effect of All Thermal Properties on HMA Distress

In case of HMA pavements, thermal conductivity, mix coefficient of thermal contraction (CTC) and heat capacity does not affect any distress except surface shortwave absorptivity (SSA) and airvoid. The main reason why thermal conductivity has no effect on the performance is because; moisture content has an influence upon the thermal conductivity of asphalt concrete. If the moisture content is small, the differences between the unfrozen, freezing and frozen thermal conductivity are small. Only when the moisture content is high (e.g greater than 10%) does the thermal conductivity vary substantially [4]. In the present study, Minneapolis comes under wet and freeze climate zone where the average annual moisture content is definitely greater than 10% and hence thermal conductivity should play a major role in performance predictions in Minneapolis. But MEPDG is not able to capture this

effect. Also, as CTC increases, cracking in HMA pavements increases which again is not captured by MEPDG.

As seen below, SSA affects total rutting (TR) more compared to alligator cracking (AC) and smoothness (IRI). This is true because, SSA has a direct impact on the surface heating of the pavements. As SSA increase the surface of the pavement absorbs more radiation and since asphalt is very sensitive to heat, the surface layer becomes more plastic and when combined with loads lead to more rutting.

Air-void content affects AC more compared to TR because as air-void content increases the stiffness of the surface layer decreases leading to more cracks (AC) at the bottom of the layer which propagate to the surface under repeated load applications.

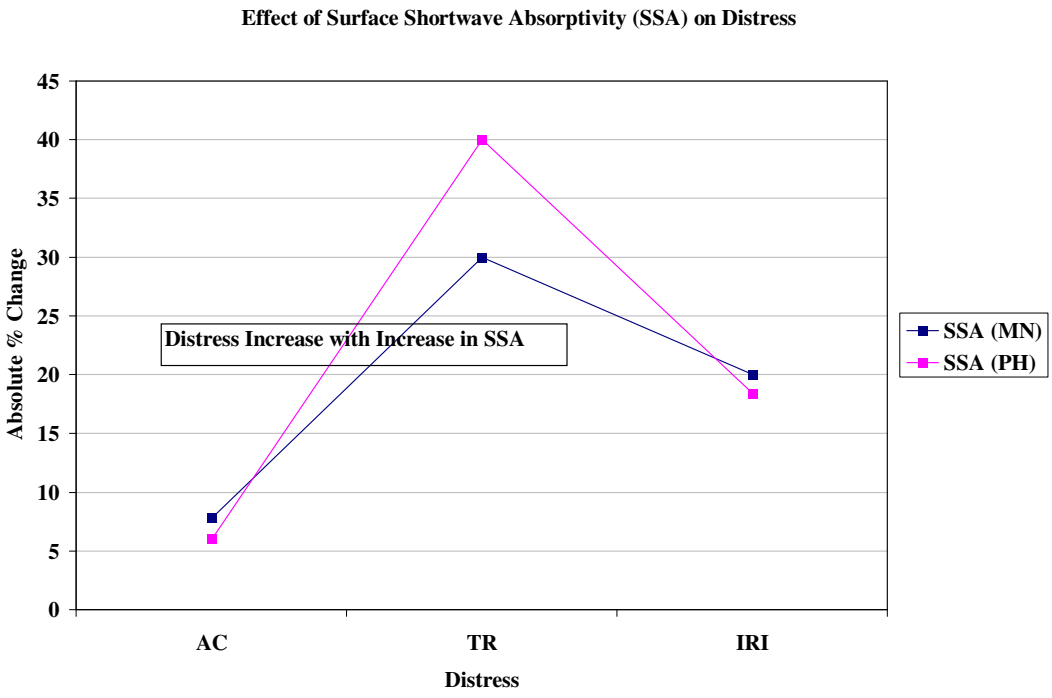

Figure 4.61 Effect of SSA on HMA distress

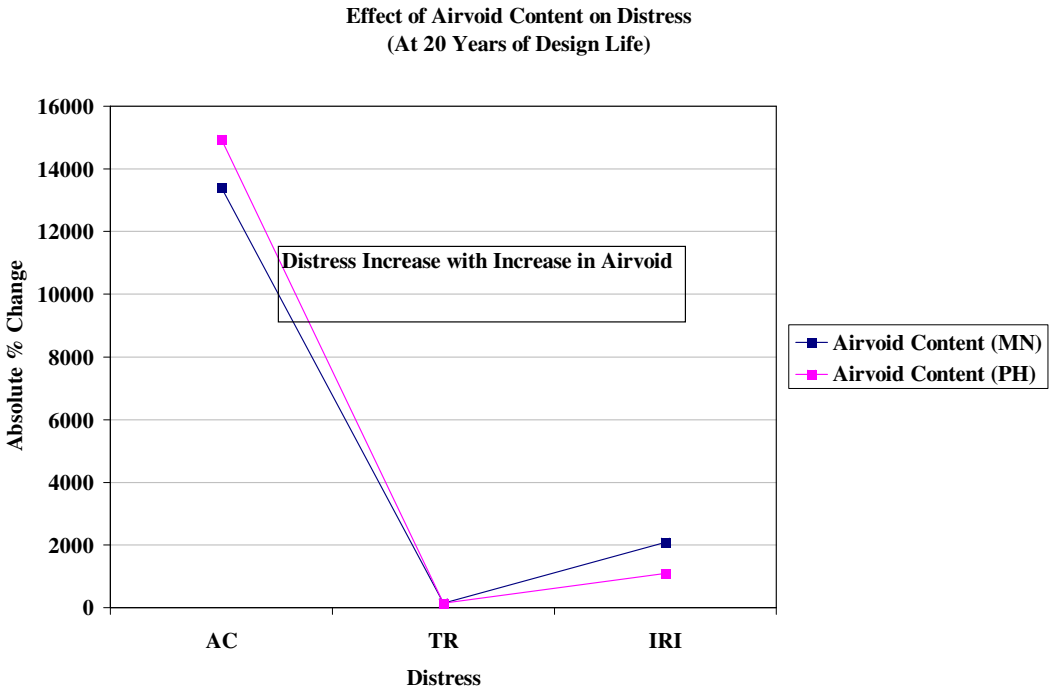

Figure 4.62Effect of airvoid content on HMA distress

4.5 Anomalies in the MEPDG Predictions

4.5.1 Anomalies in JPCP Performance Predictions

Surface Shortwave Absorptivity

Transverse cracking in JPCP's occur due to a combination of repeated loads and high temperature gradients through the depth of the pavement. It has been observed in the previous sections that SSA has no effect on JPCP transverse cracking which seems unreasonable. In the sensitivity studies, while changing the SSA values from 0.5 to 1.0 other thermal properties were kept at a standard value. For a given thermal conductivity, as SSA increases, the temperature gradients across the pavement depth increase, increasing the transverse cracking. But this behavior is not seen in the MEPDG results.

Ultimate Shrinkage Strain

According to MEPDG, ultimate shrinkage strain has no effect on transverse cracking which seems unreasonable. As shrinkage strains increases, warping stresses in PCC slabs increase leading to more cracking.

4.5.2 Anomalies in HMA Performance Predictions

From the sensitivity results of HMA thermal properties, it's clear that thermal conductivity and mix co-efficient of thermal contraction has no effect in HMA distress predictions which seems unreasonable. Also, according to MEPDG, climate has no effect on alligator cracking when clearly alligator cracking is governed by climate for the reasons explained in the alligator cracking section. Transverse cracking or thermal cracking model in the software is insensitive to all variables which evidently prove that there is some problem with the model.

4.6 Finite Element Method Analysis of Heat Transfer in Pavements

The finite element method (FEM) is used for finding approximate solutions of partial differential equations (PDE) as well as of integral equations such as the heat transport equation. In the previous chapters it has been revealed that rigid and flexible performance predictions are highly sensitive to some of the thermal parameters. Further research is needed to address issues pertaining to the impact of thermal properties on design. Standard test methods or protocols for laboratory or field-testing of some of these parameters are currently either nonexistent or unknown to the pavement community. The ultimate goal of this section is to address the capabilities of the finite element methods in predicting the sensitivity of thermal properties of pavement materials in predicting the heat flow in pavements.

4.6.1 Experiment Design

In MEPDG, a one dimensional finite element difference method has been used to populate the temperature profiles in all the pavement layers which in turn are used to predict pavement response. But the draw back of this one dimensional finite difference method is that each layer has been divided into sub-layers where the material is considered uniform within that finite layer and the thermal properties are fixed for each of these layers. But in reality the various materials in the pavements have different thermal properties and hence its not reasonable to assume uniform layers for predicting the temperatures in the pavement layers. This section predicts the temperature profiles in a pavement layer by considering the thermal properties of its constituent materials.

Effect of material thermal properties on Heat Transfer in Pavements

Thermal properties of the materials used in the pavements determine the heat flow in the pavements and eventually affect the performance of the pavements in a considerable way. A FEM model has been developed to simulate the heat transfer in asphalt pavements given the different thermal properties of constituent materials. Figure 4.63 shows the template used for the FEM analysis. The entity in the middle of the template is the material whose thermal properties are changed and in the present study airvoid, water, granite and limestone are considered. The material around the entity is asphalt concrete. Table 4.1 shows the materials which have been considered for the simulation. A temperature difference of 27^0C has been chosen. One end of the pavement is fixed at 313 K and the other end at 286 K. The boundaries have been insulated to make the flow uni-directional. The FEM simulation has been carried out using COMSOL Multiphysics software which has readily available heat

transfer modules which can carry out conduction, convection and radiation in different materials. In the present preliminary study, only conduction has been considered. In future studies conduction, convection and radiation will be considered.

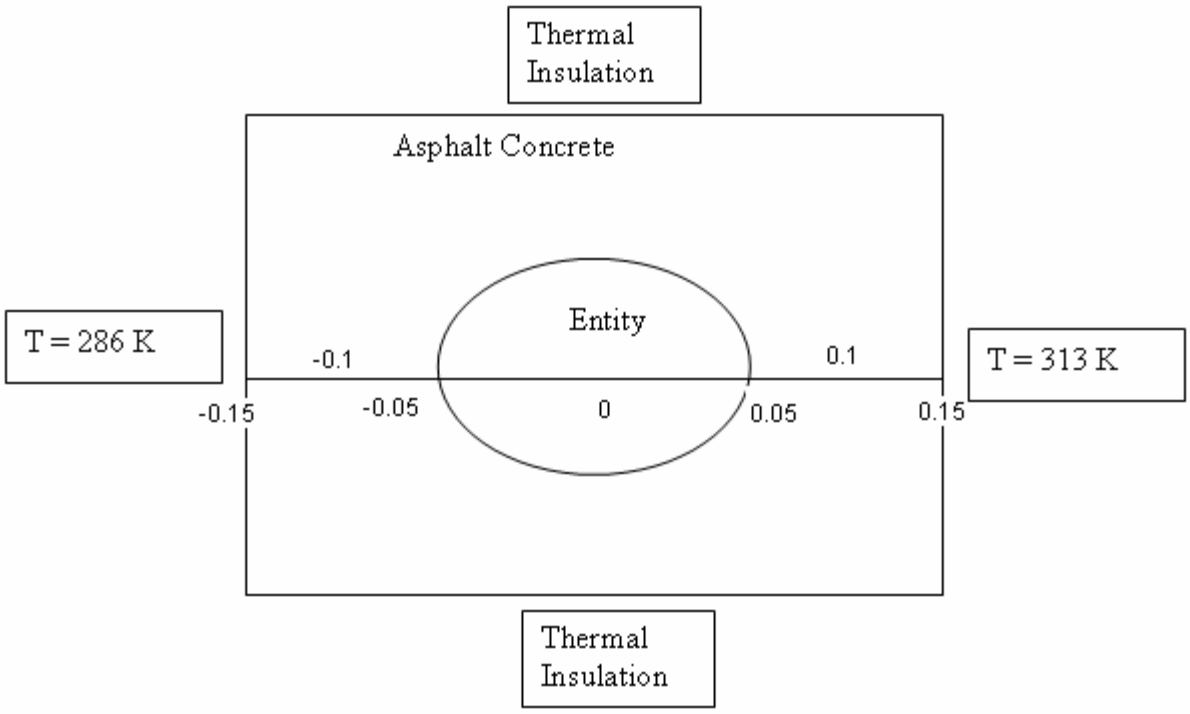

Figure 4.63 Pavement template used for the FEM analysis

Results

Temperature profiles are taken at the following Locations (0, 0.15), (0, 0.1) and (0.05) which are in front of the entity, (0, 0) the center of the entity and (0,-0.05), (0,-0.1) and (0,-0.15) which are behind the entity. The temperature profiles have been taken for each entity at these locations at steady state and are plotted together as shown below. The objective of these locations is to see how heat flow is affected before and after entering the entity based on their

thermal properties which are very important and this is discussed later in this report. The results for the temperature profiles for different entities are plotted as shown in the Figure 4.64.

Table 4.1Thermal properties of constituent materials used in the FEM analysis

Material Entity	Density $\rho\ (kg/m^3)$	Thermal Conductivity $K\ (w/m.k)$	Heat Capacity $C_p\ (J/kg.k)$
Granite	2600	4	790
Air-void	1	0.025	1012
Water	1000	0.58	4181.3
Lime Stone	1760	1.33	840
Asphalt	1100	0.75	920
Concrete	2300	1.8	880

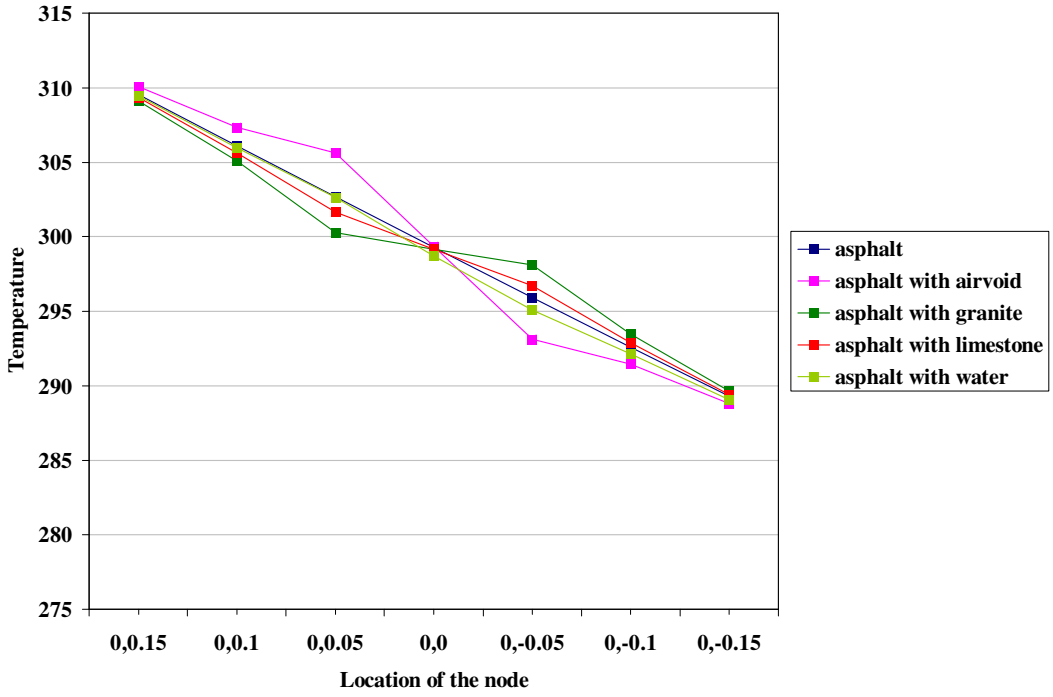

Figure 4.64 Temperature profiles with different entities

As seen from Figure 4.64, temperatures before an entity are higher in airvoid followed by asphalt, water, limestone and granite. However, after the heat wave has passed the entity, temperatures are high in granite followed by limestone, asphalt, water and airvoid. This evidently explains the fact that, airvoid which has almost zero thermal conductivity does not allow the heat wave to pass the entity, hence the temperatures are high before the entity and lower behind the entity. Hence as thermal conductivity of an entity increases, heat wave passes more effectively. To simulate the heat transfer in a pavement with all of the above materials, another template was created which is shown in Figure 4.65. Boundary conditions chosen for the simulation are shown in the Figure 4.65. Results of the simulation are shown below.

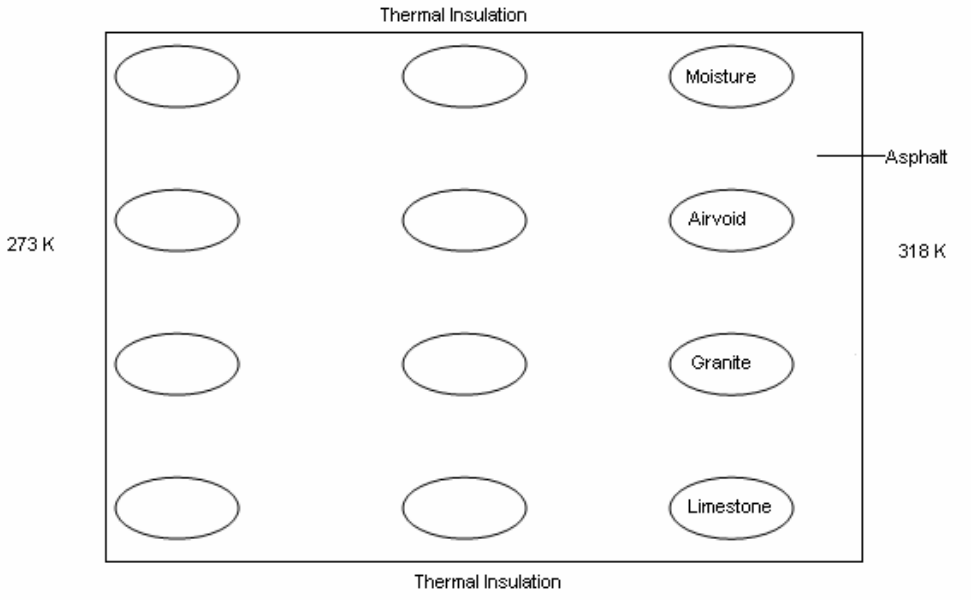

Figure 4.65 Template to simulate heat transfer with different materials

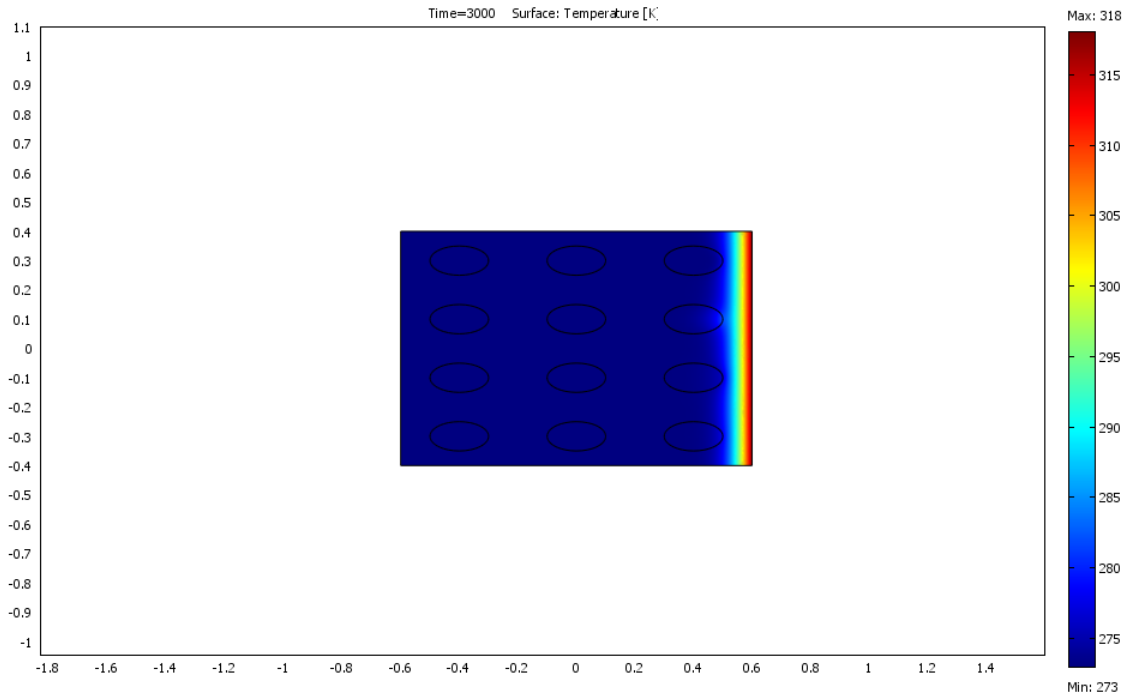

Figure 4.66 Screen shot of simulation at time = 3000 s

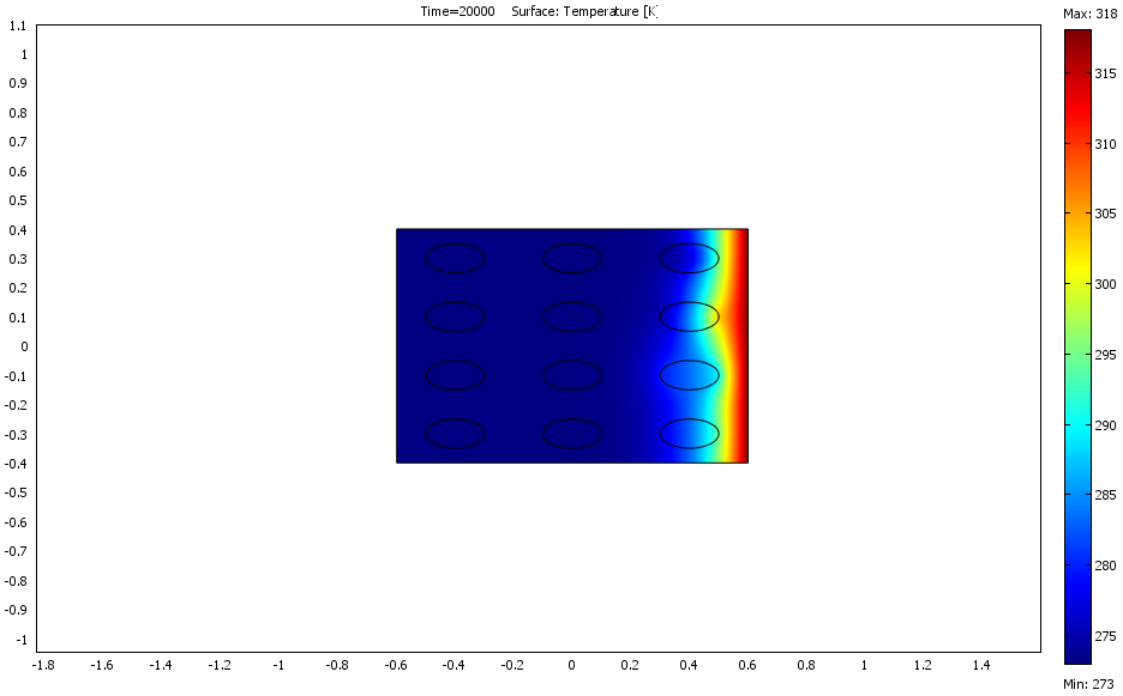

Figure 4.67 Screen shot of simulation at time = 20000 s

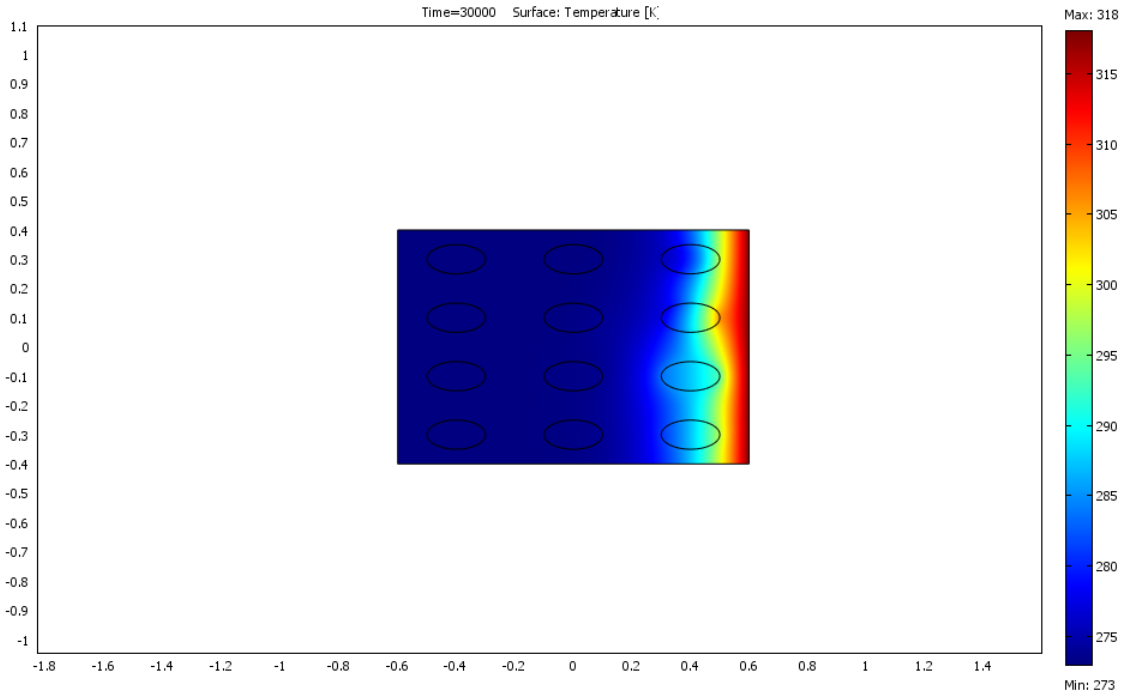

Figure 4.68 Screen shot of the simulation at time = 30000 s

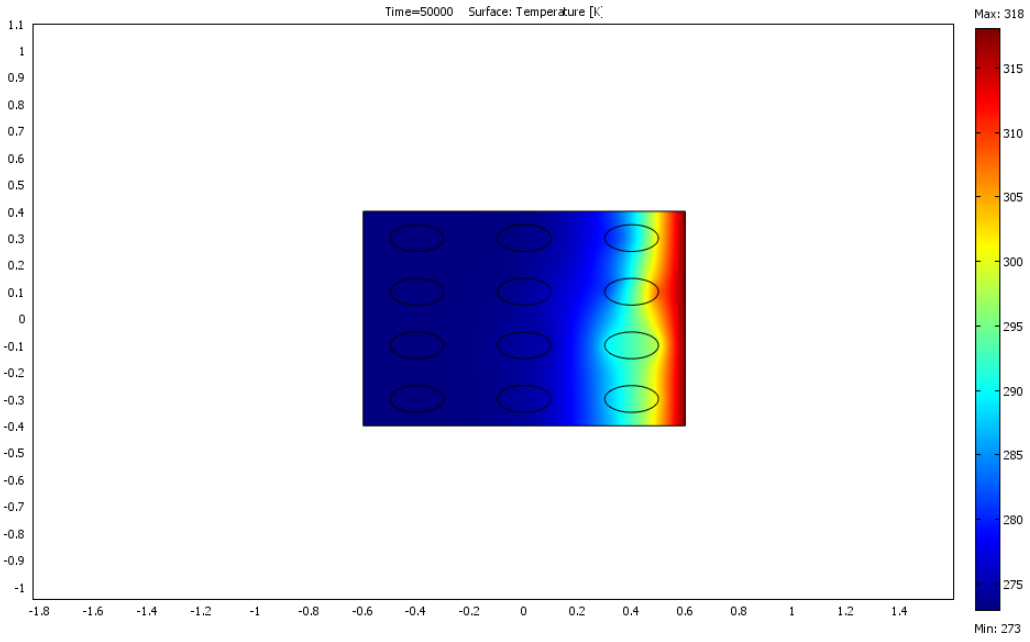

Figure 4.69 Screen shot of simulation at time = 50000 s

Chapter 5 Conclusions and Future Work

5.1 Conclusions for Sensitivity Analysis

Sensitivity analysis done as part of this study helped to identify the basic behavior of the models and to identify some flaws in the MEPDG models and the software. From all the cases run as part of this study, the following conclusions have been drawn:

1. In spite of requiring a large number of inputs, the software is very user-friendly with very useful help files.

2. Some of the inputs required by the software are hard to obtain, since there are no standard test methods for these inputs, so the designer has to rely on default values suggested by the Design Guide or use approximate values. Some of the inputs for which default values are assumed have significant impact on predicted performance.

3. On average, in JPCP's, both the cracking and faulting models show trends that agree with prevailing knowledge in pavement engineering. According to MEPDG, JPCP transverse cracking is sensitive to thermal conductivity, coefficient of thermal expansion (CTE), and climate zone. Faulting, according to MEPDG, is sensitive to dowels, thermal conductivity, co-efficient of thermal expansion, surface shortwave absorptivity (SSA) and climate zone. IRI, according to MEPDG, is sensitive to thermal conductivity, CTE and SSA.

4. On average, in CRCP's, punchout and IRI models show trends that agree with prevailing knowledge in pavement engineering. According to MEPDG, CTE is the most sensitive parameter to punchouts followed by crack spacing, ultimate shrinkage strain, climate, SSA and thermal conductivity. IRI, according to MEPDG, is sensitive to CTE.

5. On average, in HMA pavements, rutting, alligator cracking, longitudinal cracking and IRI models shows trends that agree with prevailing knowledge in pavement engineering. According to MEPDG, airvoid content, traffic volume, thickness of the asphalt layer, SSA and climate zone are the most sensitive parameters which affect rutting and alligator cracking followed by heat capacity and thermal conductivity.

6. According to MEPDG, in JPCP's, thermal conductivity, heat capacity, SSA and CTE affect cracking the most compared to faulting and smoothness(IRI).However, ultimate shrinkage affects faulting the most.

7. According to MEPDG, in CRCP's, thermal conductivity, ultimate shrinkage, heat capacity, SSA and CTE affect punchouts the most compared to smoothness (IRI).

8. According to MEPDG, in HMA pavements, thermal conductivity and heat capacity does not affect any distress, SSA affects total rutting (TR) more compared to alligator cracking (AC) and smoothness (IRI). Percentage Airvoid content affects AC more compared to TR and IRI.

9. There are some specific cases for which the models predict results that do not agree with accepted pavement knowledge.

- Anomaly, applicable to JPCP transverse cracking is SSA. It is a redundant variable for cracking.
- Anomaly, applicable to HMA rutting, cracking and IRI, is mix co-efficient of thermal contraction which is a redundant variable.
- Anomaly, applicable to HMA pavements, thermal cracking module is insensitive to all variables.
- Anomaly, applicable to HMA alligator cracking, climate has no effect.

This study is by no means exhaustive. A couple of related sensitivity studies have been performed to evaluate the impact of some of the variables that were not included in the report. There could still be some flaws that were unidentified and there still could be some variables that seem very innocuous but have significant impact on distress models. Overall the rigid and flexible part of the MEPDG Version 1.0 produces reasonable predictions of pavement performance. However, the accuracy of the predictions needs to be validated by using field data. If MEPDG Version 1.0 needs to be used for pavement design, it should be used with some caution, keeping in mind the anomalies mentioned in the report.

5.2 Conclusions for FEM Analysis

Heat transfer in asphalt pavements has been simulated by taking into account the thermal properties of the constituent materials. In case of asphalt pavements, it is clearly shown that heat flows uniformly until it reaches an entity whose thermal properties are different from that of asphalt. It is seen that the heat front enters into air voids first when compared to water, limestone and granite. But since the thermal conductivity of air is nearly zero it does not propagate the heat front further, trapping the heat in its empty space where as heat flows smoothly through granite and limestone. Same is the case with water, because of its low thermal conductivity when compared to granite and limestone, heat front passes much faster in granite and limestone when compared to water. This leads to conclusion, that it is not recommended to have more air voids or water on the surface of the pavement because it leads to more heat getting absorbed into the surface but not propagating further down the pavement depth making the heat trapped on the surface and this is a disadvantage for the pavement

surface. The more heat gets trapped on the surface, the more the asphalt gets aged and less performance because of distresses.

5.3 Future Work

The main objective of the future study would be to simulate heat transfer in real pavements by considering conduction, convection and radiation. To capture the real interiors of the pavement structure, with the shape of the aggregates and airvoid distribution, for which X-ray Tomography Technique is one of the best tools available in the pavement community.

5.3.1 X-ray Tomography Technique

X-ray computed tomography (CT) is a completely nondestructive technique for visualizing features in the interior of opaque solid objects (in our case, concrete and asphalt cores) to obtain digital information on their 3-D geometry and properties [24]. It is also known as computerized axial tomography, computed assisted tomography, or CAT scanning. An illustration of a typical X-ray CT system is given in Figure 5.1. The system is composed of an X-ray source, a collimator (window), and a detector. In principle, planar X-rays are directed towards the specimen, and the specimen absorbs some portion of the X-rays. Unabsorbed portion is detected by an array of detector cells in the detector. The ratio of unabsorbed X-rays to the X-rays coming from the source gives a CT number (Figure 5.1b). As the specimen is rotated, CT numbers are collected from various different directions. After a full 360- degree rotation, a set of CT numbers collected for all directions generates an image slice. Then, the specimen is shifted vertically by a certain amount and entire process is repeated to obtain additional slices. The amount of vertical shift was determined by the thickness of the detector aperture, t_d; i.e. the specimen is shifted at an interval of t_d so the

image of the entire specimen can be captured. As a result, the total number of image slices for a specimen is the height of the specimen divided by t_d. A three dimensional image of the specimen can be generated by stacking these image slices as shown in Figure 5.2.

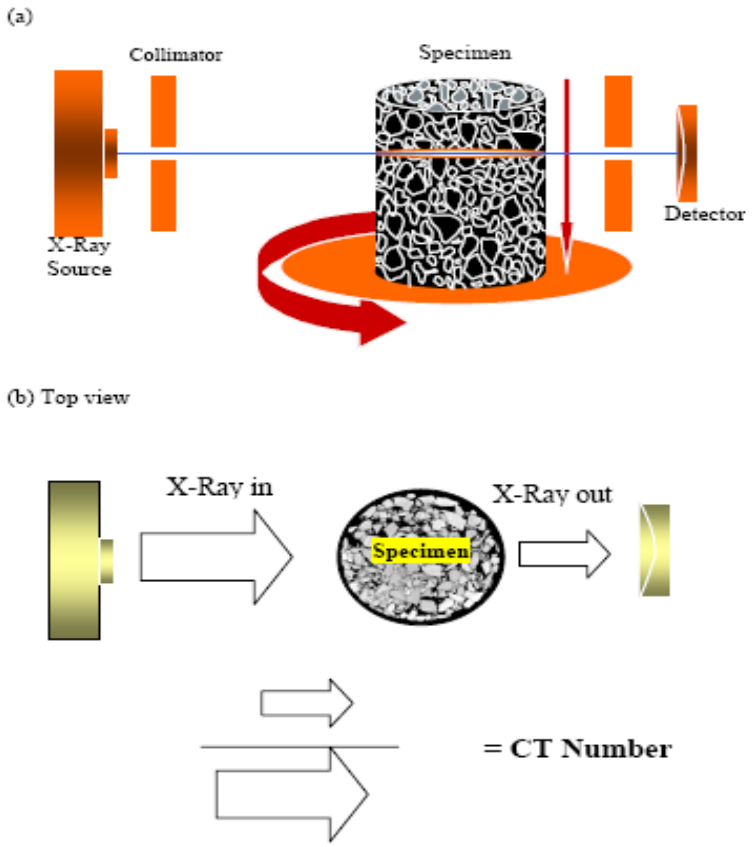

Figure 5.1Illustration of (a) a typical X-Ray CT system, and (b) acquiring CT number [24]

The magnitude of X-rays sent to the specimen should be carefully selected during scanning. If too much X-rays are sent to a low density material, CT number shown in Figure 5.1b will be very high, i.e., most of the X-rays will pass through the material. This may lead to poor contrast within different regions in a test specimen. Therefore, before scanning the entire

specimen, preliminary scans should be conducted at different X-ray levels until the best contrast is achieved. Research is now underway at Federal Highway Administration (FHWA) to develop a finite element heat transfer model which takes this 3D digital structure, obtained by X-ray CT, and develops thermal models from the thermal properties of the constituent materials. As part of the research, different aggregates have already been scanned using X-ray CT and two of the scans with different aggregates are shown below in Figures 5.3 and 5.4. A small code has already been written in MATLAB to import the X-ray CT image into COMSOL and a preliminary heat transfer is simulated in COMSOl as shown in Figure 5.5. Future research would be basically to develop the 3D images of the asphalt and concrete cores using X-ray CT and then importing them into finite element software like COMSOL and then prepare finite element models for heat transfer in pavements by considering conduction, convection and radiation.

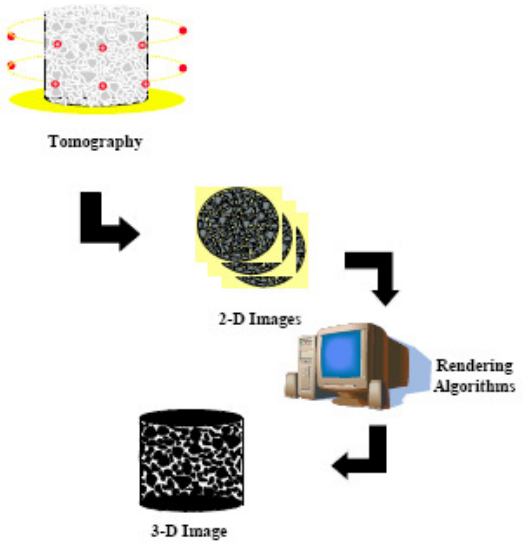

Figure 5.2 Illustration of generation of 3D structure from X-Ray CT [24]

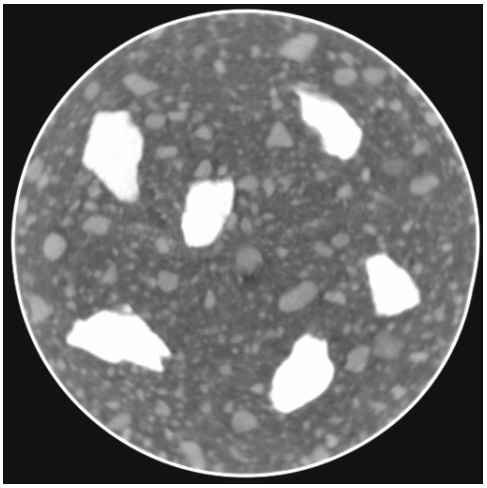

Figure 5.3 X-ray Tomography Image of Granite Aggregates in Cement Powder

.

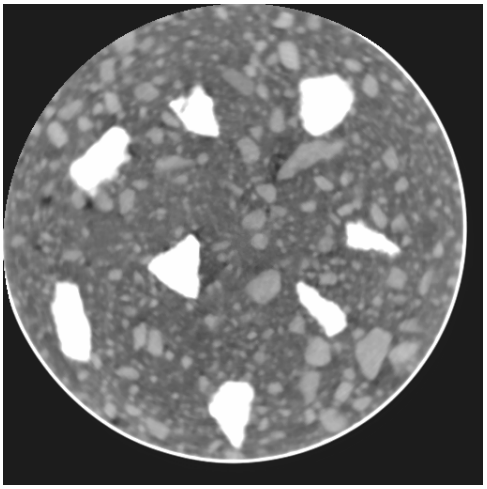

Figure 5.4 X-ray Tomography Image of Alf-Diabase Aggregate in Cement Powder

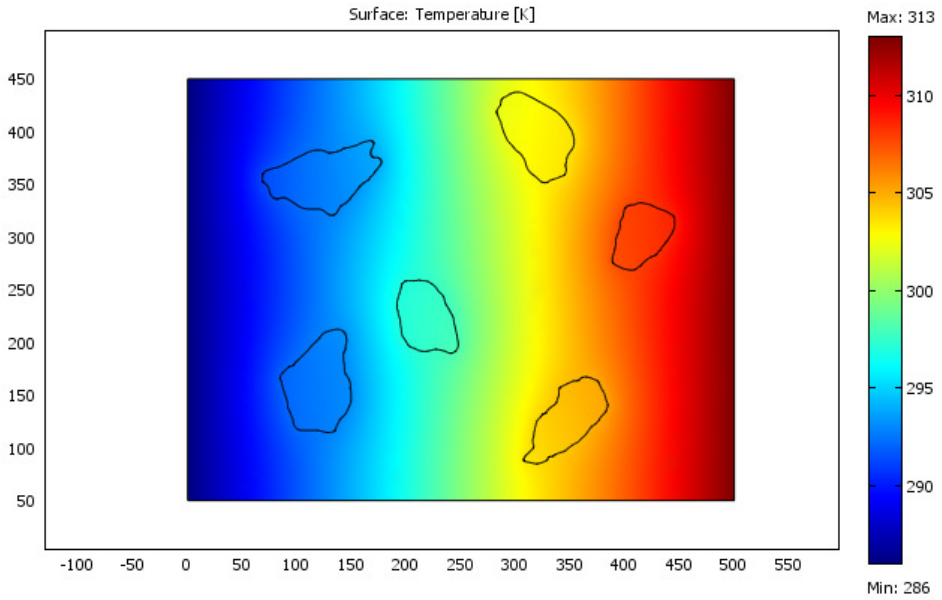

Figure 5.5 Preliminary heat transfer simulated in X-ray CT image by COMSOL

References

[1] Yoder, E.J. and Witczak, M.W., "Principles of Pavement Design: 2nd Edition", John Wiley, New York, 1975

[2] ERES Division of ARA, Inc., "Guide for Mechanistic-Empirical Design of New and Rehabilitated Pavement Structures: Part2. Chapter 2.", NCHRP,1-37A, 2004

[3] ERES Division of ARA, Inc., "Guide for Mechanistic-Empirical Design of New and Rehabilitated Pavement Structures: Part1. Chapter 1.", NCHRP,1-37A, 2004

[4] ERES Division of ARA, Inc., "Guide for Mechanistic-Empirical Design of New and Rehabilitated Pavement Structures: Part3. Chapter 3.", NCHRP,1-37A, 2004

[5] ERES Division of ARA, Inc., "Guide for Mechanistic-Empirical Design of New and Rehabilitated Pavement Structures: Part3. Chapter 4.", NCHRP,1-37A, 2004

[6] John, S.M and William, Y.B., "Distress Identification Manual for the Long-Term Pavement Performance Program: 4th Edition", Publication FHWA-RD-03-031, FHWA, U.S. Department of Transportation, 2003

[7] Kannekanti, V. and Harvey, J., "Sensitivity Analysis of 2002 Design Guide Rigid Pavement Distress Prediction Models", Publication UCPRC-DG-2006-01, California Department of Transportation, 2006

[8] Guclu, A. and Ceylan, H., "Sensitivity Analysis of Rigid Pavement Systems Using Mechanistic-Empirical Pavement Design Guide", Proceedings of the 2005 Mid-Continent Transportation Research Symposium, Iowa, 2005

[9] Sunghwan, K., Ceylan, H. and Michael, H., "Sensitivity Study of Design Input parameters for Two Flexible Pavement Systems Using the Mechanistic-Empirical Pavement Design Guide", Proceedings of the 2005 Mid-Continent Transportation Research Symposium, Iowa, 2005

[10] Ali, A.S., "Service Life of Corrosion-Damaged Reinforced Concrete Bridge Superstructure Elements", NCHRP 18-6A, 2006

[11] Ceylan, H., Sunghwan, K., Dennis, J. T., Robert, O. R., George, K. C., Jim, G., Kasthurirangan, G., "Impact of Curling, Warping, and Other Early-Age Behavior on Concrete Pavement Smoothness: Early, Frequent, and Detailed (EFD) Phase II Study", Publication FHWA DTFH61-01-X-00042 (Project 16), Center for Transportation Research and Education, Iowa State University, 2007

[12] Thermo Technologies Homepage, " Variation of Solar Radiation", http://www.thermomax.com/usdata.htm, Accessed August 16, 2007

[13] Rao, S. and Roesler, J. R., "Characterizing Effective Built-in Curling from Concrete Pavement Field Measurements", Journal of Transportation Engineering, Vol. 131, No.4, pp. 320-327, 2005

[14] Janssen, D.J., "Moisture in Portland Cement Concrete", Transportation Research Record, Vol. 1121, pp. 40-44,1987

[15] ERES Division of ARA, Inc., "Guide for Mechanistic-Empirical Design of New and Rehabilitated Pavement Structures: Appendix JJ", NCHRP,1-37A, 2003

[16] ERES Division of ARA, Inc., "Guide for Mechanistic-Empirical Design of New and Rehabilitated Pavement Structures: Appendix PP", NCHRP,1-37A, 2001

[17] Darter, M.I., LaCourseiere S.A., and Smiley, S.A., "Performance of Continuously Reinforced Concrete Pavement in Illinois." Transportation Research Record No. 715, Transportation Research Board, Washington, DC, 1979.

[18] LaCourseiere, S.A., Darter, M.I., and Smiley, S.A., "Structural Distress Mechanisms in Continuously Reinforced Concrete Pavement," Transportation Engineering Series No. 20, University of Illinois at Urbana-Champaign, 1978.

[19] Zollinger, D.G., Buch, N., Xin, D., and Soares, J., "Performance of CRCP Volume 6 – CRCP Design, Construction, and Performance," Publication FHWA-RD-97-151, U.S. Department of Transportation, Washington, DC, 1998.

[20] ERES Division of ARA, Inc., "Guide for Mechanistic-Empirical Design of New and Rehabilitated Pavement Structures: Appendix LL", NCHRP,1-37A, 2003

[21] ERES Division of ARA, Inc., “Guide for Mechanistic-Empirical Design of New and Rehabilitated Pavement Structures: Appendix GG-1”, NCHRP,1-37A, 2004

[22] ERES Division of ARA, Inc., “Guide for Mechanistic-Empirical Design of New and Rehabilitated Pavement Structures: Appendix II-1”, NCHRP,1-37A, 2004

[23] ERES Division of ARA, Inc., “Guide for Mechanistic-Empirical Design of New and Rehabilitated Pavement Structures: Appendix HH”, NCHRP,1-37A, 2003

[24] Emin, K.M., “Modeling Moisture Transport in Asphalt Pavements”, PhD Thesis, University of Maryland, 2005

Appendix A: Screenshots from the MEPDG Software

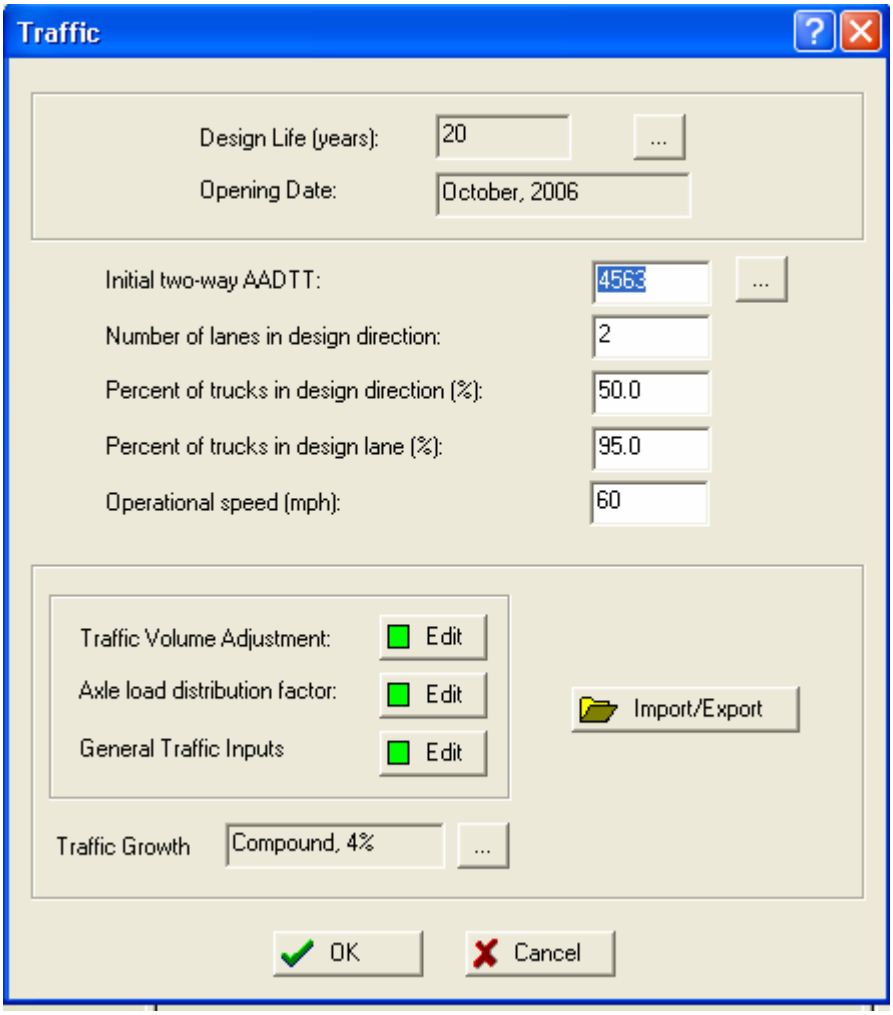

Figure A.1 General Traffic inputs used for both flexible and rigid pavements

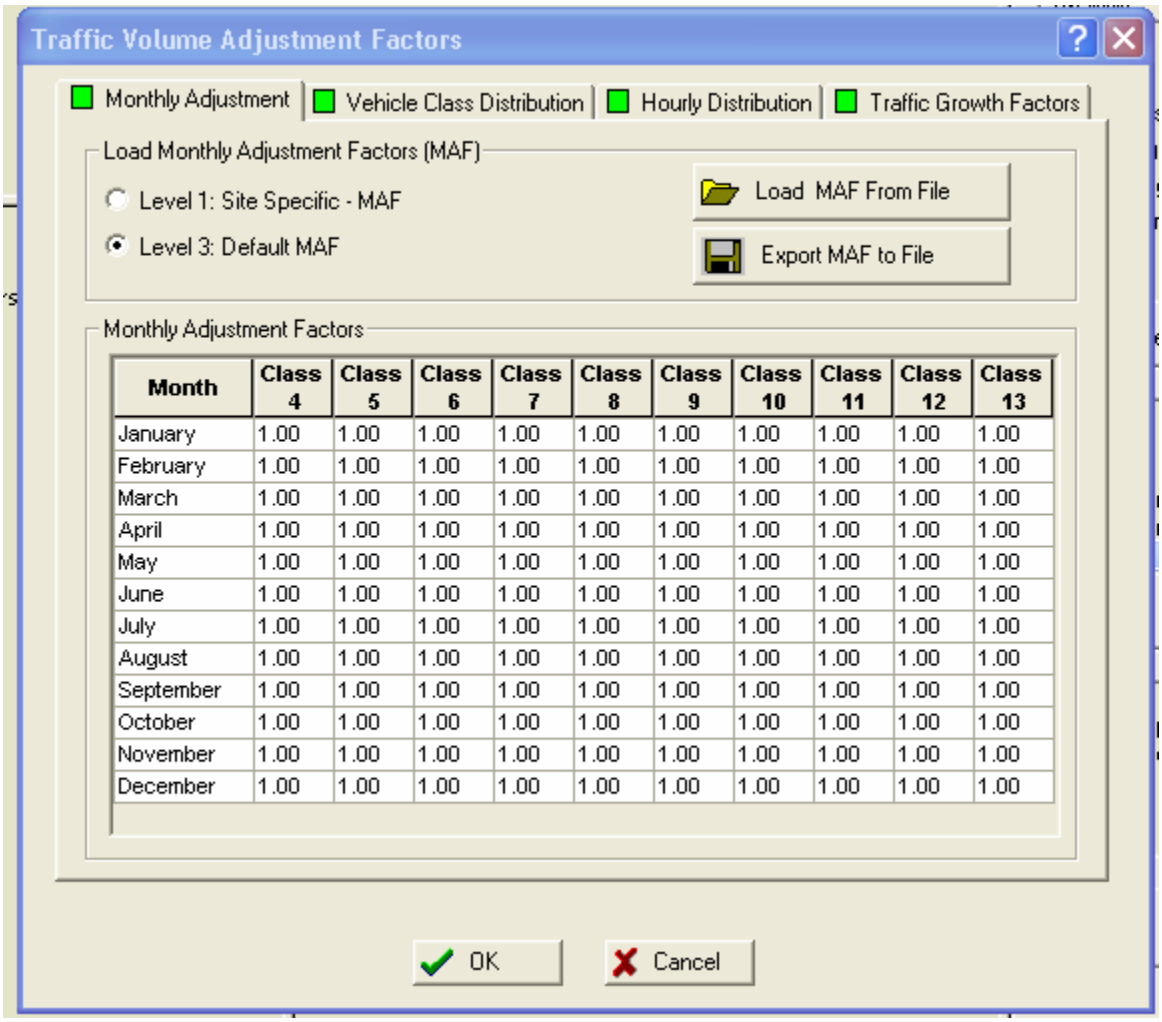

Month	Class 4	Class 5	Class 6	Class 7	Class 8	Class 9	Class 10	Class 11	Class 12	Class 13
January	1.00	1.00	1.00	1.00	1.00	1.00	1.00	1.00	1.00	1.00
February	1.00	1.00	1.00	1.00	1.00	1.00	1.00	1.00	1.00	1.00
March	1.00	1.00	1.00	1.00	1.00	1.00	1.00	1.00	1.00	1.00
April	1.00	1.00	1.00	1.00	1.00	1.00	1.00	1.00	1.00	1.00
May	1.00	1.00	1.00	1.00	1.00	1.00	1.00	1.00	1.00	1.00
June	1.00	1.00	1.00	1.00	1.00	1.00	1.00	1.00	1.00	1.00
July	1.00	1.00	1.00	1.00	1.00	1.00	1.00	1.00	1.00	1.00
August	1.00	1.00	1.00	1.00	1.00	1.00	1.00	1.00	1.00	1.00
September	1.00	1.00	1.00	1.00	1.00	1.00	1.00	1.00	1.00	1.00
October	1.00	1.00	1.00	1.00	1.00	1.00	1.00	1.00	1.00	1.00
November	1.00	1.00	1.00	1.00	1.00	1.00	1.00	1.00	1.00	1.00
December	1.00	1.00	1.00	1.00	1.00	1.00	1.00	1.00	1.00	1.00

FigureA.2 Traffic volume adjustment factors used for both flexible and rigid pavements

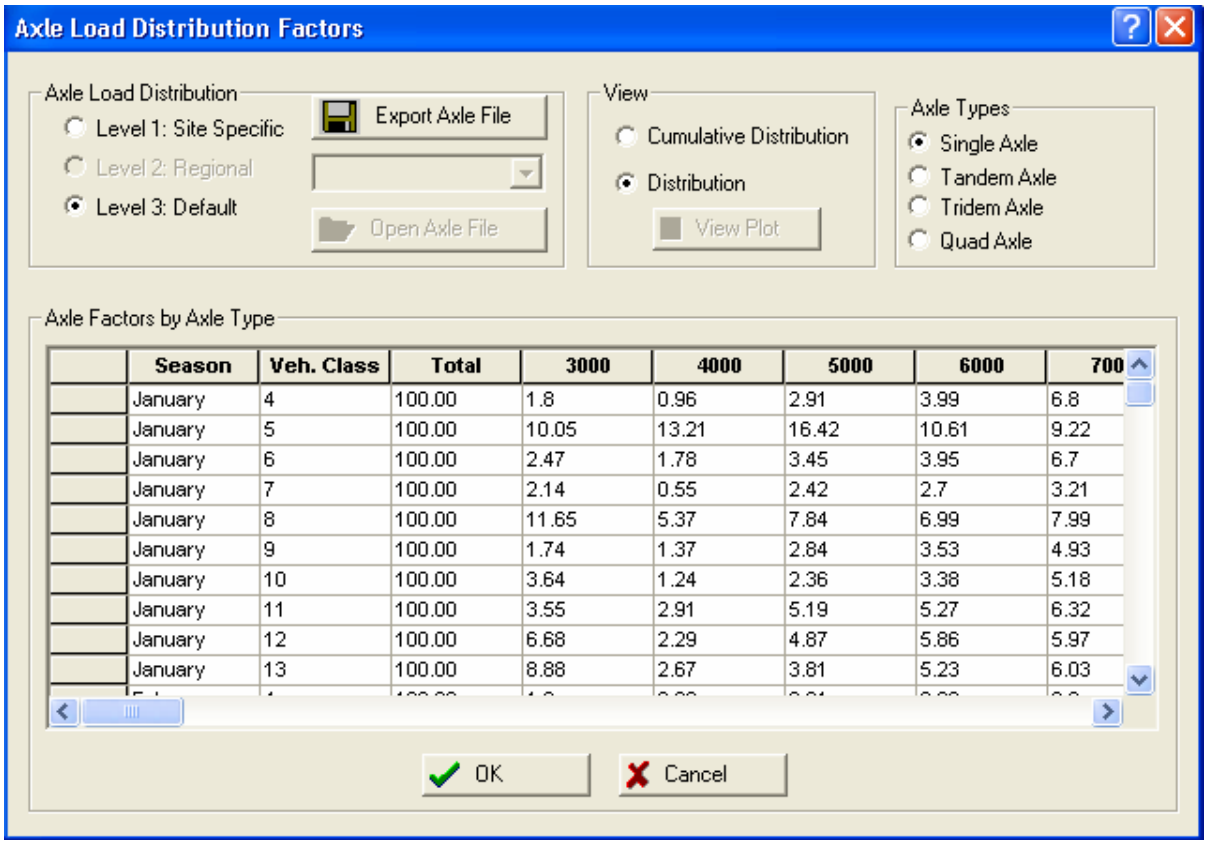

	Season	Veh. Class	Total	3000	4000	5000	6000	700
	January	4	100.00	1.8	0.96	2.91	3.99	6.8
	January	5	100.00	10.05	13.21	16.42	10.61	9.22
	January	6	100.00	2.47	1.78	3.45	3.95	6.7
	January	7	100.00	2.14	0.55	2.42	2.7	3.21
	January	8	100.00	11.65	5.37	7.84	6.99	7.99
	January	9	100.00	1.74	1.37	2.84	3.53	4.93
	January	10	100.00	3.64	1.24	2.36	3.38	5.18
	January	11	100.00	3.55	2.91	5.19	5.27	6.32
	January	12	100.00	6.68	2.29	4.87	5.86	5.97
	January	13	100.00	8.88	2.67	3.81	5.23	6.03

Figure A.1 Axle load distribution factors used for both flexible and rigid pavements

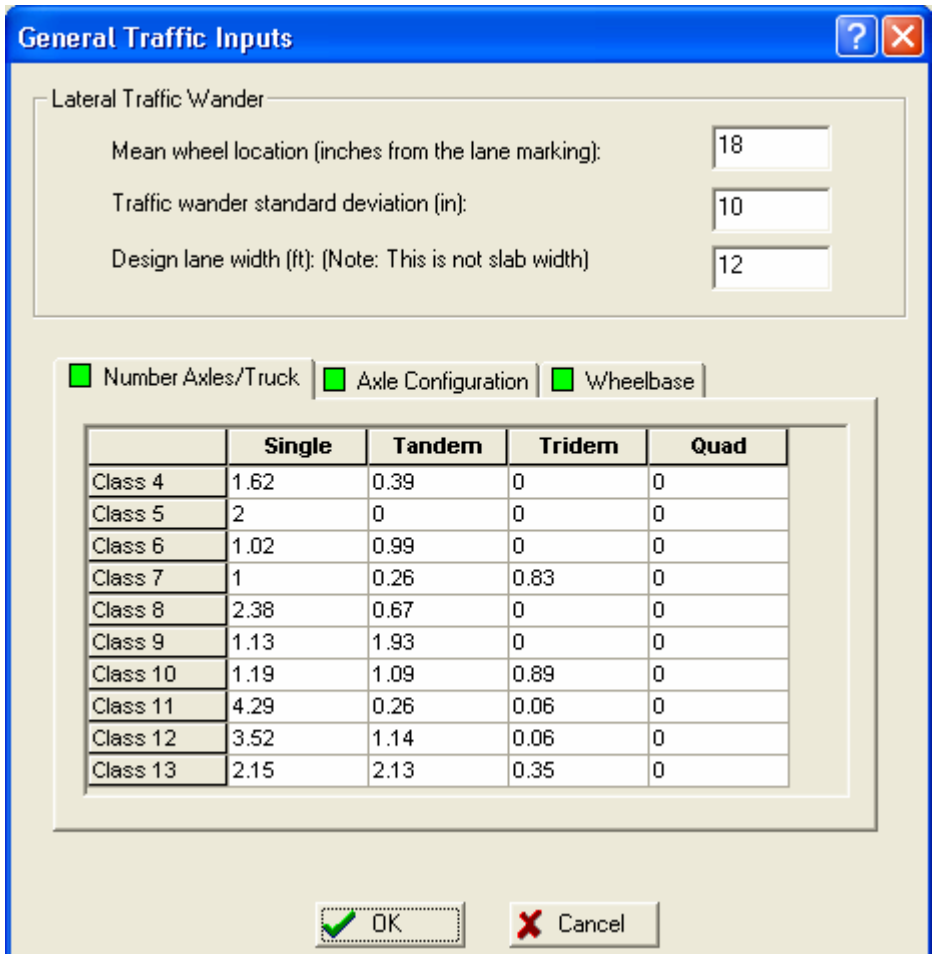

	Single	Tandem	Tridem	Quad
Class 4	1.62	0.39	0	0
Class 5	2	0	0	0
Class 6	1.02	0.99	0	0
Class 7	1	0.26	0.83	0
Class 8	2.38	0.67	0	0
Class 9	1.13	1.93	0	0
Class 10	1.19	1.09	0.89	0
Class 11	4.29	0.26	0.06	0
Class 12	3.52	1.14	0.06	0
Class 13	2.15	2.13	0.35	0

Figure A.2 General traffic inputs

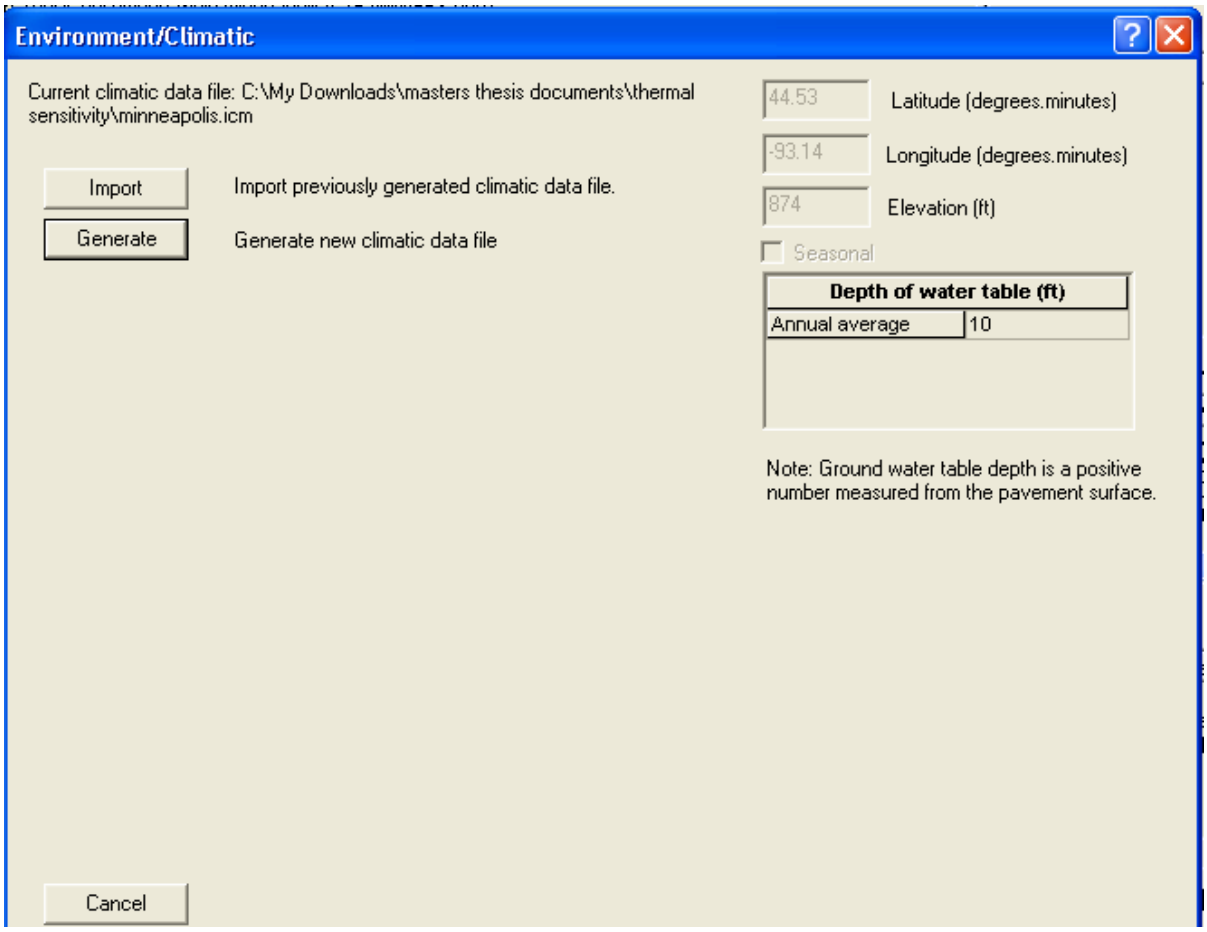

Figure A.3 Climate input window

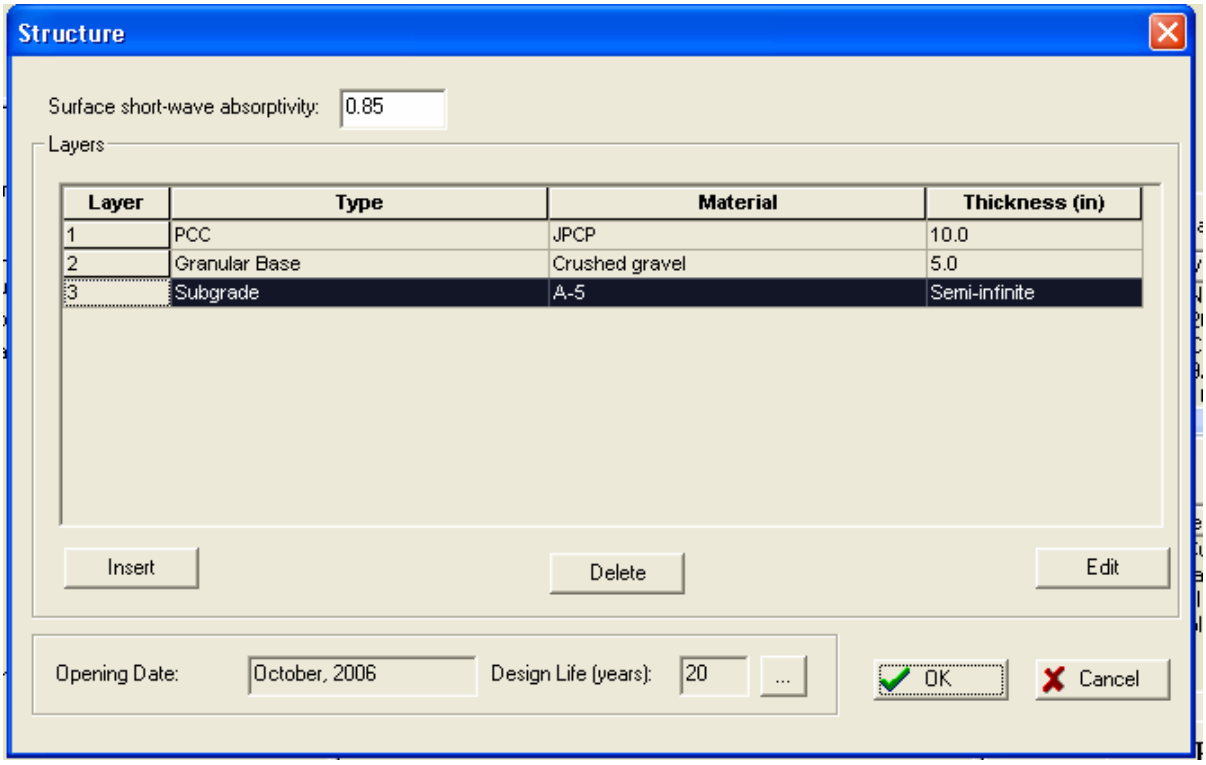

Figure A.4 JPCP structure design template

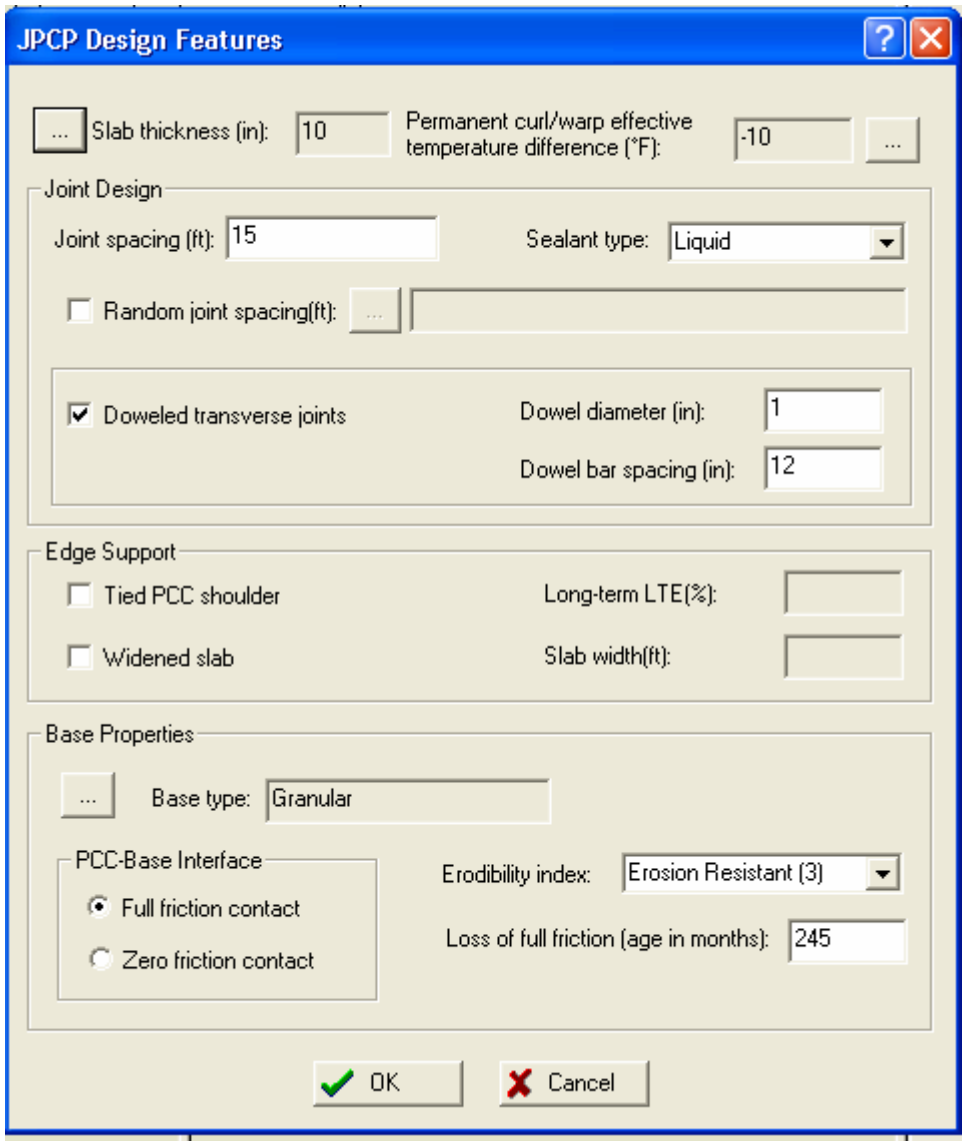

Figure A.5 JPCP Design Features

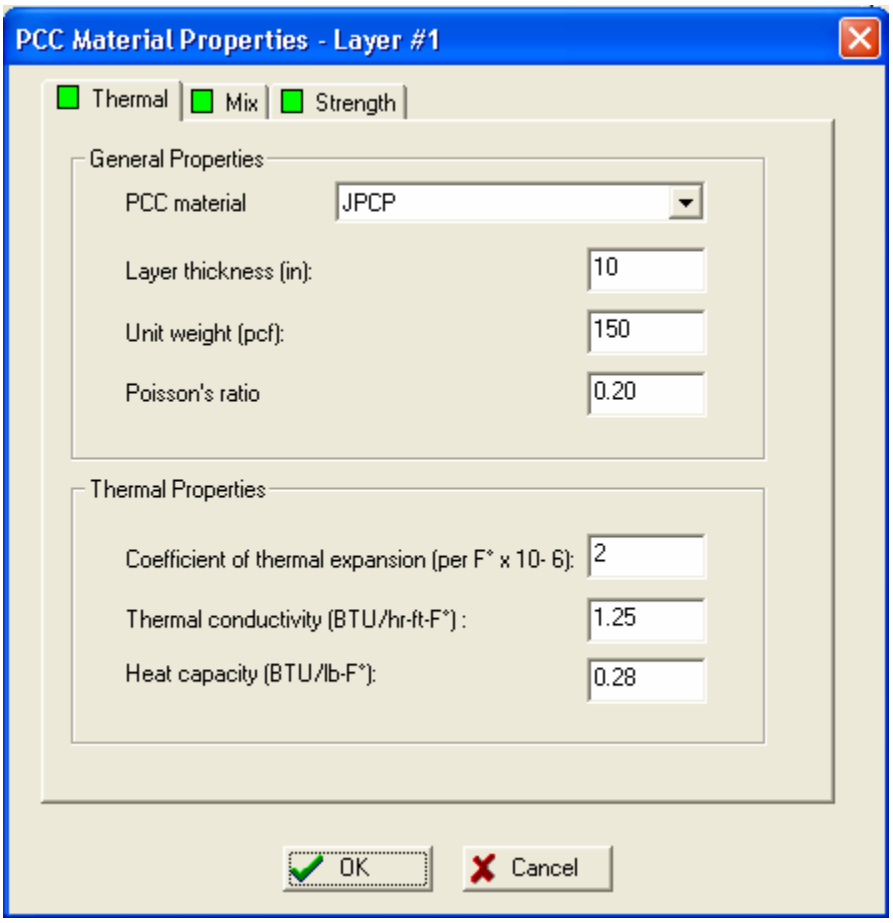

Figure A.6 PCC material properties input template

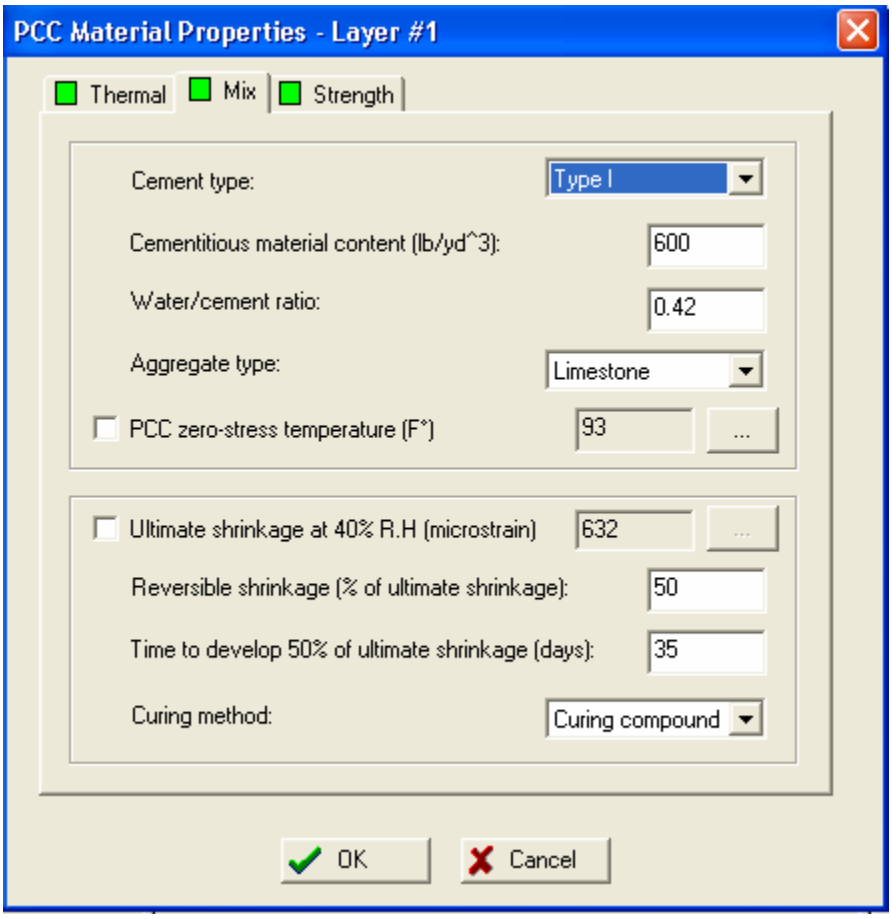

Figure A.7 Mix properties input template

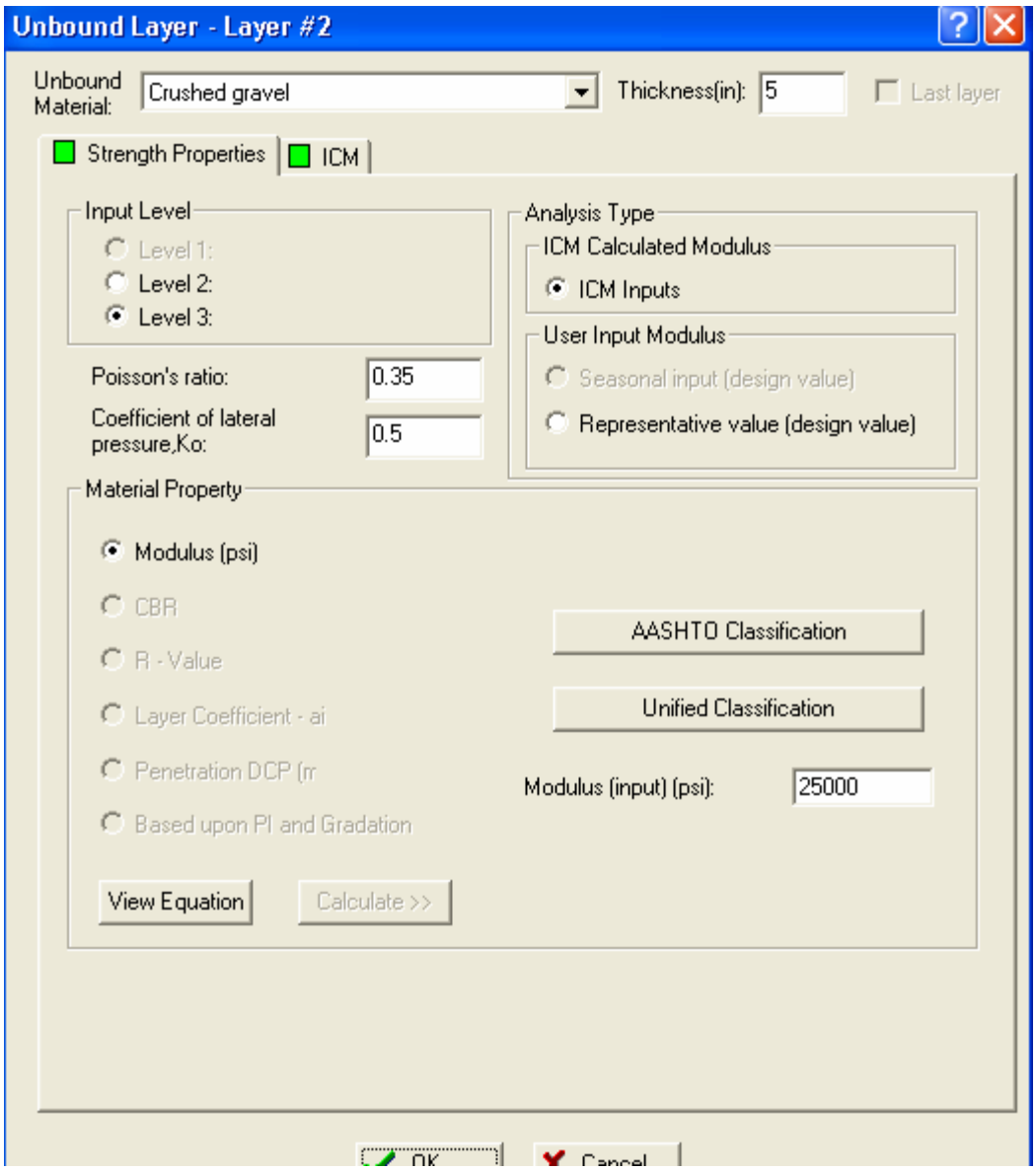

Figure A.8 Base properties input template

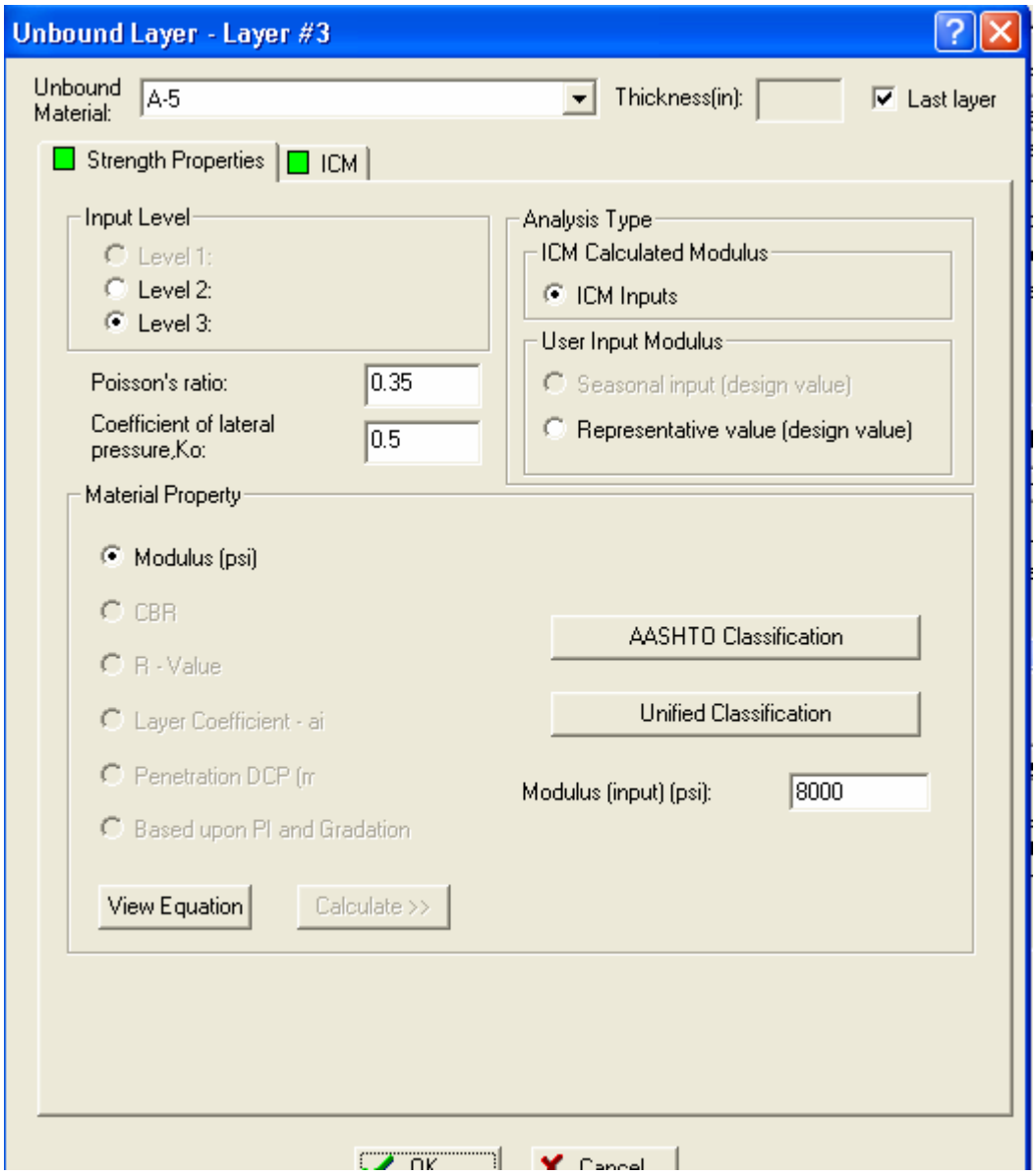

Figure A.9 Subgrade input template

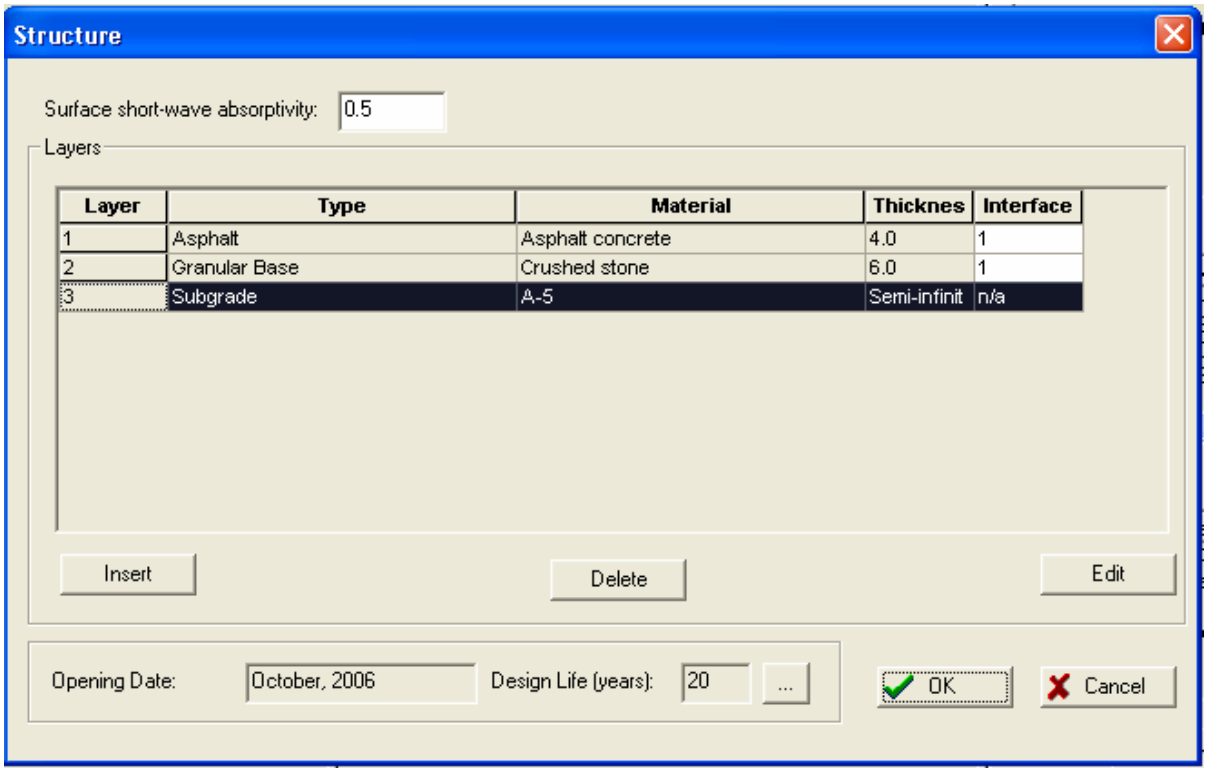

Figure A.10 HMA pavement structure input template

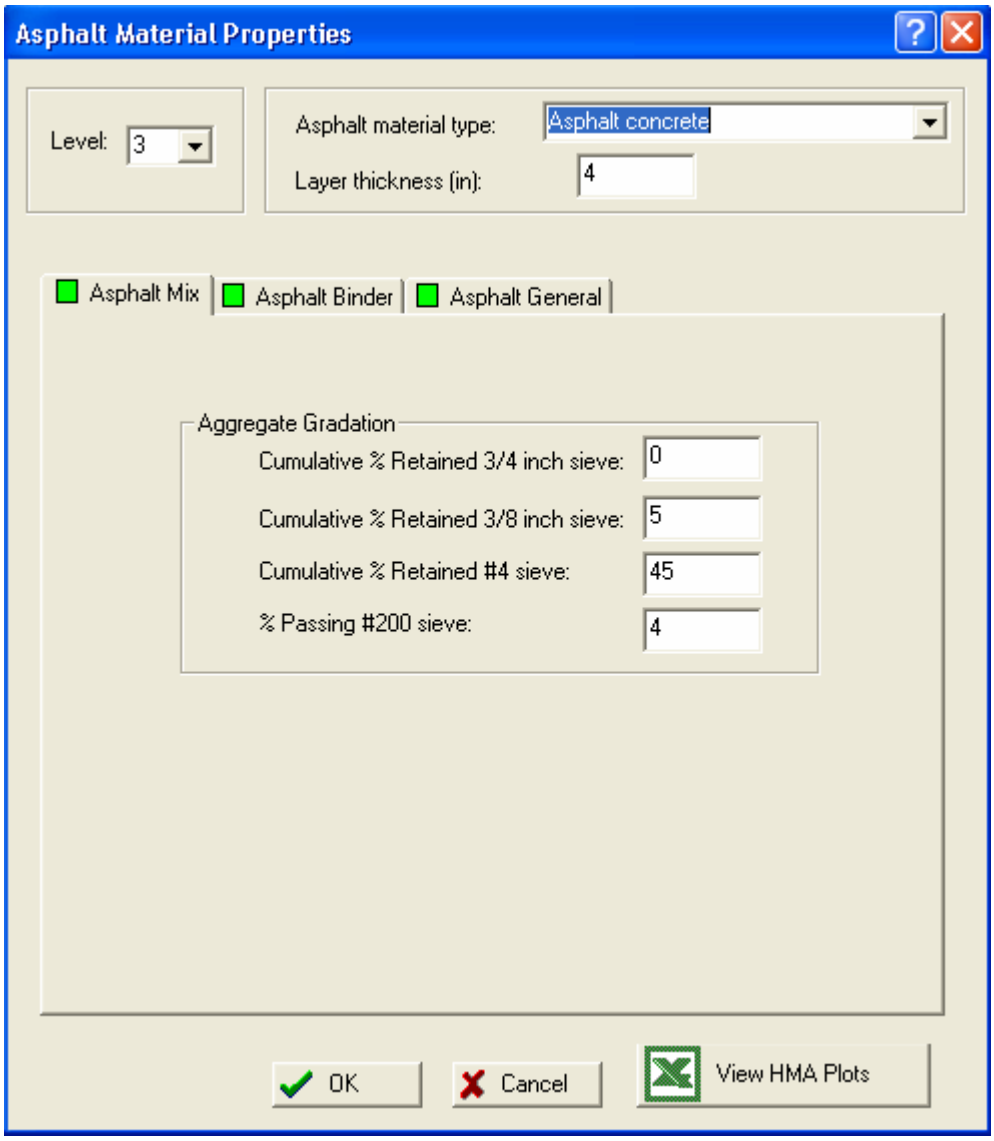

Figure A.11 HMA material properties input template

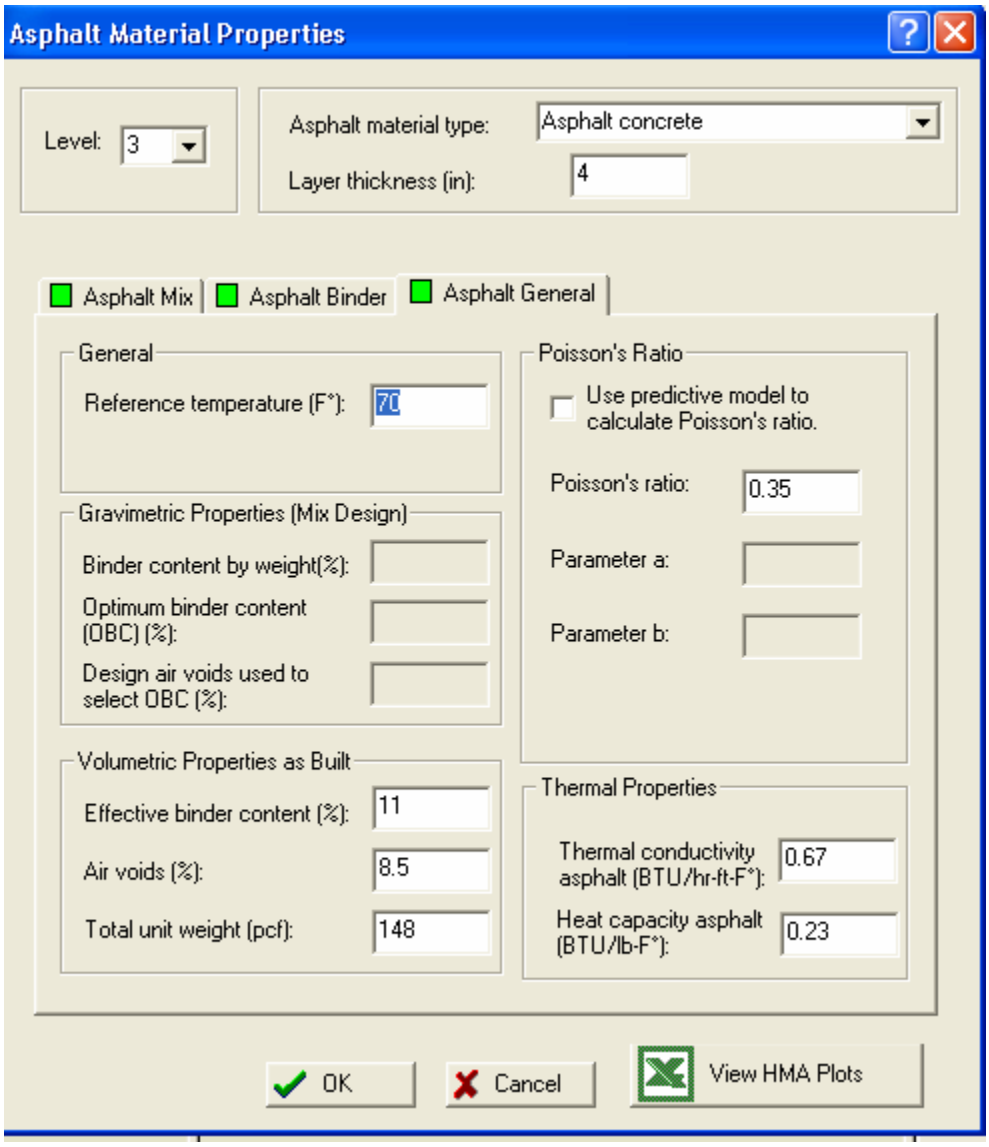

Figure A.12 HMA material properties input template

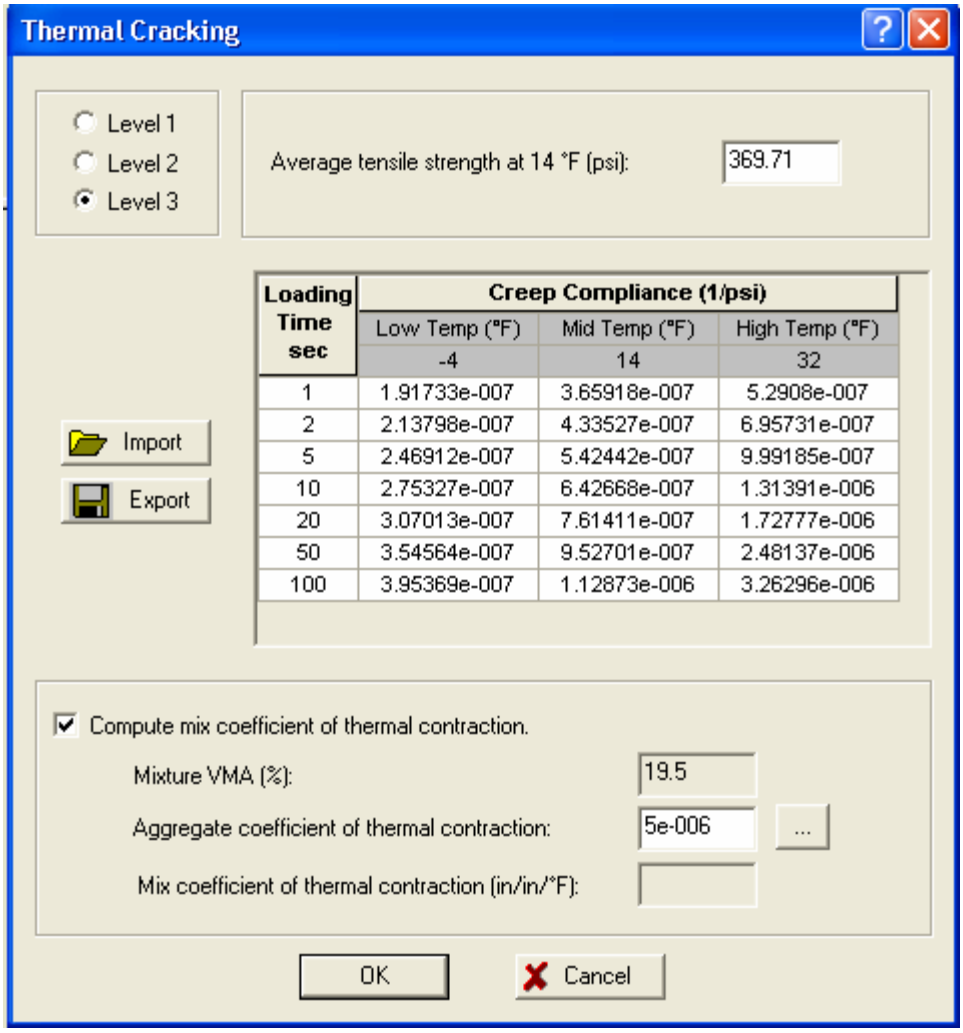

Figure A.13 Thermal cracking input template

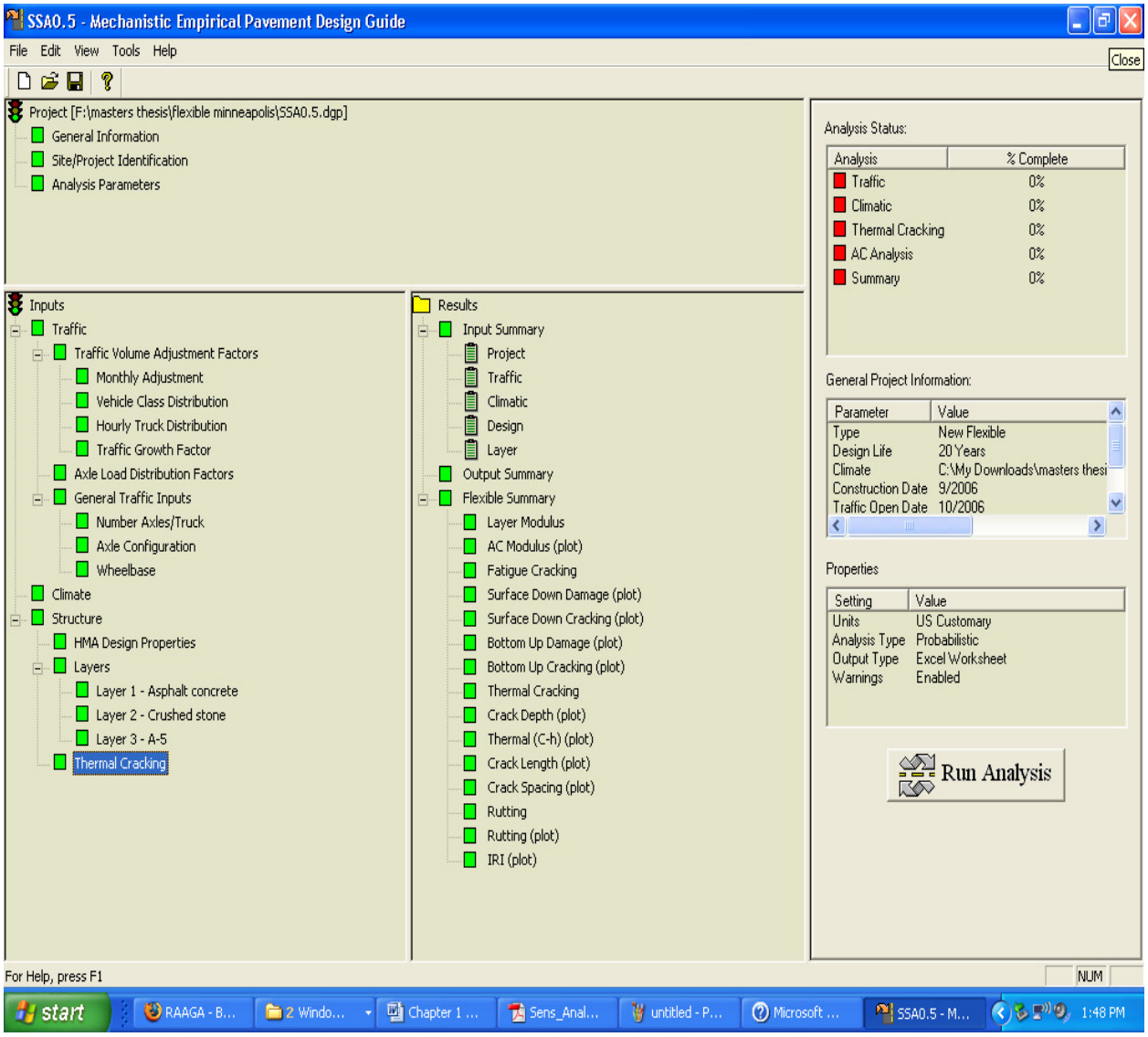

Figure A.14 MEPDG software